

# Session 3: Mathematical and physical models

Objektyp: **Group**

Zeitschrift: **IABSE reports = Rapports AIPC = IVBH Berichte**

Band (Jahr): **46 (1983)**

PDF erstellt am: **16.05.2024**

## **Nutzungsbedingungen**

Die ETH-Bibliothek ist Anbieterin der digitalisierten Zeitschriften. Sie besitzt keine Urheberrechte an den Inhalten der Zeitschriften. Die Rechte liegen in der Regel bei den Herausgebern.

Die auf der Plattform e-periodica veröffentlichten Dokumente stehen für nicht-kommerzielle Zwecke in Lehre und Forschung sowie für die private Nutzung frei zur Verfügung. Einzelne Dateien oder Ausdrucke aus diesem Angebot können zusammen mit diesen Nutzungsbedingungen und den korrekten Herkunftsbezeichnungen weitergegeben werden.

Das Veröffentlichen von Bildern in Print- und Online-Publikationen ist nur mit vorheriger Genehmigung der Rechteinhaber erlaubt. Die systematische Speicherung von Teilen des elektronischen Angebots auf anderen Servern bedarf ebenfalls des schriftlichen Einverständnisses der Rechteinhaber.

## **Haftungsausschluss**

Alle Angaben erfolgen ohne Gewähr für Vollständigkeit oder Richtigkeit. Es wird keine Haftung übernommen für Schäden durch die Verwendung von Informationen aus diesem Online-Angebot oder durch das Fehlen von Informationen. Dies gilt auch für Inhalte Dritter, die über dieses Angebot zugänglich sind.

**SESSION 3****Mathematical and Physical Models****Modèles mathématiques et physiques****Mathematische und physikalische Modelle**

Leere Seite  
Blank page  
Page vide

## Structural Analysis of the Dome in Florence

Analyse structurelle de la coupole du dôme à Florence

Analyse des Tragsystems der Domkuppel in Florenz

### S. DI PASQUALE

Professor  
Univ. of Florence  
Florence, Italy



S. Di Pasquale, born 1931, received his architect degree at the University of Naples, Italy, and worked in the field of Space Structures. From 1976 he was involved in structural masonry problems.

### SUMMARY

The results of research carried out on the dome of the Duomo in Florence, since 1976 are presented. Details are given of the characteristics of the non-linear problem due to the material properties, and about the theory proposed for its solution. Finally, a solution for non-consolidation is determined.

### RESUME

Le rapport présente les résultats de recherches effectuées pour le Dôme à Florence dès 1976. La nature du problème non-linéaire est dû aux propriétés du matériau; une théorie est utilisée pour sa résolution. Une solution de non-consolidation est enfin déterminée.

### ZUSAMMENFASSUNG

Es werden die Forschungsergebnisse über die Untersuchungen der Domkuppel in Florenz, die seit 1976 unternommen wurden, vorgestellt. Besonders wird über die durch das Materialverhalten bedingte Nichtlinearität des Problems und die theoretischen Annahmen für seine Lösung hingewiesen. Ferner wird eine Lösungsmöglichkeit ohne Verstärkung aufgezeigt.



## 1. INTRODUCTION

Paradoxically, could Filippo Brunelleschi have known the famous " $\pi$  theorem", many problems arising today from the stability of his dome should appear as feigned problems. Built in the years between 1420 and 1436, the florentine S. Maria del Fiore dome is probably the greatest masonry dome all over the world. It shows an eight-edged plan, 52 mt from the ground level, inscribed within a circle with a 45 mt inner and 54 mt outer diameter. There are also an inner 2.20 mt average thickness dome and an outer one 0.80 mt thick, bound together by eight corner arches and by other sixteen ribs. At the top, about 90 mt from ground level, there is an about 800 tons heavy lantern. Over the dome, being of fair weight of 25,000 tons, there is a wide-spreading fracture pattern, common to all wide-span masonry domes. Four major fractures bypass both the inner and outer domes and are spreading from the basis of the drum to about two thirds of the meridian length.

There are also capillary fractures, sometimes even well appreciable at a glance, actually spreading all over the structure. The problem of these fractures, and of the strengthening project, is not recent. By the end of the 17th century the dome already raised some troubles. Many were concerned with the problem in turn; V. Viviani, the famous pupil-biograph of Galileo, other less renowned architects in the 18th century, P. L. Nervi since 1940, W.B. Parsons in the same years and, more recently, R. Mainstone.

The structural analysis of this last author is particularly interesting. Though performed assuming a membrane behaviour and a fictitious rotational dome within the real one (following some hints already expressed in nuce by L.B. Alberti). In such an analysis, the problem of the static behaviour of the dome during the years of its construction is taken into consideration for the first time. The results obtained by Mainstone, although affected by rough approximations, may be confirmed today by the more sophisticated analysis recently performed. All the work done by us about this problem since 1977 cannot be conveniently summarized in the available space. Together with researches about the mechanical problem - described in what follows - other investigations have been made about worksite management, the load-lifting devices used for the construction, the history of mechanics in Renaissance. These last researches gave a confirmation of the results obtained by all the structural analyses : the fracture phenomenon had its origins before the dates stated by known documents, maybe already at the time of its construction.

The dome structure has been studied with several methods, with the aim of obtaining results which could be compared.

Before explaining such results, some basic considerations will be very useful, mainly about the contribution given by technological and scientific research to the problem of restoration of monuments. The clause I of the Venice Chart - ruling the restoration projects - raised several perplexities among the specialists of restoration, mainly about the several conclusions and the use of not-ever justifiable strengthening techniques.

The lacking of a specific theory of masonry mechanics in many cases produced structural analyses where masonry is a no-tension material; hence, fractures take place where tensile stresses show the greatest values. The theoretical mistake affecting the so-obtained results is quite self-explanatory and needs no remark.

Obviously, where a restoration project need be quickly and pressingly worked out, such procedures may be used and cautiously accepted. From our point of view, however, the not so-pressing problem of the SMF dome quite deserves a more rigorous formulation.



To this aim a mechanical theory has been proposed, viewing masonry as no-tension materials. Since this theory is complete up to date, as for the evaluation of stresses and fractures, it needs only existence and uniqueness theorems relating to particular compliance conditions of loads and constraints. Quite general results have been already obtained for plane problems, stating the theorems governing the fracturing and neglecting body forces.

In the already tested computational techniques, the no-tension behaviour has been simulated by suitable distortions or fractures. Convergence is achieved by setting zero the constrained energy due to fracture simulating distortions. Such numerical procedures followed mechanical analyses on masonry samples in order to obtain the values of elastic coefficients.

## 2. Mechanical properties of materials

This section of the research is aimed to the evaluation and knowledge of the materials of the Dome, including the materials of the foundations and the analysis of sub-soil.

The historical research has been done mainly on the documents of the "Opera del Duomo"; it has permitted the characterization of the materials by their source of origin. Destructive tests have been done on mortar, bricks and stones, using samples obtained from cores with a diameter 7 cm. and length which varies with the thickness of the vault. Mineralogical-petrographical, physical and spectrographical tests were done with the aid of Manganelli Dal Fà and Franchi at "Centro di studio sulle cause di deperimento e metodi di conservazione delle opere d'arte" - CNR - University of Florence all of this to determine the components of such materials for an ultimate control.

The availability of wood kilns for the firing of pozzolans and clays, together with aging chambers, lets us hope for good results.

In the meantime, tests have been done on the individual components and on contemporary masonry, so as to be able to compare the old and the new. This will allow an ample experimental research that uses components available today, avoiding thus further sampling. Here under we list the results of the tests done up to today, neglecting all technical information acquired by the readings of archival documents.

A relationship between a stratigraphical model, obtained from drillings performed in the surroundings of Santa Maria del Fiore, and the units that constitute the florentine sub-soil, have been deduced. Of such units have been determined the granulometric characteristics and the mechanical properties.

In a similar way we shall summarize the results of tests done on old and new materials in the following table:

	A	$\gamma_d$ Ncm <sup>-3</sup>	$\gamma_w$ Ncm <sup>-3</sup>	$\sigma_c$ Ncm <sup>-2</sup>	$\sigma_t$ Ncm <sup>-2</sup>	$E_c$ Ncm <sup>-2</sup>	$\nu$
antique brick	18,14	16,18	19,22	2772	260	1108530	0,18
recent brick	18,63	16,87	20,01	2943	256	961380	0,14
antique mortar	17,67	16,57	19,52	1962	387	784800	0,27
recent mortar	-	-	-	2118	465	794610	0,22



Where

- $A$  = coefficient of imbibition
- $\gamma_d$  = dry density
- $\gamma_w$  = wet density
- $\sigma_c$  = ultimate compressive strenght
- $\sigma_t$  = ultimate tensile strenght
- $E_c$  = Young's modulus     $\nu$  = Poisson's ratio

### 3. Structural static and dynamic analysis

3A) Static analysis was performed as stated in what follows:

- i) The order of magnitude of tensile stresses has been obtained by membrane and membrane & bending mechanical models, assuming perfectly linear elastic behaviour of materials.
- ii) A mechanical model has been considered, where the fractures already spread up to the basis of the lantern, in order to evaluate the structural stability in such configuration.
- iii) A particular no-tension finite-element has been implemented for accounting for the actual behaviour of masonry. Thus a dead load condition alone and combined with thermal loads have been considered.

A short survey of the massive results obtained leads to the following remarks. Type A-i simulations may all be compared to each other, but they do not exactly comply with the fracture pattern. This is due to the assumptions about material behaviour, which is actually no-tension.

Type A-ii simulation and its results are a basic reference for the analysis of the future fracture progress. In such a model the greatest values of stresses are found at the basis of the lantern: 10, Ncm-2 in tension and 75. Ncm-2 in compression.

We ought to remark that in this model the thrust-line holds always within the sections of the structure, except than at the basis of the lantern.

Type A-iii simulation has been performed on a 171 degrees-of-freedom model, corresponding to 1/16th of the whole structure, accounting also for the great openings at the levels of two internal platforms: these are the two weakest-links within the structure. These are very interesting results as far as they give the loading factor corresponding to a possible failure, due to yield compression stresses. Furthermore, we should remark that no-tension structural models lead in general to under-determined configurations, i.e. in unstable equilibrium under prescribed external loads: thus it may be viewed as a limit-model. In the fractured wones the material behaves as a semi-fluid, although satisfying the Drucker stability postulates.

### 3B) Dynamic linear analysis of the SMF Dome

In what follows a finite-element numerical model will be described, used to investigate the structural behaviour of the S. Maria del Fiore Dome subjected to road-traffic excitations: such dynamic analysis aimed to be compared with experimentally evaluated data.

These are several available approaches to perform a linear elastic analysis of structures subjected to any dynamic loads; these are described by several authors, but the main topics may be summarized by K.J. Bathe and E.L. Wilson ("Solution



methods for EigenValue problems in Structural Mechanics", Int. Jour. Num. Meth. in Eng., 6, n. 2, 1973) and by R.W. Clough and J. Penzien ("Dynamics of Structures", McGraw, 1975).

As a matter of fact, the structural analysis of the SMF Dome needed to account also for pier and buttresses down to the ground level, where constrained nodes are subjected to dynamic loads. These are defined as input acceleration diagrams ( $g'/g$  versus time), obtained by evaluation of amplitudes and frequencies of vibrations corresponding to several traffic conditions. Obviously, locally-acting dynamic loads cannot be considered, but a global ground-level accelerogram may be properly defined in the different loading conditions. Furthermore, the dome-geometry has been defined taking the main fracture pattern into account; this means to include proper disconnections at midspan of four horizontal edges, between an upper and lower fracture-level.

The actual double-layer vault geometry has been replaced by a simple layer node mesh, both for the Dome and the vertical structures. Furthermore, a forced-response by modal superposition technique has been used to solve the so-obtained problem. This required the previous computation of  $p$  M-orthonormalized eigenvectors. This one proves to be a very efficient technique especially when several acceleration input diagrams must be considered, or when a fairly long time interval is defined for dynamic loads, particularly when little time steps are used for final integration. The latter, besides, ought to account also for the higher frequencies which contribute to the dynamic response. Furthermore, we should remark that a particular structural assembly and geometry suggested to properly extend the modal analysis, i.e. the dimensions of the subspace defined by eigenvectors. The aim was to get sufficient accuracy of results, within the limits of the accuracy degree of the structural model, both for geometrical and mechanical aspects.

A first step of the computational procedure was the proper definition of the integration time step to be used for the integration of dynamic equilibrium equations. The unconditionally stable theta-Wilson integration scheme has been used, and in this first step direct-response and modal superposition techniques have been both extensively used and compared to each other, in order to achieve the desired accuracy in the  $p$ -dimensional principal subspace and with a computed time integration step.

The used computational procedure is the well-known SAP IV program, implemented by K.J.Bathe, E.L.Wilson and F.E.Peterson for the static and dynamic analysis of linear structures. The finite element model more extensively used was the shell & plate one, including membrane and bending stresses, while few elements were isoparametric plane-stress. We need to remark that the required accuracy in the problem formulation allows a linear approach, since the stresses produced by slight traffic-accelerations would justify - at least partially - the use of a linearly-elastic material model.

The same reasons suggested not to take into account damping effects in masonry, because sufficient experimental data and results are not completely yet in this field of investigation. Even within such and other approximations, due for instance to the geometrical and mechanical uncertainties of the assumed model, a linear dynamic analysis of a many-degrees of freedom elastic structure seems to be a useful tool for effective comparison with experimental results. Furthermore, this could be a starting point toward the implementation - in a close future - of an optimal control procedure i.e. of a real-time static and dynamic analysis of such monumental structures, already affected by wide-spreading fracture patterns. Besides, the usefulness of a numerical model ought to be viewed also in the possibility of easily changing the dynamic input, using the same procedure.

From this point of view we wanted to draw the attention of Public Municipal Au-



thorities - contractors of some investigations - on the problem of seismic reliability of such structures. Taking into account some recent aspects of Italian seismic codes about masonry structures, once again a linear approach to this problem seemed to be quite sufficient; so, an El-Centro, 1940, NS earthquake accelerogram has been given as input in the same procedure of forced response by modal superposition. Obviously, in this case the assumed elasticity behaviour does not comply with the resulting relevant stresses, due to the most unfavorable static plus dynamic loading condition. On the other hand, we shall recall that the Italian seismic code for masonry structures allows linear-elastic computations, providing at the same time rather high values of the safety factors, much greater than those assumed for r.c. or steel structures.

#### 4. Hypothesis of structural non-consolidation

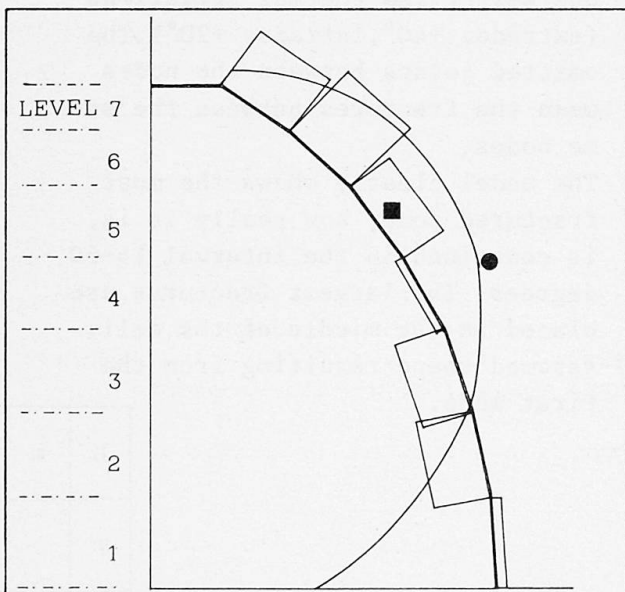
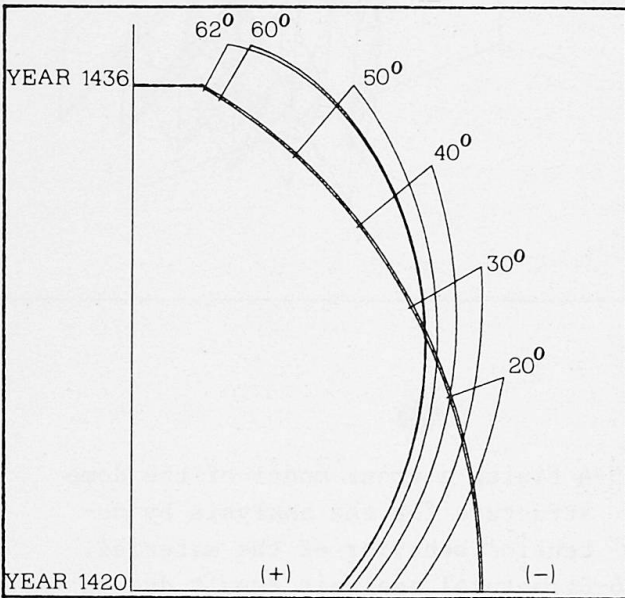
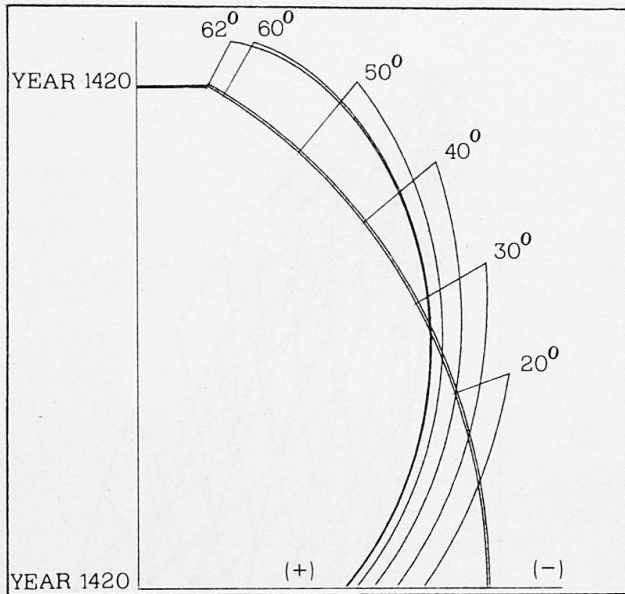
The History of the dome and the results of the theoretical, experimental and numerical researches bring about the following considerations:

- i) The fracture pattern of the dome has remote origins in respect to the evolutions that we have been able to control in the last forty years.
- ii) The history of this monument shows that the fracture pattern is in progress towards a "statically determinate" configuration. This has been the object of particular attention so as to evaluate the ultimate safety factor.
- iii) The accuracy of the ultimate safety factor can be furtherly increased through a nonlinear analysis which accounts for other phenomena, for example: the fluage, the creep, the fatigue due to mechanical and thermal loads.
- iv) The presence in site of a thick mesh of thermo-dilatometers measuring devices will permit the control in real time of the actual state of the structure. This will allow the evaluation of the ratio between the instantaneous safety factor and the ultimate one computed in ii) and iii).

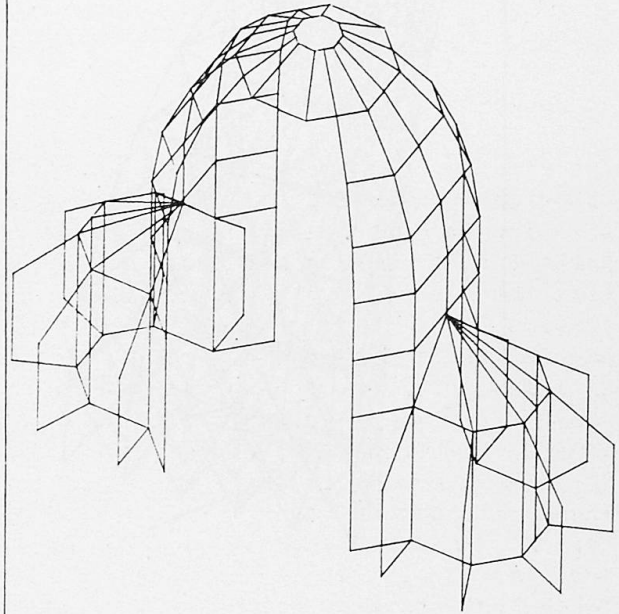
Taking into consideration the cyclical mechanisms of fractures due mainly to thermal loads, we may assume a first stage restoration of the fracture-scheme, viewed as an elimination of the constraints that prevent the natural behaviour of the structure. Thus, the mesh of measuring devices will be able to furnish information about the progress of the fractures, without all possible perturbations due to the falling of fragments within the fractures. A future project for the strengthening of materials or the stiffening of the structure can be brought forward on basis of the former considerations.

REFERENCES : Works produced about this problem by the Research group

- S.DI PASQUALE, The Dome of S.M.F.: an opportunity to state a theory of masonry structures, IASS, Madrid, 1979
- P.FOCARDI, V.VASARRI, Ricerche su fondazioni di monumenti fiorentini, XIV Congresso A.G.I., Firenze, 1980
- S.DI PASQUALE, Distorsioni fittizie per problemi a vincoli unilateri, AIMETA, Palermo, 1980
- S.BRICCOLI-BATI, A. BOVE, B.LEGGERI, Geometrically nonlinear analysis of contact problems in elastic continua, GAMM Kongr., Copenhagen, 1977
- A. BOVE, M.PARADISO, G.TEMPESTA, Relaxation technique for variational inequality problems in strict analysis, IX Int.Kongr.Anw.Math., Weimar, 1981
- S.DI PASQUALE, Application de la recherche scientifique a l'analyse et a la consolidation des struct. arch., Rapp.Gen., ICOMOS, Roma, 1981
- A. BOVE, M.PARADISO, G.TEMPESTA, Problemi di complementarietà lineare nell'analisi di strutture discretizzate a comportamento elasto-plasto-fragile, AIMETA, Genova, 1983
- S.DI PASQUALE, Questioni di meccanica dei solidi non reagenti a trazione, AIMETA, Genova, 1982



### A FINITE ELEMENT MODEL FOR DYNAMIC ANALYSIS



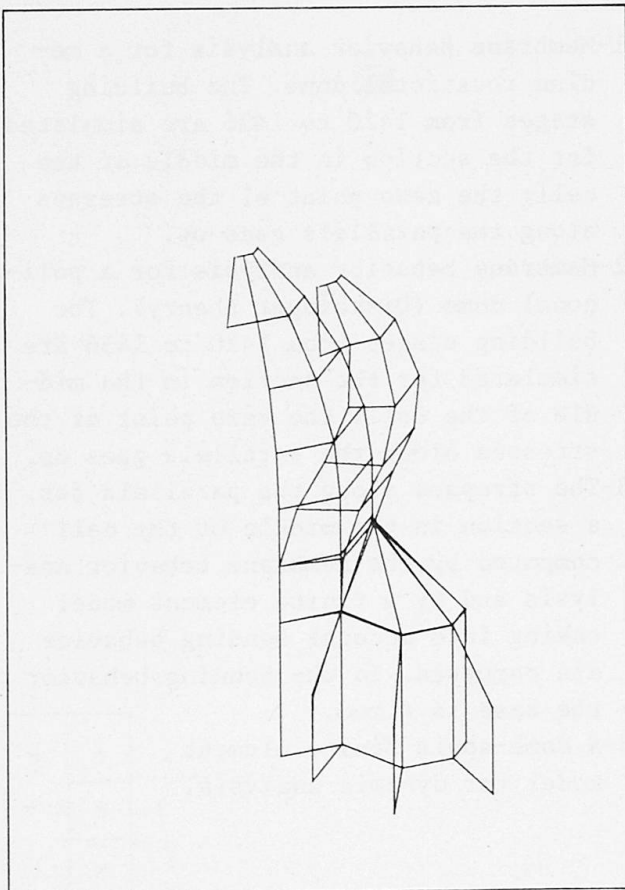
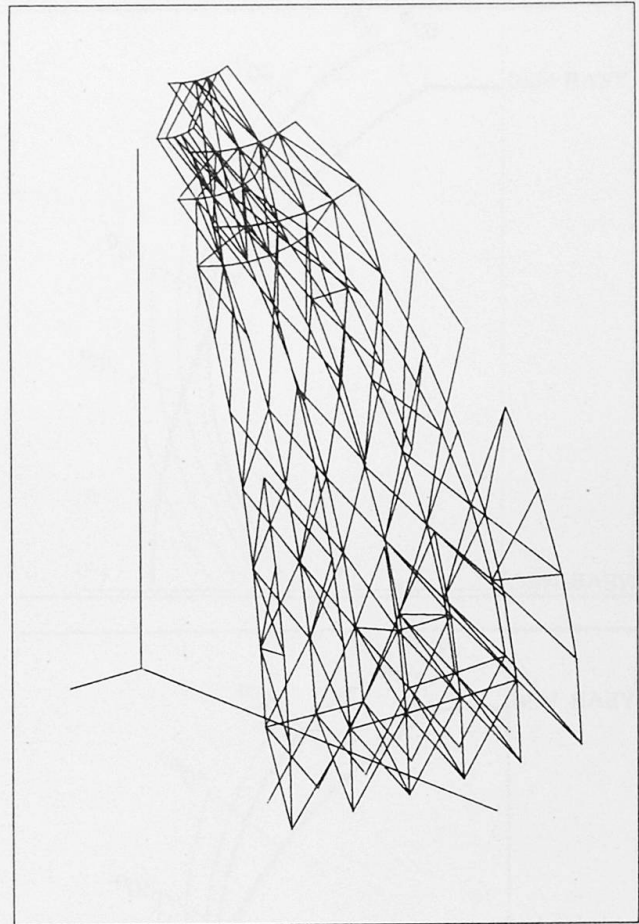
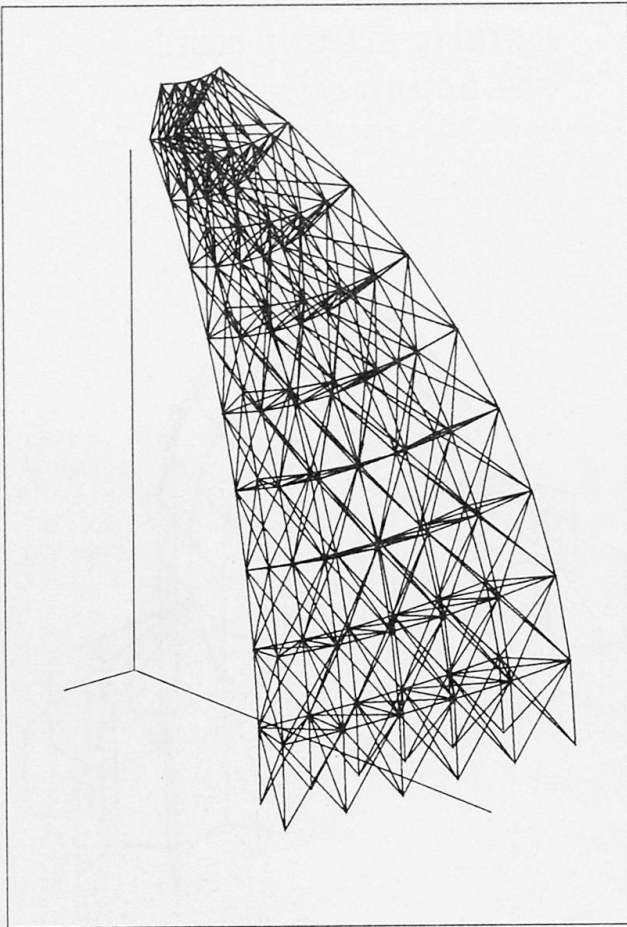
1-Membrane behavior analysis for a medium rotational dome. The building stages from 1420 to 1436 are simulated for the section in the middle of the cell: the zero point of the stresses along the parallels goes up.

2-Membrane behavior analysis for a polygonal dome (Dischinger theory). The building stages from 1420 to 1436 are simulated for the section in the middle of the cell: the zero point of the stresses along the parallels goes up.

3-The stresses along the parallels for a section in the middle of the cell computed by the membrane behavior analysis and by a finite element model taking into account bending behavior are compared. In the bending behavior the base is fixed.

4-A dome-apsis finite element model for dynamic analysis.

1	4
2	
3	



5-A finite element model of the dome structure for the analysis by no-tension behavior of the material.

6-Structural analysis result due to own weight and thermal variations (extrados  $+40^\circ$ , intrados  $+20^\circ$ ). The omitted joints between the nodes mean the fractures between the same nodes.

The model clearly shows the most fractured zone, how really it is, is contained in the interval 15-50 degrees. The largest fractures are placed in the middle of the cell.

7-Assumed shape resulting from the first mode.

5	6
7	

## Analysis of a Brunelleschi-Type Dome Including Thermal Loads

Analyse d'une coupole tenant compte des effets thermiques

Untersuchung von Kuppeln unter Berücksichtigung thermischer Belastungen

### A. CHIARUGI

Professor  
Univ. of Florence  
Florence, Italy

Born in 1937 in Florence. Took his Civil Engineer degree in Bologna, where he began his career as a University Professor in 1965. He has been teaching Structural Technology since 1972 at the Engineering Faculty of Florence.



### M. FANELLI

Professor  
ENEL-CRIS  
Milano, Italy

Born in 1931 in Florence. Civil Engineer degree cum laude in 1954. Concerned with computer analysis of structural and hydraulic problems. Head of the Theoretical Analysis Service of the CRIS of ENEL. Since 1981 is Chairman of WC VI of IABSE



### G. GIUSEPPE

Engineer  
ENEL-CRIS  
Milano, Italy

Born in 1945 in Pesaro, obtained her degree in Civil Engineering (Transport) in 1969. She was engaged at ENEL in 1971 and now she is coordinating the activity of a group in the field of advanced structural analysis.



### SUMMARY

This paper deals with an important historical monument: the Florence Cathedral dome. A Brunelleschi-type octagonal double-shell dome structure, was studied using a finite element model which reproduced its general geometry and various cases of load and restraint. The material was assumed to be linear-elastic, however, non-linear geometry was introduced by analysing gradual crack development as indicated by the present situation. Besides static loads with various assumed restraints, thermal loads were also considered in accordance with yearly periodic variations. The superposition of these effects gives some hints on the origin of the present cracks and the static performance of the cracked structure.

### RESUME

Il s'agit d'une contribution à la connaissance d'un important monument historique: la coupole de la Cathédrale de Florence. Sur un modèle à éléments finis reproduisant sa géométrie générale, on a étudié plusieurs cas de charge et de liaison. Le matériau est censé être élastique-linéaire, mais on introduit des variations de géométrie qui représentent le développement progressif des fissures jusqu'au niveau actuel. En plus du poids propre, on a considéré des charges thermiques d'après un cycle annuel schématique. La superposition des effets donne quelques idées sur l'origine des fissures actuelles ainsi que sur la performance statique de la coupole fissurée.

### ZUSAMMENFASSUNG

Der Beitrag gibt Aufschlüsse über ein wichtiges historisches Baudenkmal: die Kuppel des Doms von Florenz. Die doppelschalige, achteckige Kuppel wurde unter Beachtung der Geometrie des Bauwerks mit einem Modell aus finiten Elementen nachgebildet. Unter der Annahme linear-elastischen Materialverhaltens und der Berücksichtigung nicht-linearer Geometrie aus der Beobachtung des Rissverhaltens wurden verschiedene Lastfälle und geometrische Restriktionen erfasst. Neben den statischen Lasteneinwirkungen wurden unter Berücksichtigung verschiedener, angenommener Spannungszustände auch hypothetische thermische Belastungen, entsprechend den jährlichen Temperaturschwankungen, untersucht. Die Ueberlagerung der verschiedenen Einwirkungen liefert interessante Hinweise über die Entstehung der vorhandenen Risse und das statische Verhalten der gerissenen Kuppel.



1. FOREWORD - In order to fight the deterioration of historical monuments, all means made available by today technology should be used. In this spirit -heeding the damaged state of the Dome of Florence Cathedral- we deemed useful to attempt an analysis effected according to methods perfected for studying the most complex present structures, so as to gain a better insight of the statical conditions. We defined a numerical F.E. model of a Brunelleschi-type dome, according to an overall shape reproducing, with some simplifications and regularizations, the monument own one; elastic linear behaviour was assumed for the material. In spite of these simplifications, the model is deemed rich in overall insight potentiality: used as a "verification" tool, indeed, it allows to gain some pregnant trends of the mechanical behaviour of a structure. These, together with physical evidence desumed from direct observation of the dome, can yield useful contributions to the diagnosis of a structural damage. With the present paper we intend to illustrate, apart from yet unwarranted geometrical and mechanical refinements, only a few of the 26 cases of load and constraint analyzed, emphasizing how these results can be useful in the abovesaid sense.

## 2. DESCRIPTION OF THE MATHEMATICAL MODEL USED AND ITS

RESULTS - In order to achieve the abovesaid aims we defined at first the geometry of an ideal octogonal, regular, double-shell symmetric dome, the vertical profiles at corners being circular. The two shells are connected not only by the corner ribs, but also by two equally spaced ribs for every panel. To this model we attributed ideal mechanical characteristics of an elastic, homogeneous, isotropic solid (Young modulus  $E = 50,000 \text{ kgcm}^{-2}$ ; Poisson ratio 0.2; thermal dilatation coefficient  $\alpha = .8 \cdot 10^{-5} (\text{°C})^{-1}$ ; thermal diffusivity  $a = 16 \text{ cm}^2\text{h}^{-1}$ ). We intended to assess on such a structure -in this preliminary phase- only the effects of deadweight and of yearly sinusoidal thermal variations. To this end a F.E. mesh was built up for one quarter of the dome, cut by two orthogonal vertical symmetry planes (fig. 1 a). In order to better define the constraint conditions at the dome basis a quarter of the underlying drum, as schematized by the F.E. mesh of fig. 1 b, was later joined to the dome quarter of fig. 1 a. In this "dome plus drum" mesh there are 428 elements (2nd order, isoparametric ones with 20 or 15 nodes) and 2667 nodes. Some first-approach computations concerned only the dome, under different constraint hypotheses at the basis, assuming different degrees of participation for the outer shell, and also applying stiffness and deadweight either in one stage or in 7 successive stages broadly simulating the construction process. Passing over these first approaches, we intend here to illustrate the main results obtained by analysing the "dome plus drum" structure with complete constraints at the drum basis, under deadweight (including that of the skylight, acting on the upper rim of dome) and yearly periodic temperature variations. All these conditions were applied both to the intact and the cracked structure (see fig. 2, [1]). The position of cracks was defined by schematizing the actual cracking pattern, i.e. following vertical planes symmetrically intersecting four out of the eight dome panels (those at  $45^\circ$  from the plan cross axes). As concerns the extension in height of the cracks, an iterative computation was performed by raising in steps the upper tip of the cracks, until the tensile stresses that tended to

appear (in a direction perpendicular to the crack planes) above the tip became negligible. This condition obtained for cracks extending up to about  $2/3$  of the dome height, in good agreement with the observed present crack development. As concerns the stress analyses pertaining to thermal loads, it was necessary to obtain first the 3-D, time dependent temperature distribution inside the shells. Boundary thermal conditions were assumed with a common average of  $+15^{\circ}\text{C}$ , on which sinusoidal waves were superposed, with amplitude  $\pm 15^{\circ}\text{C}$  on the outer surface,  $\pm 5^{\circ}\text{C}$  on the inner surface; for the latter also a time-lag of one month with respect to outside was introduced. Intermediate boundary conditions were assumed for the cavities between the two shells. Figs. 3 to 10 represent graphically some results of the above-cited analyses. By considering these results, together with observations on the crack pattern (on every other panel: actually, those panels are cracked that stem from the four massive pillars of the cross-vault, whereas the other four panels, springing from arch supports, are practically uncracked, see fig. 2), we deemed it useful to analyse in detail the structure underlying the drum. To this end we discretized, by the F.E. mesh of fig. 11, the structure lying between the dome basis (third gallery level) and the first gallery level. 188 isoparametric, 2nd order elements with 1232 nodes were used for this mesh. This structure was constrained completely at the nodes of lower surface, whilst on the side vertical planes obvious symmetry conditions were applied for the intact structure. On the upper surface, two different load conditions were considered:

- a vertical, uniformly distributed pressure amounting to about  $3 \text{ kgcm}^{-2}$  (the integral of which roughly balances the weight of overlying masonry masses);
- a unit horizontal load ( $1 \text{ kgcm}^{-2}$ ), uniformly distributed across the thickness, thrusting outward perpendicularly to each octagon side.

Some of the results are illustrated in figure 12. In particular, the stress pattern seen from fig. 12a is confirmed by results of theoretical studies concerning curved wall-beams on interrupted supports [2] and continuous, curved intrados beams [3]. The upshot of it all is that the difference in stiffness between "solid" panels and "arch-supported" ones produces a bias in the horizontal tensile stresses at panel centers, especially under vertical loads. This bias is enhanced by the stress-concentration effect due to the "eyes" piercing the drum panels. If we analyze the possible superpositions of the previously considered stress states, it looks as if the structure possessed a natural propensity to cracking just in the "solid-supported" panels, starting from the "eyes" and following nearly vertical paths.

3. CONCLUSIVE REMARKS - The foregoing material aims at setting up a definite example of the possibilities offered by numerical analysis methods, as well as a first contribution - even if under sketchy hypotheses - to the diagnosis of the monument conditions. No more is attempted, in fact, than quantifying hints on the preferential bias of the structure to damage, as actually observed, and evaluating the broad lines of the present static conditions with open cracks. It is evident that even this diagnostic phase is far from concluded. It will, indeed, be necessary to effect further analyses - not only static, but also dynamic ones - , improving the model with geometrical, thermal and mechanical characteristics more in tune with actual properties.



We shall, moreover, need accurate experimental data (thermal and mechanical measurements), in order to effect a more proper numerical simulation as well as to validate the mathematical model; this will allow, in turn, to orient more specific experimental checks. By thus proceeding, clearly, not only the set of informations needed to complete the diagnostic phase will be more accurately drawn up, but a possibility will be opened toward setting up means for checking the effects of any type of "therapy". Indeed, if we should pass to a phase of "design" of any intervention upon an already built structure, we should be able to forecast the actual response of the monument.

#### ACKNOWLEDGEMENTS

Heartfelt thanks are expressed to ISMES (Bergamo, Italy) who kindly allowed to use its stress-analysis "FIESTA" system for all numerical analyses. Special gratitude is reserved for Mr. Franco Pari, of ENEL/CRIS, who cared after all the numerical and graphical work with unrelenting competence and assiduousness.

#### BIBLIOGRAPHIC LIST

- [1] FONDELLI M., FERRI W., FRANCHI P., GRECO F.  
"Il rilevamento fotogrammetrico della Cupola di S. Maria del Fiore in Firenze", Istituto Geografico Militare di Firenze, 1971
- [2] POZZATI P., "Tubo cilindrico ad asse verticale appoggiato in corrispondenza di alcuni tratti del bordo", Costruzioni in Cemento Armato, Studi e Rendiconti, Vol. 4, 1967
- [3] CECCOLI C., MERLI M., "Trave-parete ad intradosso curvo"  
Giornale del Genio Civile, fasc. 7, 8, 9, 1976

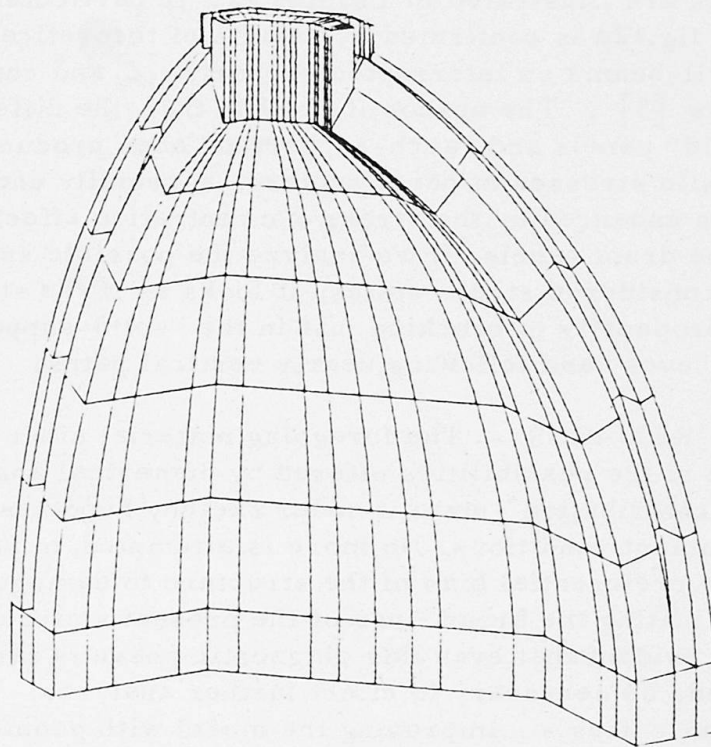


Fig. 1 a)

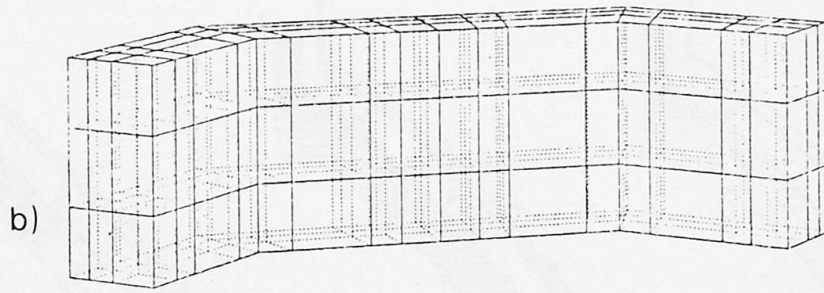


Fig. 1 - a) F.E. mesh of a quarter of the dome ; b) F.E. mesh of the drum underlying the dome

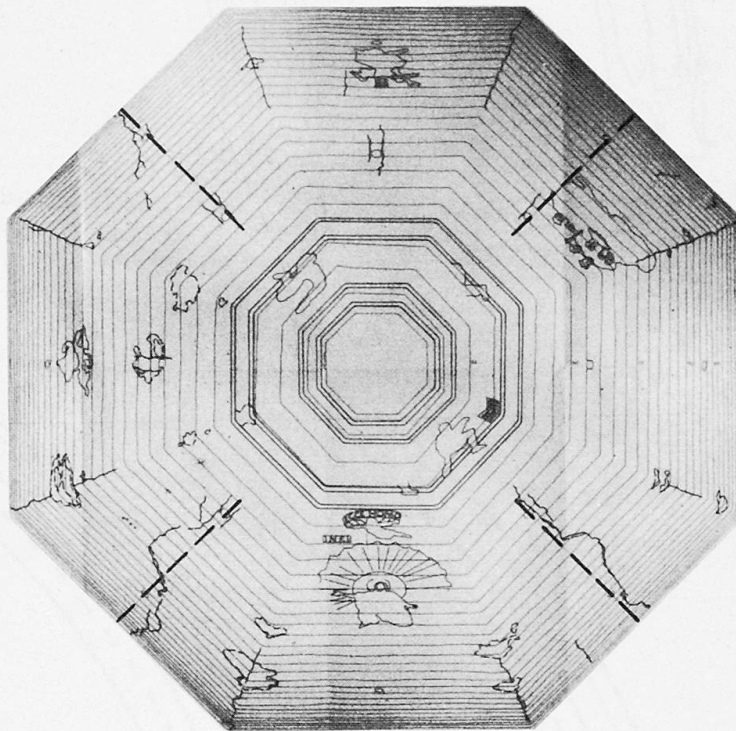


Fig. 2 - Nadiral view of crack pattern in Florence Cathedral dome  
(-----) assumed cracks

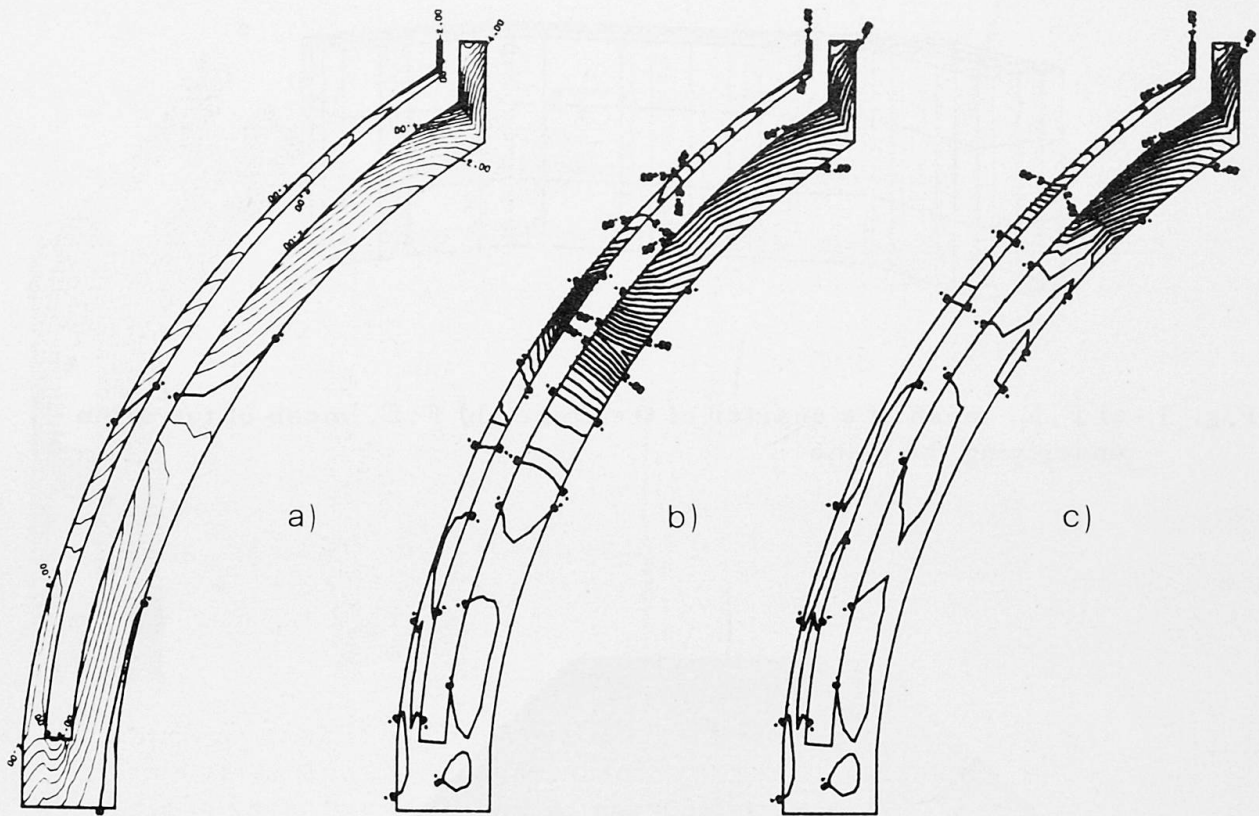


Fig. 3 - Contour lines of  $\sigma_x$  in the cross-section at mid-panel (load = dead-weight) ; a) uncracked structure; b) crack up to one-half height; c) crack up to two-third height

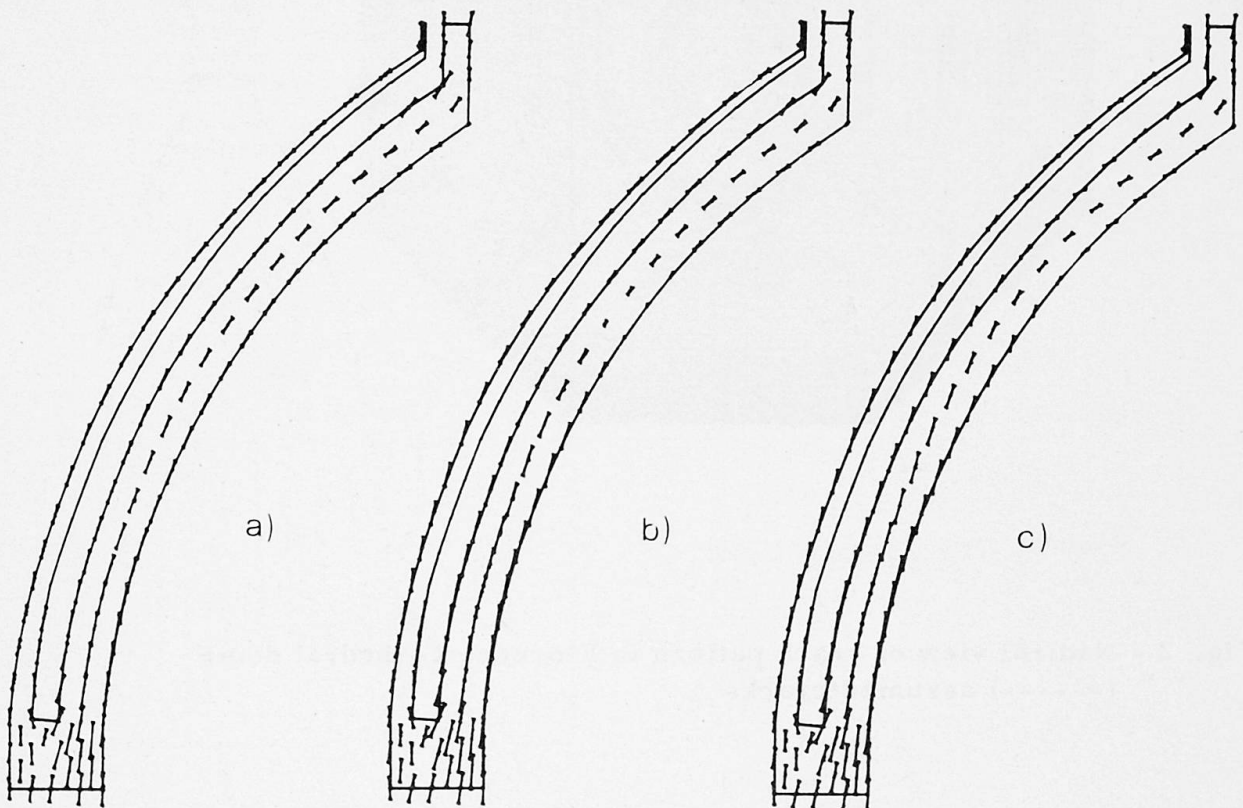


Fig. 4 - Principal stresses in cross-section at mid-panel: a) b) c) as in fig. 3 (load=deadweight)

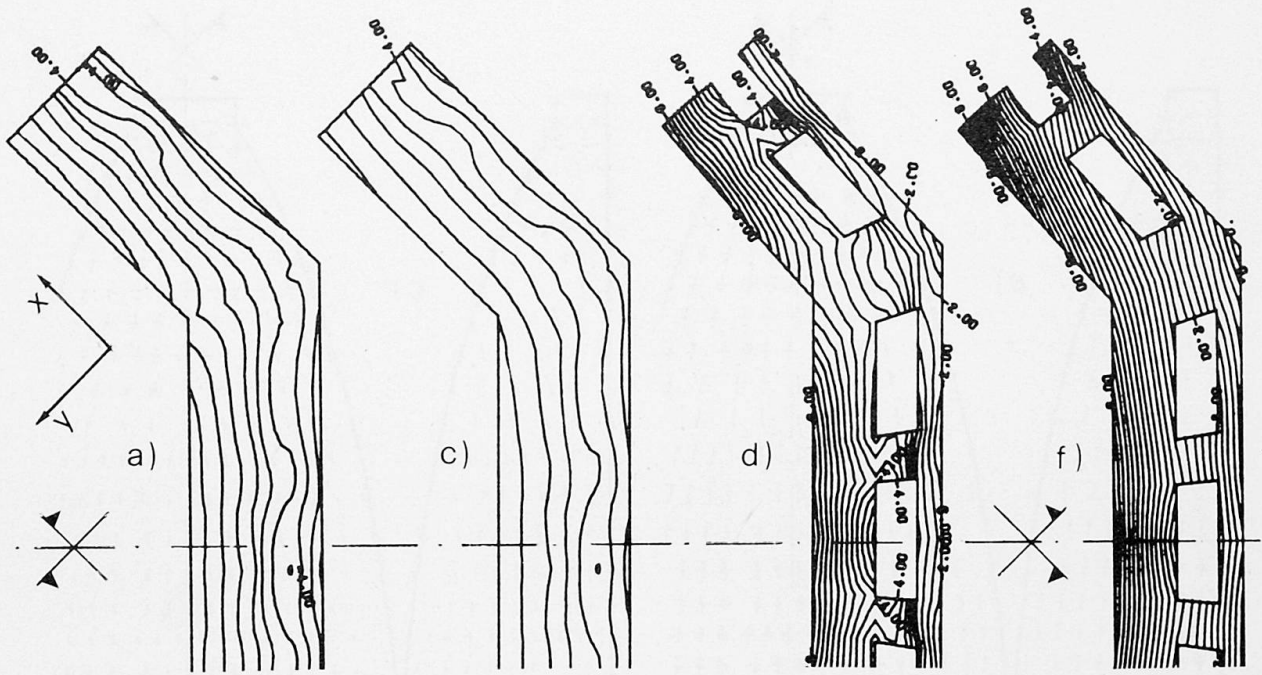


Fig. 5 - Contour lines of  $\sigma_z$  in horizontal sections : a) c) as in fig. 3 for hor. sect. at level of first gallery (load=deadweight); d) f) same as a) c) but for hor. sect. at level between second and third layer of elements in fig. 1 a)

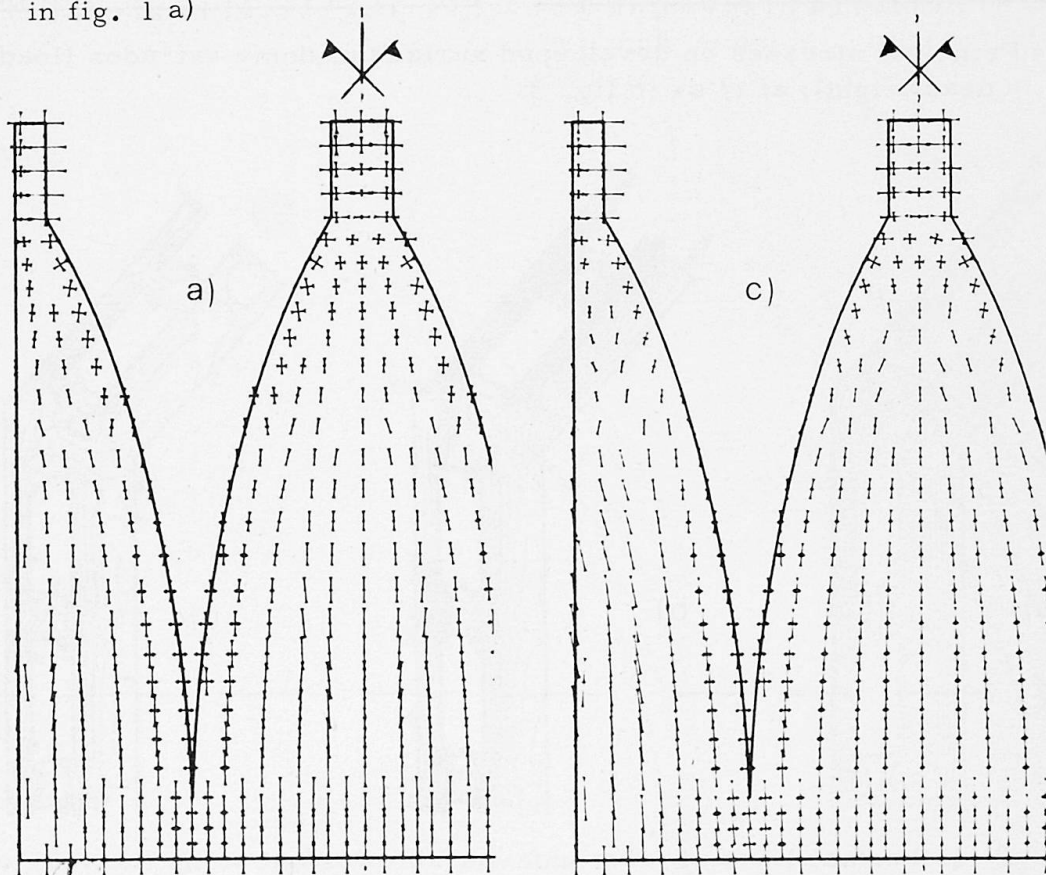


Fig. 6 - Principal stresses on developed surface of dome intrados (load = deadweight); a) c) as in fig. 3

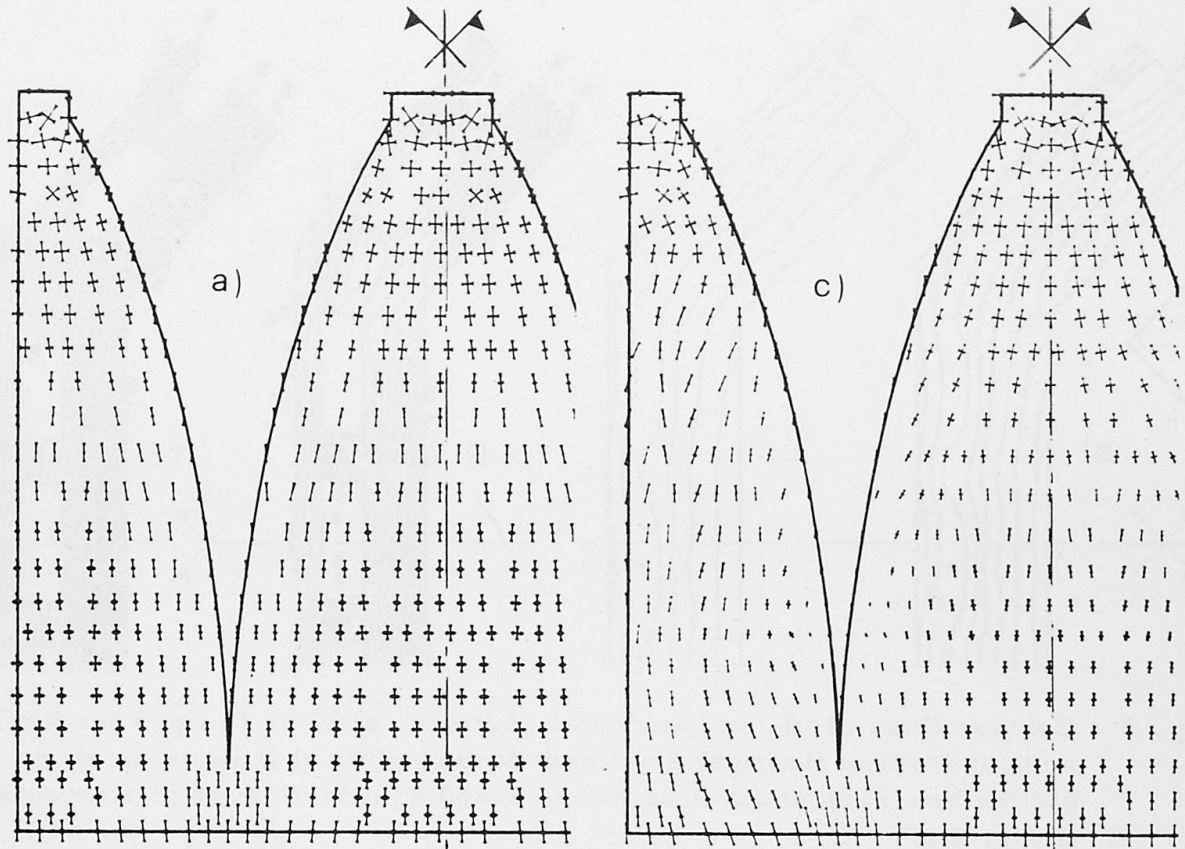


Fig. 7- Principal stresses on developed surface of dome extrados (load = deadweight); a) c) as in fig. 3

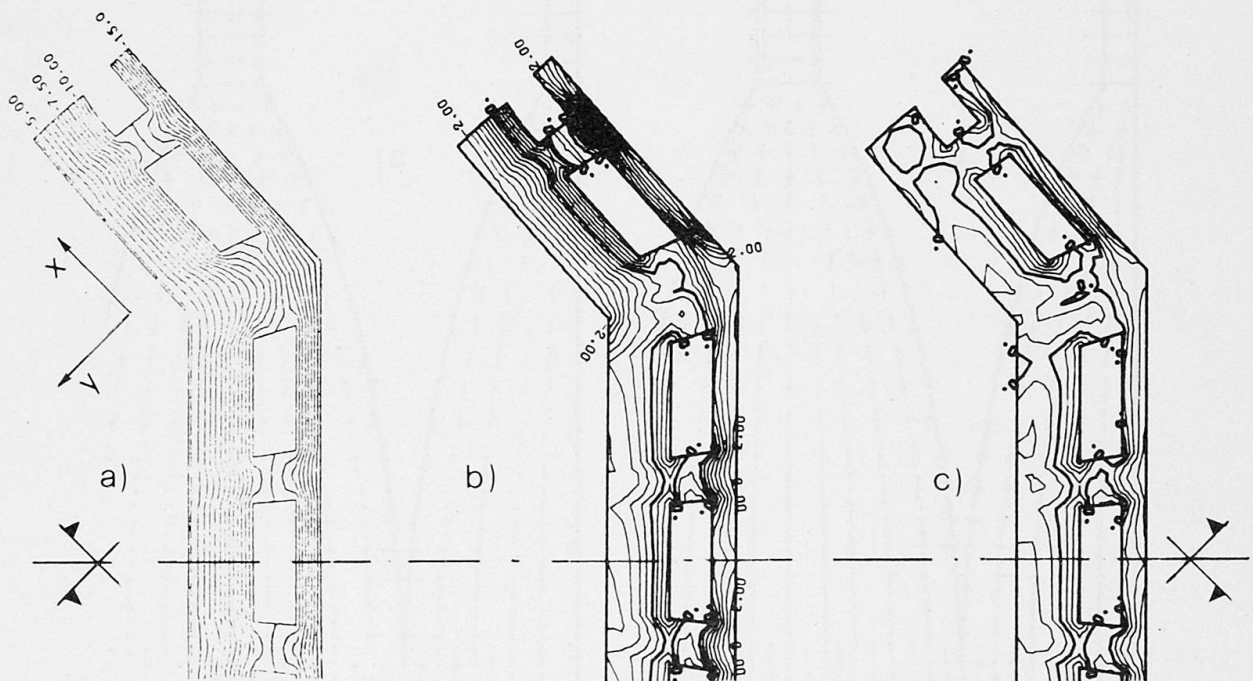


Fig. 8 - a) Isothermal lines at most unfavourable instant along the yearly cycle (Jan.) at hor. sect. between second and third layer of elements in fig. 1 a); b) Horiz. sect. between second and third layer of elements in fig. 1 a): contour lines for  $\sigma_x$ , uncracked structure, thermal load at Jan.; c) as b), but for cracked structure, maximum extension of cracks

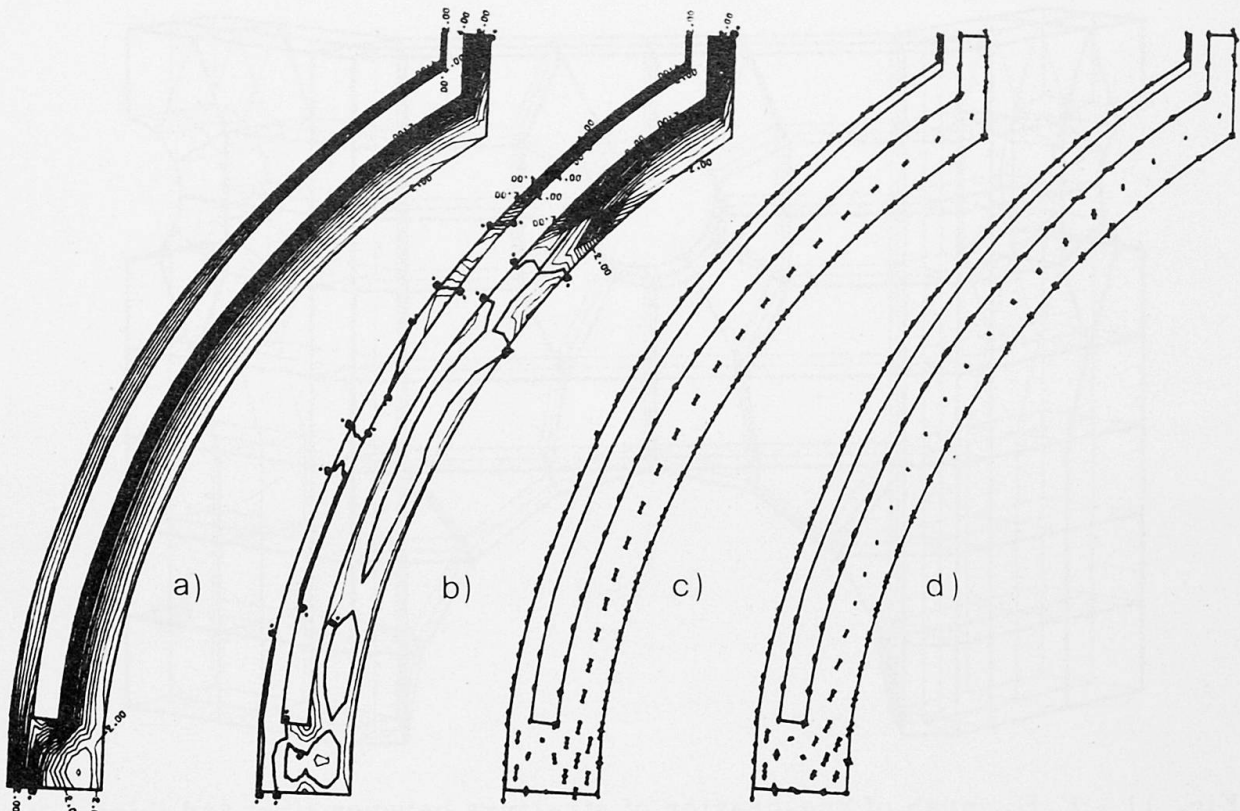


Fig. 9- a) Contour lines for  $\sigma_x$  on vertical cross-section at mid-panel, uncracked structure, thermal load at Jan.; b) as a), but for cracked structure, max. extension of cracks; c) principal stresses on vertical cross-section at mid-panel, uncracked structure, thermal load at Jan.; d) as c), but for cracked structure, max. extension of cracks

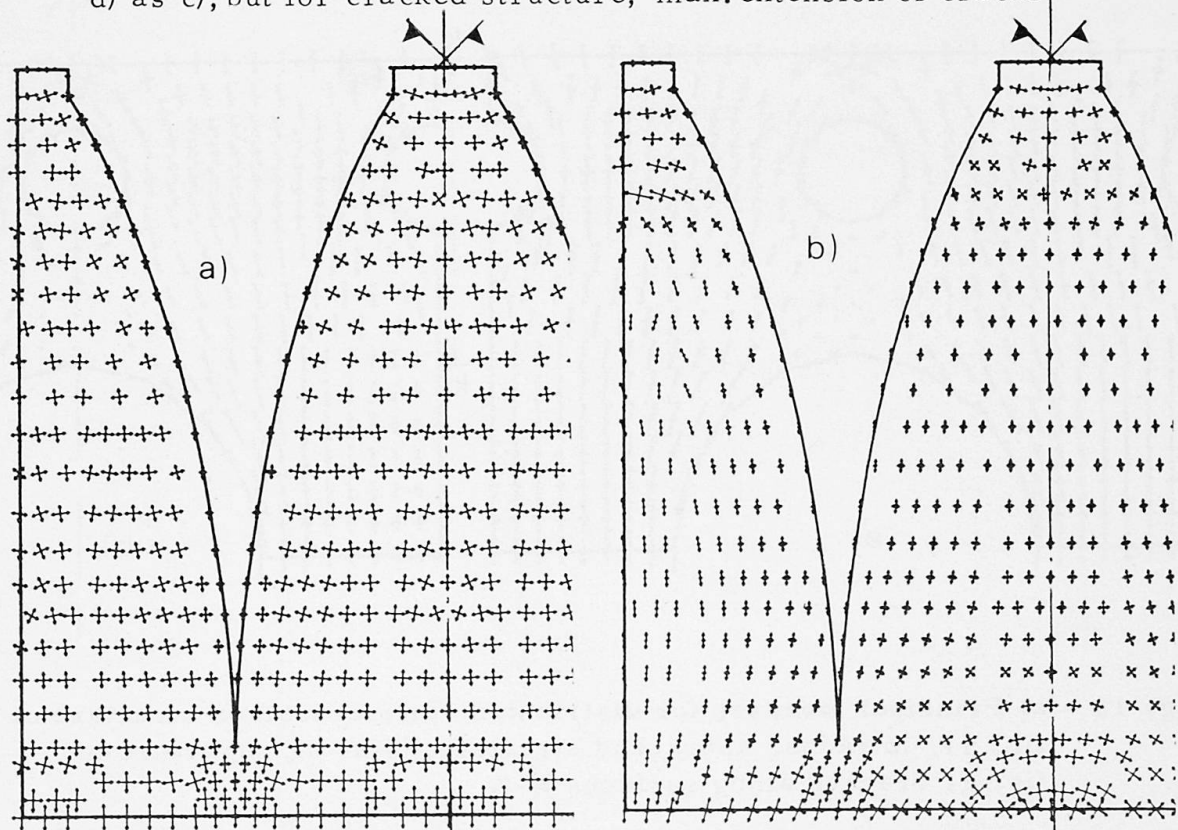


Fig. 10 - a) Thermal load at Jan., uncracked structure; principal stresses on extrados; b) as a), but for cracked structure, max. extension of cracks

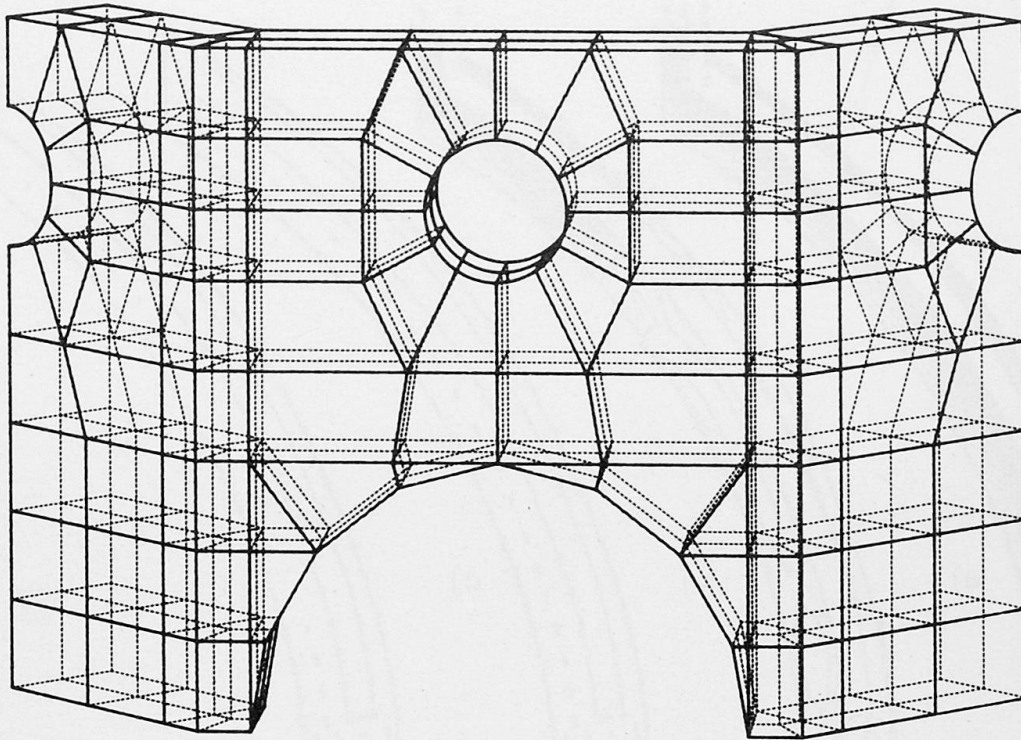


Fig. 11 - F.E. mesh of one-quarter of structure between first and third gallery

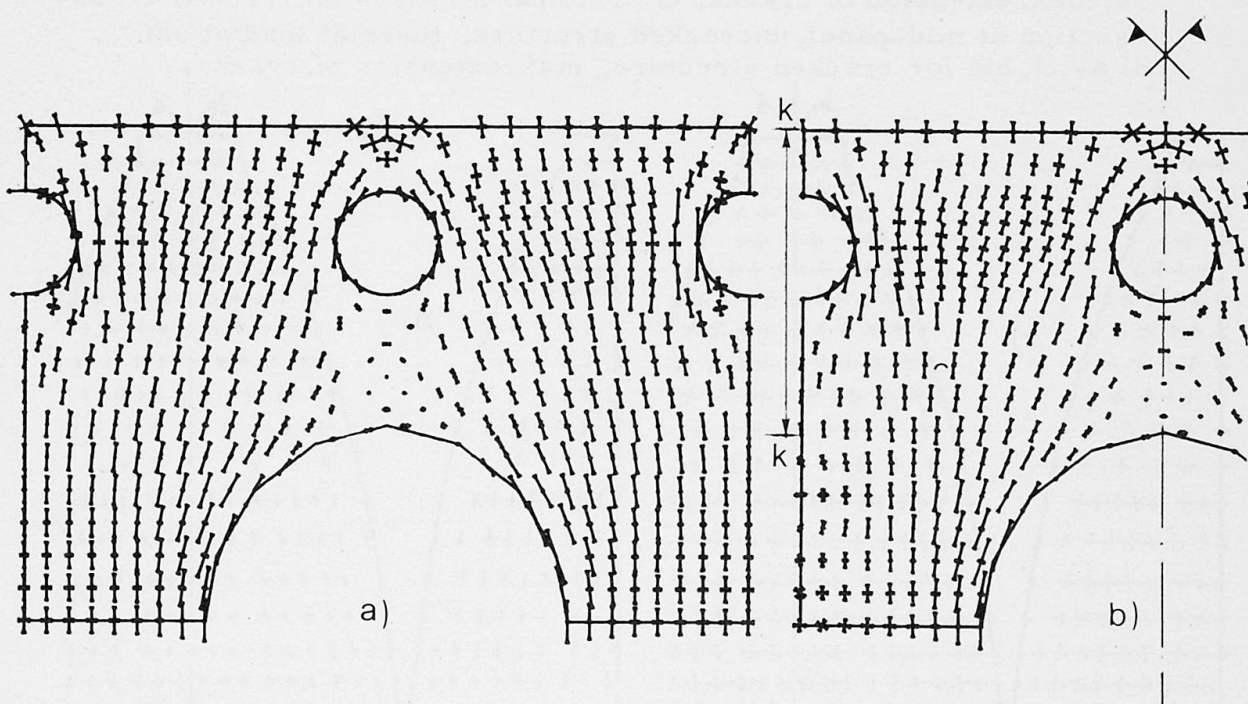


Fig. 12 - a) Principal stresses for distributed vertical load on structure of fig. 11, intrados, uncracked structure; b) as a), structure of fig. 11 cracked along surfaces K-K

## Non Conventional Finite Element Model for Strengthening of Masonry

Modèle à éléments finis pour le renforcement de murs en maçonnerie

Ein Finites-Element-Modell für die Verstärkung von Mauerwerk

### Gian Michele CALVI

Postgraduate Student  
University of Pavia  
Pavia, Italy



Author of a thesis dealing with the subject of the paper, with extensive numerical and experimental applications to masonry and reinforced masonry.

### Armando GOBETTI

Associate Professor  
University of Pavia  
Pavia, Italy



Author of several papers on finite element techniques, particularly in the plastic and non-linear field.

### Giorgio MACCHI

Professor  
University of Pavia  
Pavia, Italy



Formerly (1970-1973) Director of the Institute of Construction, Faculty of Architecture, Venice, then Dean of the Faculty of Engineering, University of Pavia, Chairman of Commission «Structural Analysis» of CEB. Author of several papers on non-linear analysis of structures as well as on masonry and reinforced masonry under seismic actions.

## SUMMARY

Damaged masonry walls and their reinforcement are studied using a plane stress finite element model specifically derived to simulate non-linear behaviour and anisotropy in an advanced state of cracking, as well as for modelling the addition of bonded or unbonded steel reinforcement.

## RESUME

Les murs en maçonnerie endommagés et leur renforcement sont étudiés au moyen d'un modèle à éléments finis en état plan de contraintes, établi pour simuler le comportement non-linéaire et l'anisotropie dans un état avancé de fissuration, ainsi que pour tenir compte de l'association avec des armatures d'acier, adhérents ou non-adhérents.

## ZUSAMMENFASSUNG

Das beschädigte Mauerwerk und seine Bewehrung werden mit Hilfe eines Modells aus finiten Elementen im ebenen Spannungszustand untersucht. Das Modell berücksichtigt nicht-lineares Verhalten, die Anisotropie im fortgeschrittenen gerissenen Zustand wie auch die Bewehrungseinlagen mit oder ohne Verbund.



## 1. INTRODUCTION

Conventional linear-elastic finite element techniques cannot adequately describe the behaviour (nor assess the safety) of damaged masonry walls, because the non-linearity and the anisotropy created by cracking and by the material deterioration play an essential role both in the distribution of action among walls, and in the state of stress within the walls. A plane stress model already developed by the Authors and simulating cracking has proved to be in good agreement with wall tests in axial and diagonal compression performed at the University of Pavia. |4|

The adopted approach, using bulk modulus and shear modulus (both variable in non linear field) seems to be convenient:

- load/displacement equations are decoupled;
- stress tensor and strain tensor invariants can be used;
- K and G have a clear physical meaning.

The aim of the present study is to check the validity of the approach in the case of coupled shear walls in an advanced state of cracking and deterioration, and to extend it to the assessment of strengthened masonry walls by improving the model with bonded or unbonded reinforcing steel bars.

## 2. THE MODEL UTILIZED IN SIMULATING MASONRY

### 2.1 General considerations

The model utilizes an eight node plane stress element. It is an isotropic model, but takes into account the anisotropy due to cracking, by changing with continuity its elastic properties. Cracking is considered as smeared over the entire element. The non-linear constitutive equations are written making use of the bulk modulus (K) and the shear modulus (G). |1| |2| |6|

### 2.2 Criteria for crack formation

Two different criteria have been considered for cracking. The first one is based on the attainment of tensile strength in the principal direction. The second one is based on the attainment of the tensile strength normal to the loading direction, due to the interaction between bricks and mortar (coaction criterion).

### 2.3 The bulk modulus K

The bulk modulus (K) assumes only two values:  $K_1$  before, and  $K_2$  after cracking. The second one is quite frequently less than zero: it means that the Poisson modulus is greater than 0.5. This happens because cracks are considered as a part of masonry, so that the volume of an element may grow under a mean compressive stress. |9|

### 2.4 The shear modulus G

The formulation used for G is already known for some geotechnical problems:

$$G = G_0 + \gamma_1 \sigma_m + \gamma_2 \sqrt{J_2}$$

in which  $\sigma_m$  is the third of the first invariant of the stress tensor and  $J_2$  is the second invariant of deviatoric stress tensor.

$G_0$ ,  $\gamma_1$ ,  $\gamma_2$  are constants to be determined by tests on a given type of masonry.

### 2.5 The input parameters

Nine input parameters are needed for the definition of the constitutive equations of the material:  $K_1$ ,  $K_2$ ,  $G_0$ ,  $\gamma_1$ ,  $\gamma_2$ ,  $\sigma_{cm}$ ,  $\sigma_{cb}$ ,  $C_1$ ,  $C_2$ .

$\sigma_{cm}$  is the cracking tensile stress of masonry

$\sigma_{cb}$  is the cracking tensile stress of a brick

$C_1$ ,  $C_2$  are constants (functions of the properties of bricks and of masonry) utilized in the coaction cracking criterion.

A more exhaustive description of the model can be found in |8|

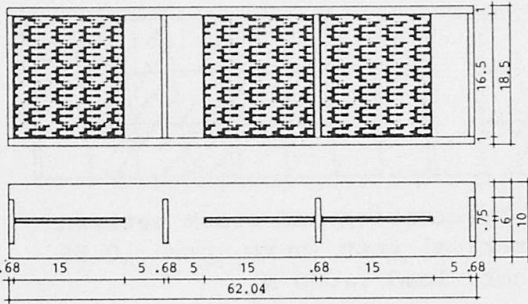


Fig.1 - Geometrical characteristics of Hendry's specimen (inches).

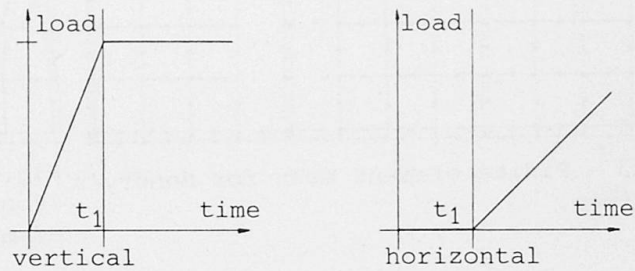


Fig.2 - Numerical loads laws

### 3. MODELLING OF THE ORIGINAL TESTS

#### 3.1 Characteristics of the experimental tests

The original experimental tests [3] were performed on coupled plain masonry walls confined by a thin reinforced concrete frame (Fig.1). The masonry structures were built by one-sixth-scale bricks and a ratio 1:4 cement and sand mortar. The horizontal load was increased under constant vertical precompression (Fig.2) in each test. Different tests had different vertical precompression.

#### 3.2 Problems in numerical simulation

In Fig.3 the very simple mesh used is shown. Not all the needed parameters were available from tests. The set was completed using values obtained from other experimental tests carried out on plain masonry. The constants used are:

$$\begin{aligned} K_1 &= 7000 \text{ N/mm}^2 \cong 1000000 \text{ psi} \\ K_2 &= -7000 \text{ N/mm}^2 \cong -1000000 \text{ psi} \\ G_0 &= 1400 \text{ N/mm}^2 \cong 200000 \text{ psi} \\ \gamma_1 &= 20000 \\ \gamma_2 &= 12000 \\ \sigma_{CM} &= 0.18 \text{ N/mm}^2 \cong 25 \text{ psi} \\ \sigma_{cb} &= 2.8 \text{ N/mm}^2 \cong 400 \text{ psi} \\ C_1 &= 1 \\ C_2 &= 0.4 \end{aligned}$$

The corresponding Young modulus in the elastic stage is about  $4000 \text{ N/mm}^2$  ( $562500 \text{ psi}$ ). It is important to underline that the most relevant parameters in these tests are  $G_0$ ,  $\gamma_1$ ,  $\gamma_2$  because change of shape is the governing phenomenon. The load history (Fig.2) allows the masonry characteristics change as a function of the vertical load before the application of the horizontal load. In particular, the shear modulus increases since the ratio between  $\gamma_2$  and  $\gamma_1$  is so that a monoaxial compression decreases the shear deformability of the material. Then, during the application of the horizontal load,  $G$  begins to decrease, as the tests show.

#### 3.3 Experimental and numerical results

In Fig.4 the shape of one simulated specimen at  $10700 \text{ N}$  ( $2500 \text{ lb}$ ) is shown and the elements in which at this step the principal tensile stress is greater than  $\sigma_{CM}$  are indicated with the direction of hypothetical cracks. The experimental test shows a very similar crack pattern. In Fig.5 it is possible to compare the experimental and the numerical force-displacement curves. The principal differences are:

- experimental curves seem to start with a sensible difference in shear modulus; this fact is not evident in numerical applications;
- for the highest precompression load two experimental curves are available: the numerical one follows one of them at low horizontal load; the other one at higher horizontal load; it seems nevertheless overestimate the stiffening effect of precompression.

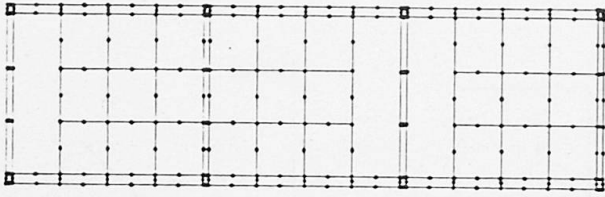


Fig. 3 - Finite element mesh for Hendry's specimen.

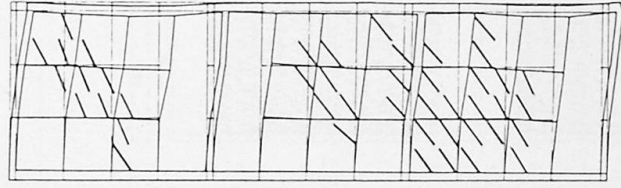
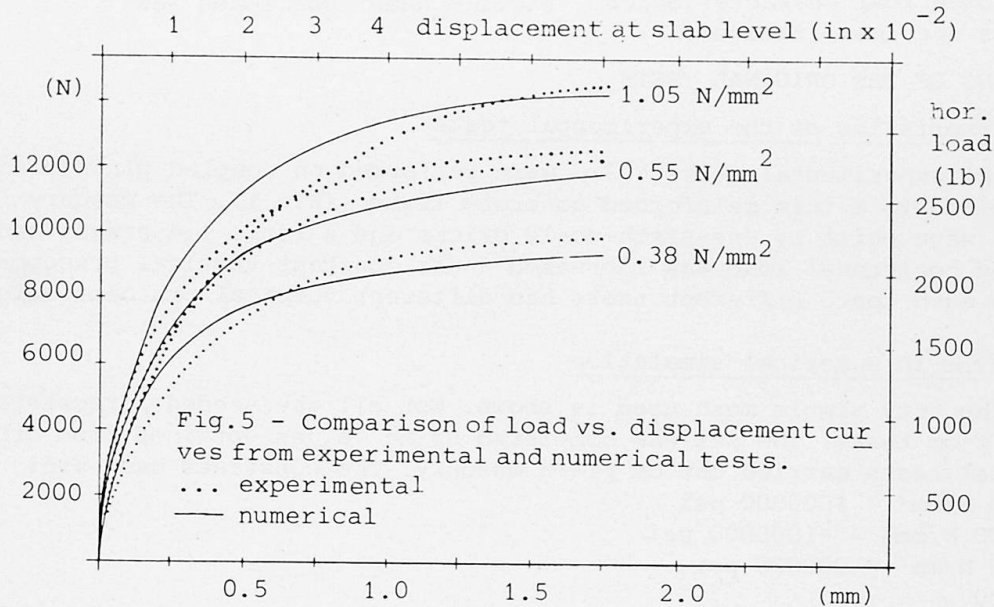


Fig. 4 - Deformation and crack pattern from numerical test (vert. prec.  $0.55 \text{ N/mm}^2$ , hor. load  $11000 \text{ N}$ ).



#### 4. MASONRY STRENGTHENED BY STEEL BARS

##### 4.1 Element used for reinforcing bars

The behaviour of reinforcing bars is simulated by truss elements having a bi-linear constitutive law. Two kinds of mesh are used: the first one has just one truss element for each reinforcing bar; in the second mesh each bar is simulated by several trusses connected to the wall in intermediate nodes (Fig. 6). From a physical point of view one may think to an external bar fixed at the ends to the masonry or to a reinforcement connected with continuity to the masonry by bond (concrete, shot-concrete, epoxy).

In both cases the reinforcement alone has no stiffness; in the second case each element works as a stiffening of the single connected plane stress element.

##### 4.2 Bond

Bond between bars and masonry is taken into account only in a global way, it means that the corresponding nodes are simply connected one to each other. The use of bond elements is not necessary for two reasons:

- the global behaviour is studied, and not the local stress situation between bars and masonry.
- masonry in tension is already taken into account in the formulation of the constitutive law.

The apparent increase of stiffness of bars due to the stress transmission to masonry is obtained by simply increasing their Young modulus. [12]

#### 4.3 Loads

As seen before, in the case of plain masonry confined by a R.C. frame, horizontal loads were applied at an edge of the upper slab.

In the case of not confined plain masonry this is not possible.

There are two kinds of problems. The first one does not depend on the model: even if a linear elastic model is used loads do not redistribute themselves in the same way as having a rigid slab above the walls, because it becomes of some importance the compressive or tensile deformation of the wall which the load is applied to. In that case it is better to apply the load to the truss connecting the walls. If the material constitutive equations are non-linear also this procedure is not suitable because the two elements directly connected to the truss immediately degrade.

The adopted solution is to distribute also the horizontal load to all the nodes at the upper edge of walls (Fig.7).

#### 4.4 Simulated meshes

In Fig.8, on the left hand, the different meshes simulated are shown. In order to check the validity of the new model, the structure of Fig.1 has been simplified by considering the masonry panels without the r.c. frame. The two walls are connected by a rigid truss. Two principal reinforcing systems are used: the vertical one should improve the flexural behaviour; the horizontal one, coupled to the vertical, should improve the shear behaviour. Each horizontal bar has a section of  $5 \text{ mm}^2$ , each vertical bar has a section of  $8 \text{ mm}^2$ ; the horizontal reinforcement is therefore 2 per mille of the masonry section, and the vertical one is 4.5 per mille.

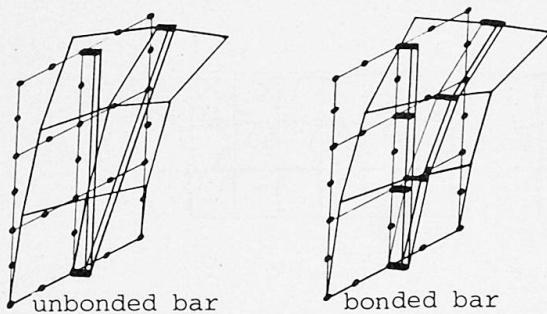


Fig.6 - Different behaviour for different simulation of bars.

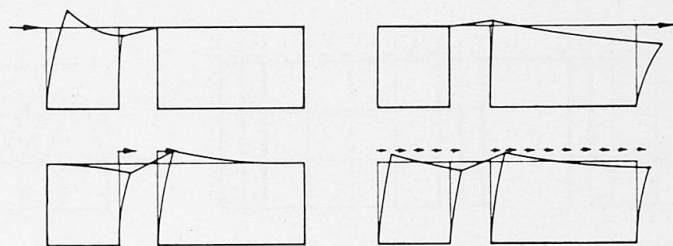


Fig.7 - Loads and deformation.

### 5. NUMERICAL RESULTS

#### 5.1 Deformation and crack pattern

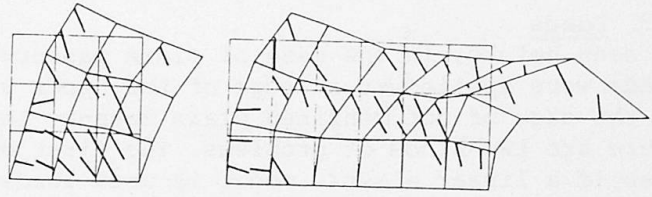
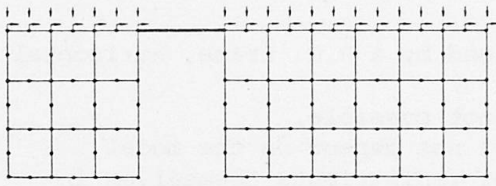
In figure 8, on the right hand, deformation and cracks of each specimen are drawn in front of the corresponding mesh. Plain masonry has both flexural and shear cracks; the deformed shape too shows that also the flexural behaviour is very important when the greatest part of tensile stress is not taken by a R.C. frame.

Cracks at the upper edge of the walls are due to the direct application of loads; the same reason justifies the large displacements at the same edge.

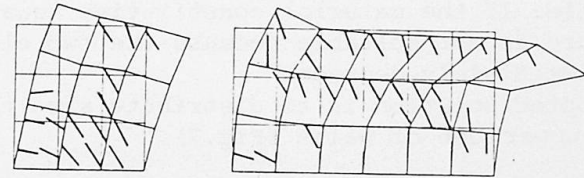
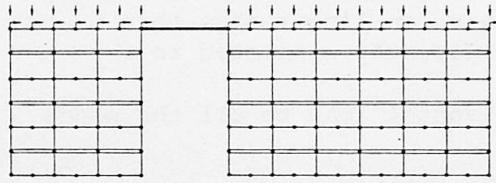
The element more interested by this behaviour is at the right upper corner, in fact it is the only one not confined for tensile stresses. When a horizontal reinforcement is added, the deformation is less; no significative difference is observed in the crack pattern. With vertical reinforcement only, the displacements become even smaller and flexural cracks disappear.

On the other hand, there is no sensible benefit for the shear cracks.

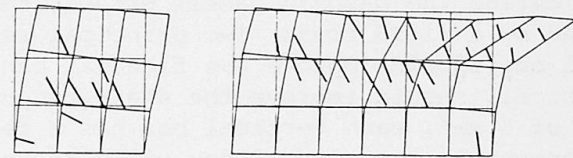
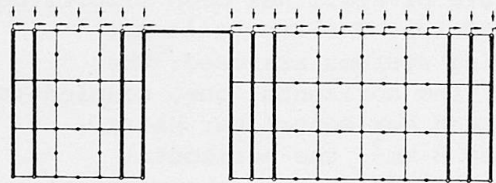
A considerable improvement is obtained, both in deformations and crack patterns, when the two kinds of reinforcement are put together. In this case also the shear cracks are much less significant.



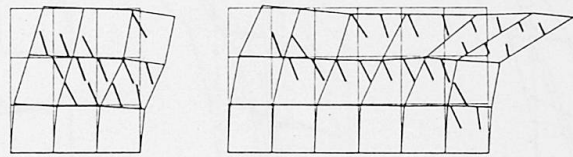
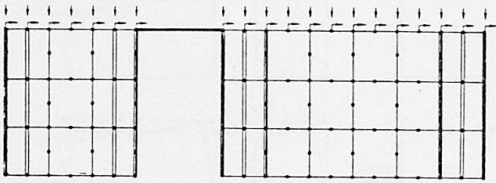
Plain masonry



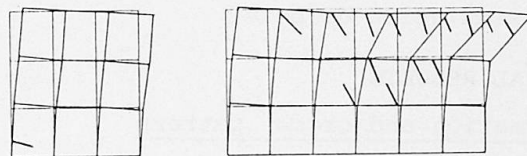
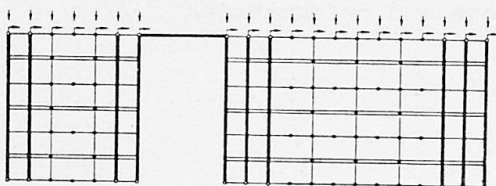
Horizontal bonded reinforcement



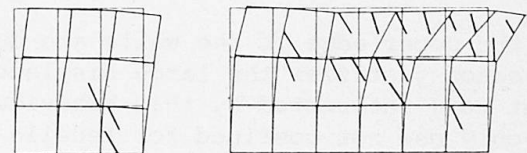
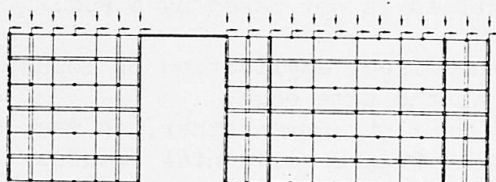
Vertical unbonded reinforcement



Vertical bonded reinforcement



Vertical unbonded horizontal bonded reinforcement



Vertical bonded horizontal bonded reinforcement

Fig.8 - Deformation and crack pattern for different kinds of reinforcement (horizontal load 8750 N).

### 5.2. Load-displacement curves

In Figure 9 the curves horizontal displacement vs. horizontal load for the different cases of reinforcement are plotted and compared.

The vertical load acting on walls is the same for all cases and has the intermediate value among the three values considered on the wall with R.C. frames.

The diagrams show the maximum horizontal displacement in each case (upper right node of the wider wall).

The following points need to be underlined:

- the sensible difference of displacements also at low load level is due to the immediate deterioration of the elements at the upper edge;
- bonded bars behave better than unbonded because they can locally delay the formation of cracks, but difference is not very large for the higher internal hypostaticity of the mesh;
- for the same reason, an increase of steel area does not affect sensibly the curves (none of the bars reached the yielding stress even when the masonry was strongly deteriorated);
- curves do not show the most important effects of reinforcement: improvement of out-of-plane strength, improvement of ductility and containment of cyclic deterioration. |4||7||10||11|

### 5.3. Loads redistribution

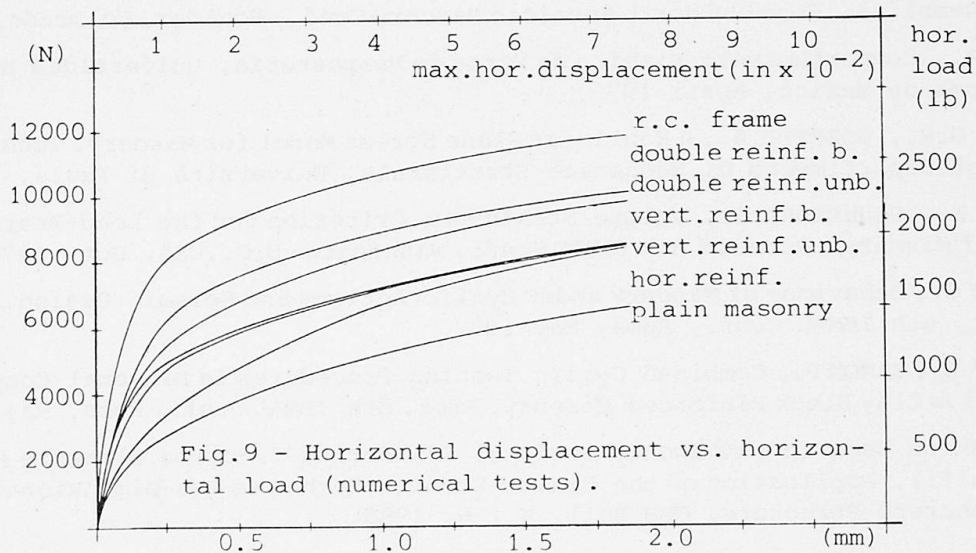
Fig.10 shows the effect of force internal redistribution in terms of the ratios between the force  $F_2$  taken by the second wall and the force  $F_1$  taken by the first wall, for different situations of applied loads and materials. It is important to underline the strong effect of a vertical precompression: the in-plane horizontal deformation due to Poisson effect causes a mutual action between the walls so that the  $F_2/F_1$  ratio is particularly affected by such phenomenon at low values of the horizontal load  $H$ .

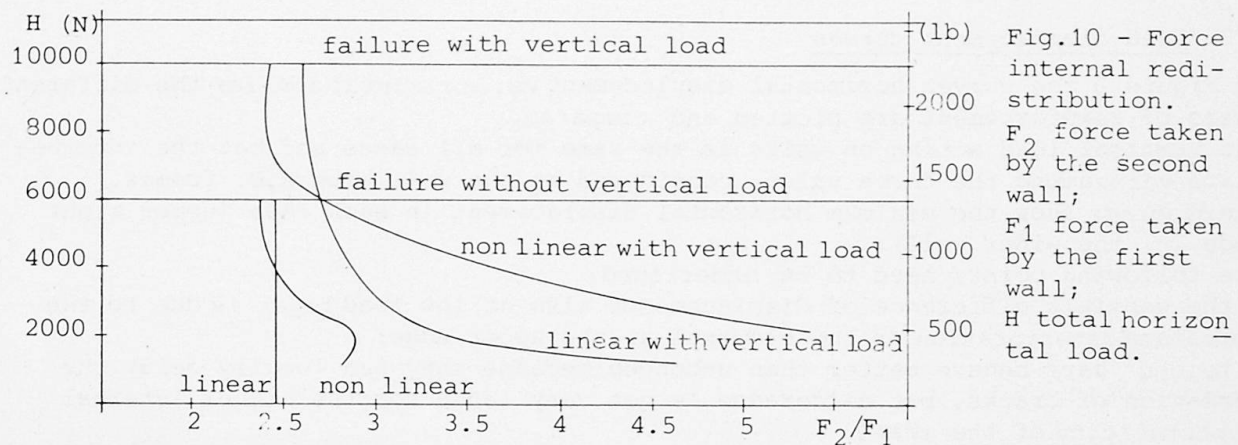
This happens also with a linear material, but may be amplified with the present model.

Curves referred to non-linear model show variations of the ratio  $F_2/F_1$  due to the different deterioration of the walls.

## 6. CONCLUSIONS

The proposed non linear plane stress model has proved to be suitable for the analysis of plain masonry shear walls, and of coupled shear walls confined by reinforced concrete frames. The effects of cracking and deterioration of plain masonry are satisfactorily described; nevertheless, the possible anisotropy of units is not yet taken into account. The redistribution of load among coupled shear walls is satisfactorily modelled.





The extension of the model to masonry strengthened by steel bars (both bonded and unbonded) has been performed in order to allow to study the effects of strengthening and its most suitable pattern. Vertical bars proved to be efficient in containing the horizontal cracking, but have a relatively small effect in containing shear deformation. Vertical and horizontal steel (even in very low percentage) sensibly improve the stiffness in the cracked stage and the strength. It has to be underlined that the model does not yet show the favourable effect of reinforcement in cyclic loading (improvement of ductility and containment of cyclic deterioration).

#### REFERENCES

1. CEB T.G. on Concrete under Multiaxial State of Stress (Eibl J. et alii), General Concepts of Constitutive Equations. CEB Bull. N.156, 1983.
2. GERSTLE R.H., Material Modelling of Reinforced Concrete. IABSE Coll. on Advanced Mechanics of Reinforced Concrete, Delft, June 1981.
3. SINHA B.P., HENDRY A.W., Racking Tests on Storey Height Shear-Walls Structures with Openings Subjected to Precompression. Proc.Int.Conf. on Masonry Structural Systems, Austin, Texas, May 1969.
4. CANTU' E., MACCHI G., Strength and Ductility Tests for the Design of Reinforced Brickwork Shear Walls. Proc. of 5th IBMAC Conf., Washington D.C., Oct.1979.
5. HILSDORF M.K., Investigation into the Failure Mechanism of Brick Masonry Loaded in Axial Compression. Proc. of Int.Conf. on Masonry Structural Systems, Austin, Texas, May 1969.
6. ARYA S.K., HEGEMEIER G.A., On Nonlinear Response Prediction of Concrete Masonry Assemblies. Proc. of North American Masonry Conf., Boulder, Colorado, Aug.1978.
7. MELI R., Comportamiento Sismico de Muros de Mamposteria, Universidad Nacional Autonoma de Mexico, April 1975.
8. CALVI G.M., GOBETTI A., A Nonlinear Plane Stress Model for Masonry. Technical Report of Dipartimento di Meccanica Strutturale, Università di Pavia, 1983.
9. MANNS W., SCHNEIDER H., Volume Strain as a Criterion for the Load-Bearing Capacity of Masonry. Proc. of 5th IBMAC Conf., Washington D.C., USA, Oct. 1979.
10. MACCHI G., Behaviour of Masonry under Cyclic Actions and Seismic Design. General Report, 6th IBMAC Conf., Roma, May 1982.
11. CANTU' E., ZANON P., Combined Cyclic Testing Procedures in Diagonal Compression on Hollow Clay Block Reinforced Masonry. Proc. 6th IBMAC Conf., Roma, May 1982.
12. CEB T.G. on Behaviour of Two-Dimensional Reinforced Concrete Elements (Mehlhorn G. et alii), Application of the Finite-Element-Method to Two-Dimensional Reinforced Concrete Structure. CEB Bull. N.156, 1983.

## Limit Load of Masonry Structures

Charge ultime de structures en maçonnerie

Die Traglast von Mauerwerk

### Matelda LO BIANCO

Research-worker  
Univ. of Palermo  
Palermo, Italy



M. Lo Bianco, born 1952, received her degree in Architecture at University of Palermo in 1975, and later began her activity as research-worker in the same Faculty. She published some papers about problems on optimum design and prestressed concrete.

### Cesare MAZZARELLA

Professor  
Univ. of Palermo  
Palermo, Italy



C. Mazzarella, born 1932, received his civil engineering degree at the University of Palermo. He published some papers on problems in Structural Engineering, such as optimum design, work-hardening adaptation and prestressed concrete.

### SUMMARY

The paper deals with the ultimate load of masonry structures conceived as discrete structures formed from rigid blocks and frictional joints. The problem is treated as one of limit analysis of a discrete rigid-plastic structure with non-associated flow rule. A numerical procedure is proposed which at first obtains a lower bound of the collapse factor and then, if necessary, calculates the true collapse factor by solving a non-linear program.

### RESUME

Le problème de la charge ultime pour les structures en maçonnerie est résolu à l'aide d'un modèle formé de blocs rigides et de joints avec frottement. Il s'agit d'un problème d'analyse limite pour une structure rigide-plastique. Une procédure numérique fournit une valeur inférieure du facteur de charge, et calcule le facteur ultime exact à l'aide d'un programme non linéaire.

### ZUSAMMENFASSUNG

Die Arbeit behandelt das Problem der Traglast von Mauerwerk. Das Mauerwerk wird als diskrete Struktur aus starren Blöcken und Fugen, welche als Reibungsflächen gedacht sind, aufgefasst. Der Grenzzustand wird mit Hilfe eines starr-plastischen Modells ohne zugeordnetes Fließgesetz erfasst. Das Berechnungsverfahren bestimmt einen unteren Grenzwert der Traglast. Wenn notwendig wird dieser mit Hilfe eines nichtlinearen Programmes optimiert.



## 1. INTRODUCTION

The collapse load of masonry structures is the oldest problem in the structural mechanics field (see [1] for an exhaustive bibliography) and the first paper on the masonry arch or dome, allowing for friction and cohesion is due to Coulomb [2]. More recently, Heymann [3-4] showed that the masonry's collapse load can be viewed as a limit analysis problem, and Livesley [5] provides a formal procedure for finding the collapse load of any structure formed by rigid blocks, with the block interfaces capable of carrying only compressive and shear stresses. Livesley's procedure maximizes the load factor  $\rho$  subjected to the linear equilibrium equations and the linearized constraints imposed by criteria of failure at block interfaces. Because the limit on the shear force is assumed to be that associated with Coulomb friction, the normality flow rule is not-satisfied and the obtained load factor is only an over-estimate of the true factor [6]. Consequentially it is necessary a post-optimality analysis to test the validity of the computed load factor.

The present paper studies the collapse load of masonry structures with the same Livesley basic assumption (*discrete rigid-plastic model with frictional interfaces*) in the general framework of limit analysis for material with non-associated flow rule [7]. For a such structure, the computation of the load collapse multiplier  $\rho$  implies the solution of a non linear, non convex mathematical program; instead it is relatively easy to construct [8] an upper bound  $\rho_u$  (or a lower bound  $\rho_l$ ) to  $\rho$ , solving, in both cases, a standard limit analysis problem of an auxiliary structure, which must have the same geometry of the original one but different constitutive equations, suitable chosen and with associated flow rule. You propose a numerical procedure formed by three steps: i) a lower bound  $\rho_l$  of the real collapse multiplier  $\rho_c$  is obtained solving a linear programming (LP); ii) a post-optimality analysis of LP solution checks if  $\rho_l$  is at the same time the real  $\rho_c$  ( $\rho_l = \rho_c$ ); iii) only if the above test fails the real multiplier is obtained solving a non-linear program.

For semplicity sake the paper deals only with plane masonry structures (as simple or multiple arches and walls) but all the results of this paper can be easily extended to spatial structures (as domes).

Matrix and vector quantities are denoted by underlined characters;  $\underline{0}$  denotes the null matrix or vector;  $\underline{A}$  or  $\underline{A}^t$  denote the transpose of  $\underline{A}$ , and superimposed dot ( $\dot{\cdot}$ ) denotes a time derivative.

## 2. THE MASONRY STRUCTURE AND THE IDEALIZED MODEL

Any (plane) masonry structure can be described as an assemblage of regular form stone blocks, with interposed mortar joints, which can carry only compressive and shear stresses. An useful approximation to the very complex behaviour of a such structure is obtained assuming the stone blocks as rigid and the joint's tickness as infinitesimal. The structural model is conceived as formed by rigid, discrete size, *nodes* ( $n$  in number) with interposed  $m$  *rigid-plastic sections* ( $m > n$ ), which have yield limits on the (generalized) *stress* vector  $\underline{\sigma} = [N \ T \ M]^t$ . The limit on the *shear*  $T$  is linearly dependent on the *normal force*  $N$  ( $N > 0$ ) with non-associated flow rule (NAFR). Because no-interaction is assumed between the shear  $T$  and the *bending moment*  $M$ , the yield domain in the  $(N, M)$  space is the usual interaction curve, suitably linearized (see Fig.1 related to a rectangular

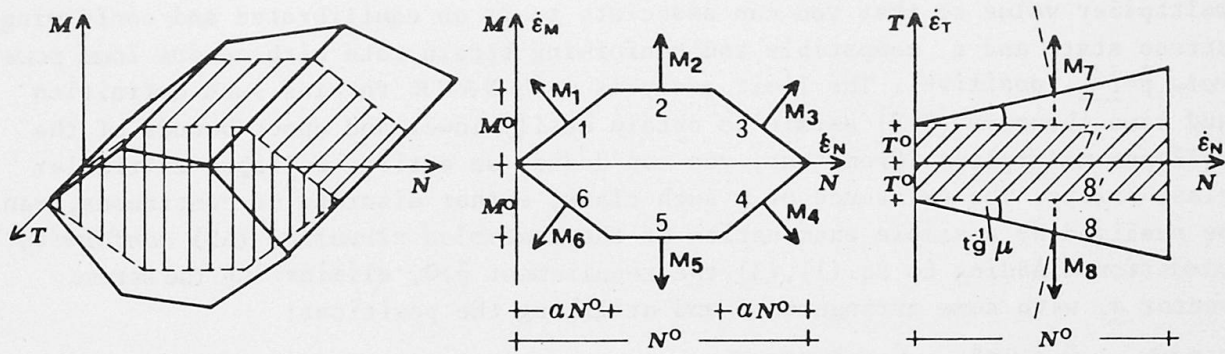


Fig.1 Elemental yield domains: axonometric and sections.

cross-section). The analytical description of this constitutive law (*elemental conformity* conditions [9]), can be given the following matricial form:

$$\begin{aligned} \underline{\varphi} = \underline{\dot{N}}^{\circ} \underline{\sigma} - \underline{k}^{\circ} \leq \underline{0}, \quad \underline{\Psi} = \underline{\dot{M}}^{\circ} \underline{\sigma} - \underline{k}^{\circ}, \\ \underline{\dot{\lambda}} \geq \underline{0}, \quad \underline{\tilde{\varphi}} \underline{\dot{\lambda}} = \underline{0}, \quad \underline{\dot{\varepsilon}} = \underline{M}^{\circ} \underline{\dot{\lambda}}, \end{aligned} \quad (1)$$

which usually refers to a single section or element, but can refer to the full element set by a suitable redefinition of the vectors and matrices as super vectors and block diagonal supermatrices. In Eq.(1)  $\underline{\varphi}, \underline{\Psi}, \underline{\dot{\lambda}}, \underline{k}^{\circ}$ , (with the same dimension) are, respectively, the (elemental) *yield function*, (*plastic*) *potential*, *multiplier rate* and (*plastic*) *resistance* vectors. Eq.(1c-d) define the flow rule: the *strain rate* vector  $\underline{\dot{\varepsilon}} = [\dot{\varepsilon}_N \ \dot{\varepsilon}_T \ \dot{\varepsilon}_M]^t$  dual in the v.w. sense of vector  $\underline{\sigma}$ , is a linear combination of the *yield modes*  $\underline{M}_i^{\circ}$  (i.e. of the plastic potential gradient), with non-negative coefficients  $\dot{\lambda}_i$ , which can be non zero only if the corresponding y.f.  $\varphi_i$  vanishes. Some remarks will be useful: i) Adding to Eq.(1b) the sign requirement  $\underline{\Psi} \leq \underline{0}$ , you can define the *reduced yield domain* with AFR, currently used to obtain a lower bound multiplier [8-9]; this definition requires a simple modify of the usual assumption:  $\underline{M}_j^{\circ}$  and  $\underline{k}_j^{\circ}$  must be interpreted as proportional to unitary external normal and to distance from the origin of the  $\Psi_j = 0$  plane. ii) The  $\underline{\varphi}$  vector can be split in two subvectors  $\underline{\varphi} = [\underline{\varphi}_a \ \underline{\varphi}_n]^t$ , where  $\underline{\varphi}_a$  collects the y.f. with AFR (1-6 in Fig.1) and  $\underline{\varphi}_n$  the y.f. with NAFR (7-8 in Fig.1); breaking in the same way the  $\underline{\Psi}$  vector, and observing that, as consequence of the assumed flow rule,  $\underline{\varphi}_a \equiv \underline{\Psi}_a$  (whereas  $\underline{\varphi}_n \neq \underline{\Psi}_n$ ), you obtain the following relations:

$$\underline{N}^{\circ} = \underline{M}^{\circ} + \underline{P}^{\circ}, \quad (\underline{N}^{\circ} = [\underline{N}_a^{\circ} \ \underline{N}_n^{\circ}], \underline{M}^{\circ} = [\underline{M}_a^{\circ} \ \underline{M}_n^{\circ}], \underline{P}^{\circ} = [0 \ \underline{P}_n^{\circ}]), \quad (2a-d)$$

where  $\underline{N}_a^{\circ} \equiv \underline{M}_a^{\circ}$  depends on the cross-section type and the assumed linearization and:

$$\underline{P}_n^{\circ} = \begin{bmatrix} -\mu & 0 & 0 \\ -\mu & 0 & 0 \end{bmatrix}^t. \quad (2e)$$

With a *redundant stresses* formulation [10], the *equilibrium* conditions for a one-parameter loading (with parameter  $\rho \geq 0$ ) and the *compatibility* condition are:

$$\underline{\sigma} = \underline{A}(\underline{f}^{\circ} + \underline{f}\rho) + \underline{B} \underline{x}, \quad \underline{\dot{u}} = \underline{A} \underline{\dot{\varepsilon}}, \quad \underline{\dot{\theta}} = \underline{B} \underline{\dot{\varepsilon}} = \underline{0}, \quad (3)$$

where the vector  $\underline{f}^{\circ}$  ( $\underline{f}$ ) collects the *nodal forces* equivalent to the fixed (variable) load system, and the vectors  $\underline{x}, \underline{\dot{u}}, \underline{\dot{\theta}}$  are respectively the *redundant stress*, the (nodal) *displacement rate* and the *distorsion rate* vectors. The *compatibility* matrices  $\underline{A}$  and  $\underline{B}$  depend only on the structure's layout and on the assumed redundant stresses.

### 3. THE COLLAPSE MULTIPLIER CLASS AND ITS BOUNDS

In the limit analysis with AFR, the collapse multiplier is the only load



multiplier value so that you can associate to it an equilibrated and conforming stress state and a compatible and conforming strain rate with *active load power rate*  $\dot{p} = \tilde{f} \dot{\underline{u}}$  positive. The limit analysis with NAFR retains such definition and same theorems [7-8] permit to obtain easily lower and upper bounds of the collapse multiplier. From that, you can deduce an entire collapse multiplier class exists. The existence of a such class, either discrete or continuous, can be realized by a simple examination of the *assembled structure (AS) conformity conditions*. Adding to Eq.(1),(3) the requirement  $\dot{p} > 0$ , eliminating the stress vector  $\underline{\sigma}$ , with some arrangements and utilizing the positions:

$$\begin{aligned} \underline{N} &= \underline{E} \underline{N}^\circ, & \tilde{\underline{n}} &= \tilde{\underline{f}} \underline{A} \underline{N}^\circ, & \tilde{\underline{k}}_{\underline{N}} &= \tilde{\underline{k}}^\circ - \tilde{\underline{f}}^\circ \underline{A} \underline{N}^\circ \\ \underline{M} &= \underline{B} \underline{M}^\circ, & \tilde{\underline{m}} &= \tilde{\underline{f}} \underline{A} \underline{M}^\circ, & \tilde{\underline{k}}_{\underline{M}} &= \tilde{\underline{k}}^\circ - \tilde{\underline{f}}^\circ \underline{A} \underline{M}^\circ \end{aligned} \tag{4}$$

you obtain the following AS conformity conditions:

$$\begin{aligned} \underline{\varphi} &= \tilde{\underline{N}} \underline{x} + \underline{n} \rho - \tilde{\underline{k}}_{\underline{N}} \leq 0 & \underline{\Psi} &= \tilde{\underline{M}} \underline{x} + \underline{m} \rho - \tilde{\underline{k}}_{\underline{M}} \\ \underline{\lambda} &\geq 0, & \underline{\varphi} \underline{\lambda} &= 0, & \underline{\theta} &= \tilde{\underline{M}} \underline{\lambda} = 0, & \dot{p} &= \tilde{\underline{m}} \underline{\lambda} = \omega > 0, \end{aligned} \tag{5}$$

where  $\underline{\varphi}(\underline{\Psi})$  can be called the AS yield function (plastic potential) vector, and  $\omega$  is a positive number.

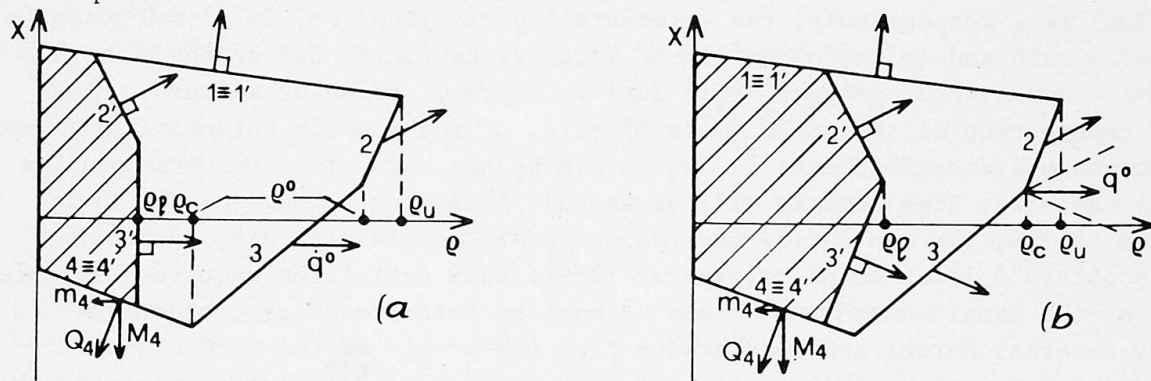


Fig.2 Assembled structure yield domains: two ideal cases.

In the  $\underline{y} = [\underline{x} \ \rho]^t$  space (the AS stress space), Eq.(5a) defines the AS rigid region, whose boundaries are the AS yield planes  $\underline{\varphi} = 0$ . Denoting with  $\underline{M}_j$  the  $j$ -th column of  $\underline{M}$  and with  $m_j$  the  $j$ -th scalar component of  $\underline{m}$ , you can say that an AS deformation mode vector  $\underline{Q}_j = [\tilde{\underline{M}}_j \ m_j]^t$  is associated to each plane  $\varphi_j = 0$ , and that the AS strain rate vector  $\underline{\dot{q}} = [\underline{\theta}^t \ \dot{p}]^t$  is obtained as linear combination of these deformation mode vectors (i.e. of the AS plastic potential gradient) with non negative coefficient  $\lambda_j$ , subjected to the complementary conditions (5d). The geometric interpretation of the AS conformity conditions (5) is formally similar to the usual for the elemental conformity conditions (1), but it is really most restrictive: it is easy to realize that the Eq.(5e-f) require only a value for  $\dot{q}$ , i.e.  $\underline{\dot{q}} = \underline{\dot{q}}^\circ = [\underline{\tilde{O}} \ \omega]^t$ , which is a vector orthogonal to the subspace  $\underline{x}$  and directed as the positive  $\rho$ -axis.

Therefore a collapse condition can be represented by those points  $\underline{y}^\circ$  of the AS rigid region boundaries to which you can associate, through the generalized flow law (5c-f), the AS strain rate vector  $\underline{\dot{q}}^\circ = [\underline{\tilde{O}} \ \omega]^t$ . For AFR structures,  $\underline{Q}_j$  coincides with the external normal to the  $\varphi_j$  plane, and the  $\underline{y}^\circ$  point set, either only a point or a continuous set, coincides with the boundaries point subset which have the greatest distance from the  $\underline{x} = 0$  plane. For NAFR structures the  $\underline{y}^\circ$  point set can be either discrete or continuous with a corresponding collapse multiplier  $\rho^\circ$

set either discrete or continuous. Fig.2 represents the AS rigid region of hypothetical structures with NA FR: in Fig.2a you have a continuous  $\underline{y}^\circ$  set and a continuous collapse multiplier  $\rho^\circ$  set, and in Fig.2b you have only a  $\underline{y}^\circ$  point and only a  $\rho^\circ$  collapse multiplier, but the point  $\underline{y}^\circ$  don't coincide with the boundaries point subset with the greatest distance from  $\underline{x}=\underline{0}$  plane. For the structural safety, the only interesting value of the  $\rho^\circ$  collapse multiplier set is the minimum value  $\rho_c$  which can be defined from the following *non linear program* (NLP):

$$\rho_c = \left\{ \min \rho \left| \begin{array}{l} \underline{\varphi} = \tilde{N} \underline{x} + \underline{n} \rho - \underline{k}_N \leq \underline{0}, \quad \underline{\dot{\lambda}} \geq \underline{0}, \quad \tilde{\varphi} \underline{\dot{\lambda}} = 0 \\ \underline{M} \underline{\dot{\lambda}} = \underline{0}, \quad \tilde{m} \underline{\dot{\lambda}} = \omega > 0, \quad \rho \geq 0 \end{array} \right. \right\}. \quad (6)$$

The NLP (6), often encountered in the structural engineering field [11-13] is a marginally non linear program (in the sense that it is a linear program at all but with the complementarity relations  $\tilde{\varphi} \underline{\dot{\lambda}} = 0$ , which makes NLP (6), strictly speaking a non convex non linear program) whose solution, theoretically and computationally speaking, is not easy.

On the contrary, it is relatively easy to construct [8] an upper bound  $\rho_u$  and a lower bound  $\rho_l$  to  $\rho_c$ , i.e.  $\rho_l \leq \rho_c \leq \rho_u$ . The upper bound  $\rho_u$  can be obtained as the collapse multiplier of an auxiliary structure which has the same geometry, load system and rigid region of the assigned one, but with AFR. The value of  $\rho_u$  can be obtained [5] solving the following LP:

$$\rho_u = \{ \max \rho \mid \underline{\varphi}_u = \tilde{N} \underline{x} + \underline{n} \rho - \underline{k}_N \leq \underline{0}, \quad \rho \geq 0 \}, \quad (7)$$

where  $\underline{\varphi}_u$  is defined in Eq.(5a), i.e.  $\underline{\varphi}_u = \underline{\varphi}$ .

The lower bound  $\rho_l$  can be obtained as the collapse multiplier of a second auxiliary structure which has the same geometry and load system of the assigned one, but a reduced yield domain with AFR. You can define [9] the elemental reduced yield domain as the envelope of the planes with external normal  $\underline{M}_j^\circ$  and passing through that points of the original polyedron face from which ortogonal projection on  $\underline{M}_j^\circ$  has the minimum value; in Fig.1 e 2 this reduced domain is depicted with dashed lines. The value of  $\rho_l$  can be obtained solving the following LP:

$$\rho_l = \{ \max \rho \mid \underline{\varphi}_l = \tilde{M} \underline{x} + \underline{m} \rho - \underline{k}_M \leq \underline{0}, \quad \rho \geq 0 \}, \quad (8)$$

where  $\underline{\varphi}_l$  is defined from Eq.(5b), i.e.  $\underline{\varphi}_l = \underline{\psi}$ . In both cases considered in Fig.2, we have depicted the points  $\rho_l$  and  $\rho_u$ .

#### 4. THE LOWER BOUND APPROACH AND THE NUMERICAL PROCEDURE

We propose a numerical procedure based on a lower bound approach, i.e. on the relation  $\rho_l \leq \rho_c$ , where  $\rho_l$  and  $\rho_c$  are obtained solving the LP (8) and the NLP (6), respectively. We call *lower bound solution* (l.b.s) the optimal solution of the LP (8), i.e. the value set  $\rho_l, \underline{x}_l, \underline{\dot{\lambda}}_l$ , which verifies the *optimality condition* [10] of the LP (8):

$$\begin{array}{l} \underline{\varphi}_l = \tilde{M} \underline{x}_l + \underline{m} \rho_l - \underline{k}_M \leq \underline{0}, \quad \underline{\dot{\lambda}}_l \geq \underline{0}, \quad \tilde{\varphi}_l \underline{\dot{\lambda}}_l = 0 \\ \underline{M} \underline{\dot{\lambda}}_l = \underline{0}, \quad \underline{m} \underline{\dot{\lambda}}_l = \omega > 0, \quad \rho_l \geq 0. \end{array} \quad (9)$$

We call *admissible collapse solution* (a.c.s.) a value set  $\rho^\circ, \underline{x}^\circ, \underline{\dot{\lambda}}^\circ$  which verifies

the constraint set of NLP (6) and the relation:

$$\rho_c \leq \rho^0. \quad (10)$$

The following theorems can now be given:

1-st Theorem. *If the lower bound solution is an admissible collapse solution, then the collapse multiplier and the lower bound multiplier values coincide (i.e.  $\rho_c = \rho_\ell$ )*

Proof. If the l.b.s.  $\rho_\ell, \underline{x}_\ell, \dot{\lambda}_\ell$ , is an a.c.s. then, by Eq.(10), you have  $\rho_c \leq \rho_\ell$ , whereas  $\rho_\ell \leq \rho_c$  by definition. The continuous inequality  $\rho_\ell \leq \rho_c \leq \rho_\ell$  implies  $\rho_c = \rho_\ell$ .

2-nd Theorem. *If the lower bound solution verifies the relation:*

$$\tilde{\sigma}_\ell P^\circ \dot{\lambda}_\ell = 0, \quad (\tilde{\sigma}_\ell = \tilde{A}(f^\circ + f \rho_\ell) + \tilde{B} \underline{x}_\ell), \quad (11)$$

then the l.b.s. is an admissible collapse solution, and, by th.1,  $\rho_c = \rho_\ell$ .

Proof. We must demonstrate that the l.b.s.  $\rho_\ell, \underline{x}_\ell, \dot{\lambda}_\ell$ , with the added condition (11) verifies the constraint set of NLP (6). This set differs from Eq.(9) only for the yield function (i.e.  $\varphi_\ell \neq \tilde{\varphi}$ ) and the complementary condition (i.e.  $\varphi_\ell \dot{\lambda}_\ell \neq \tilde{\varphi} \dot{\lambda}_\ell$ ), so it is necessary to demonstrate only that  $\varphi(\underline{x}_\ell, \rho_\ell) \leq 0$  and  $\tilde{\varphi}(\underline{x}_\ell, \rho_\ell) \dot{\lambda}_\ell = 0$ . In order to this, we observe:

i)  $\varphi_\ell(\underline{x}_\ell, \rho_\ell) \leq 0$  implies  $\varphi(\underline{x}_\ell, \rho_\ell) \leq 0$ , because the reduced yield domain  $\varphi_\ell \leq 0$  is not external to yield domain  $\varphi \leq 0$  by definition.

ii)  $\tilde{\varphi}_\ell(\underline{x}_\ell, \rho_\ell) \dot{\lambda}_\ell = 0$ , with the cond.(11), implies  $\tilde{\varphi}(\underline{x}_\ell, \rho_\ell) \dot{\lambda}_\ell = 0$ ; in the elemental stress space  $\underline{\sigma}$ , the c.c.(9c) can be written as  $(\tilde{M}^\circ \underline{\sigma}_\ell - \underline{k}^\circ)^t \dot{\lambda}_\ell = 0$ , and adding to it the cond.(11), you obtain  $(\tilde{M}^\circ + \tilde{P}^\circ) \underline{\sigma}_\ell - \underline{k}^\circ)^t \dot{\lambda}_\ell = 0$ , i.e.  $\tilde{\varphi}(\underline{x}_\ell, \rho_\ell) \dot{\lambda}_\ell = 0$  by position (2a).

Corollary. *If the lower bound solution implies a collapse mechanism without relative sliding rate at critical sections, i.e. with  $\dot{\epsilon}_{Tj} = 0$  ( $j=1,2,\dots,m$ ), then the l.b.s. is an admissible collapse solution, and, by th.1,  $\rho_c = \rho_\ell$ .*

Proof. It is easy to see, by position (2d), that  $\dot{\epsilon}_{Tj} = 0$  ( $j=1,2,\dots,m$ ) implies  $\tilde{\sigma}_\ell P^\circ \dot{\lambda}_\ell = 0$ , i.e. the l.b.s. is an a.c.s.

Adopting the lower bound approach, we propose a *numerical procedure* in three steps; the first, which requires a not-heavy computational effort, must be always executed, whereas the second and the third, which one requires a heavy computational effort, can be sometime omitted. The steps are: 1) Solve the LP(8), obtaining the l.b.s.  $\rho_\ell, \underline{x}_\ell, \dot{\lambda}_\ell$ ; if the obtained  $\rho_\ell$  is sufficient to ensure the structural safety, the procedure can be abandoned; 2) Test, using the previous corollary or Th.2, if the l.b.s. is an a.c.s.; in this case the procedure can be abandoned because  $\rho_c = \rho_\ell$ ; 3) Solve the NLP (6) to obtain the collapse solution and the collapse multiplier  $\rho_c$ .

The solution of the NLP (6) can be obtained adopting expressly conceived algorithms [11,12,14], of the branch and bound type, or transforming the NLP (6) in a mixed integer program (MIP) and solving it by commercial codes [15]. This transformation can be easily obtained replacing the complementarity cond. (6c) with an equivalent set of constraints on the yield function  $\varphi$ , the multiplier rate  $\dot{\lambda}$  and an auxiliary boolean vector  $\underline{z}$ . The MIP problem is:

$$\rho_c = \left\{ \min \rho \left\{ \begin{array}{l} \varphi = \tilde{N} x + n \rho - k_N \leq 0, \quad M \dot{\lambda} = 0, \quad \tilde{m} \dot{\lambda} = \omega > 0, \dot{\lambda} \geq 0, \\ \beta z - \varphi \leq 0, \quad \lambda + \beta z \leq \beta i, \quad z_i = (0, 1), \quad \rho \geq 0 \end{array} \right. \right\} \quad (12)$$

where  $i=(1\dots 1\dots 1)^t$  and  $\beta \gg 1$ , must be assigned to ensure always that  $-\beta < \varphi_i$  and  $\lambda_i < \beta$ . Beginning the numerical experiences, we chose to solve the NLP in the derived form MIP (12) for two reasons: i) the commercial code, with some arrangements, permit to execute automatically the necessary steps; ii) the codes available to solve the NLP (6) are not sufficiently tested even for moderately large problems. The solved problem are not so many to give a judgement about the validity of formulation (12), but we notice that the assignement of value to  $\beta$  seems to be a critical problem.

5. NUMERICAL EXAMPLE

As a simple application we consider (Fig.3) a two trapezoidal blocks (A,B), three critical section (a,b,c) plane model, with a one parameter loading system,  $f_{YA}^0 = f_{YB}^0 = -0.2 N_b^0$ ,  $f_{YA} = 0.1 N_b^0$ , where  $N_b^0$  is the yield limit to normal force  $N_b$  at sect. b, where we have assumed  $M_b = T_b = 0$ . The yield domain at sect. a and c is as in Fig.1, with yield limits  $N^0 = N_b^0 / \cos \gamma$  (where  $\gamma = 15^\circ$  is the section's inclination),  $M^0 = N^0 \ell / 8$ ,  $T^0 = 0.1 N^0$ ,  $\alpha = 0.35$  and friction angles  $\mu_a = 17^\circ$  and  $\mu_c = 13^\circ$ .

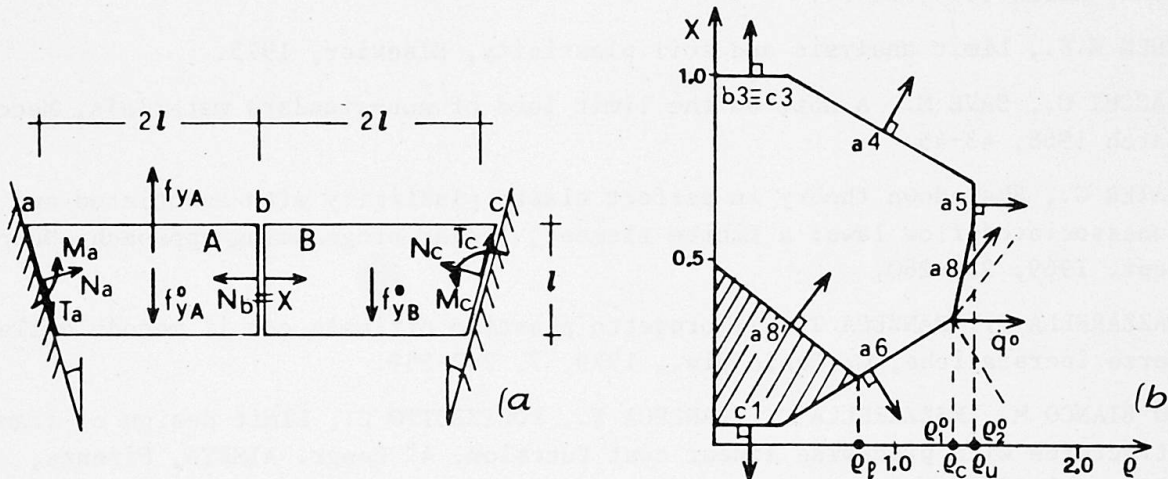


Fig.3 Structural model (a) and assembled structure yield domains (b).

We have depicted the yield domain (the reduced one with dashed lines) in the adimensional AS stress space  $\underline{y} = [x \ \rho]^t$ , where  $x = N_b / N_b^0$  is the redundant stress and  $\rho$  is the multiplier of the load  $f_{YA}^0$ . The yield planes indication meaning is: the letter denotes the section, and the following digit denotes the yield plane number in the elemental stress space (Fig.1). We remark: i) the yield plane (a5) points and the corner (a8)-(a6) point are admissible collapse solution, i.e. they are two subsets of the  $y^0$  set defined in Ch.3; ii) the collapse point, i.e. the NLP (6) optimal solution is the corner (a6)-(a8), with  $\rho_c = 1.356$ ,  $x_c = 0.385$ ; iii) the upper bound multiplier  $\rho_u = 1.415$  is, at the same time, an admissible collapse multiplier; iv) the lower bound solution is at the corner (a6)-(a8') with  $\rho_\ell = 0.773$ .



## ACKNOWLEDGEMENTS

This work has been sponsored by C.N.R. (Italian Research Council) and M.P.I. (Italian Educational Department). This support is gratefully acknowledged.

## REFERENCES

1. BENVENUTO E., La scienza delle costruzioni ed il suo sviluppo storico, Sansoni, 1981.
2. COULOMB M., Essai sur une application des règles de Maximis e Minimis à quelques Problèmes de Statique, relatifs à l'Architecture, Mem. Acad. Roy. Sc. Paris, 1776, (7), 343-382.
3. HEYMANN J., The stone skeleton, Int. J. Solids Struct., 1966, 2, 249-279.
4. HEYMANN J., On shell solution for masonry domes, Int. J. Solids Struct., 1967, 3, 227-241.
5. LIVESLEY R.K., Limit analysis of structures formed by rigid blocks, Int. J. Num. Meth. in Eng., 1978, 12, 1853-1871.
6. DRUCKER D.C., Coulomb friction, plasticity, and limit loads, J. Appl. Mech. ASME, March 1954, 71-74.
7. CHEN W.F., Limit analysis and soil plasticity, Elsevier, 1975.
8. SACCHI G., SAVE M., A note on the limit load of non-standard materials, Mecc., March 1968, 43-45.
9. MAIER G., Shakedown theory in perfect elasto plasticity with associated and nonassociated flow laws: a finite element, linear programming approach, Mecc., Sept. 1969, 250-260.
10. MAZZARELLA C., PANZECA T., Il progetto plastico ottimale con il metodo delle forze iperstatiche, G. Genio Civ., 1979, 7, 247-259.
11. LO BIANCO M., MAZZARELLA C., PANZECA T., POLIZZOTTO C., Limit design of frame structures with piecewise linear cost function, 4° Congr. AIMETA, Firenze, 1978, 313-323.
12. GIANNESI F., JURINA L., MAIER G., Optimal excavation profile for a pipeline freely resting on the sea floor, Eng. Struct., Jan. 1979, 81-91.
13. LO BIANCO M., MAZZARELLA C., Sul progetto ottimale agli stati limite delle strutture in c.a.p., Giornate AICAP, Ravenna, 1981, 27-63.
14. HALLMAN W.P., Complementary problem, Doct. Thesis, Wisconsin Un. Madison, 1979.
15. MPSX/370 with MIP/370 extension, IBM, 1975.

## Calculation of Damaged and Repaired or Strengthened Concrete Structures

Calcul de structures en béton endommagées et restaurées

Berechnung beschädigter und instandgesetzter Stahlbetonbauten

### Costas SYRMAKEZIS

Civil Eng.  
Techn. Univ. Athens  
Athens, Greece



C. Syrmakizis, born 1945. Civil Engineering and Doctoral Diplomas at the National Technical University of Athens, Greece. Lecturer in the Civil Engineering Department at the same University. National Representative for UNIDO project for Repair-Strengthening of Structures.

### Elpinicky VOYATZIS

Res. Fellow  
Natl. Techn. Univ.  
Athens, Greece



E. Voyatzis, born 1958, received her Civil Engineering Diploma at the National Technical University of Athens, Greece. She is Research Fellow at the Civil Engineering Department of the same University, working on research projects on repair and strengthening of structures.

### SUMMARY

This article presents an analytical method for an accurate calculation of the stiffness coefficients of a column, damaged or repaired and/or strengthened after damage. Analytical models are used for the description of the damaged region of the column. The jacket-column system is analysed using compatibility conditions for the deformations of the jacket and the column. Several practical conclusions and an example showing the influence of the damaged or repaired and strengthened member on the response of the overall structure, are given.

### RESUME

L'article présente une méthode analytique pour le calcul précis des coefficients de rigidité d'une colonne, endommagée ou restaurée/renforcée après l'endommagement, à l'aide d'un programme pour l'ordinateur. La description des régions endommagées de la colonne est réalisée à l'aide de modèles analytiques. Le système colonne-chemise est analysé à l'aide des conditions de compatibilité des déformations de la colonne et de la chemise. Quelques conclusions sont présentées et un exemple montre l'influence d'un élément endommagé ou restauré sur le comportement de la structure entière.

### ZUSAMMENFASSUNG

Der Beitrag gibt ein analytisches Verfahren für die genaue Berechnung des Steifigkeitskoeffizienten einer beschädigten oder instandgesetzten und verstärkten Stütze mit Hilfe eines Computerprogramms. Für die Beschreibung der beschädigten Stelle der Stütze werden analytische Modelle benutzt. Das System Ummantelung-Stütze wird mit Hilfe der Kompatibilitätsbedingung für die Verformungen des Mantels und der Stütze analysiert. Praktische Schlussfolgerungen und ein Beispiel zeigen den Einfluss des schadhafte und instandgesetzten Bauteiles auf das Verhalten der ganzen Konstruktion.



## 1. INTRODUCTION - PHILOSOPHY OF DESIGN OF DAMAGED AND REPAIRED-STRENGTHENED REINFORCED CONCRETE STRUCTURES.

One of the most important steps during a repair and/or strengthening procedure for a damaged reinforced concrete (R.C.) structure, is the estimation of the overall (residual) bearing capacity of the structure, regarding both the vertical and the horizontal actions, either immediately after damage, or after repair and/or strengthening. For such an estimation, and in order to take into account the real mode of behaviour of the structure, the calculation of the characteristics of the individual members is needed. In general, damaged building elements are suffering a certain decrease of their stiffness, while, repaired and/or strengthening building elements, may be subjected to a stiffness increase. Sometimes, members reestablished to their initial (before damage) stiffness level (e.g. epoxy injection in a crack) may still have a reduced stiffness due to very fine but extensive invisible cracks which are impossible to restore. Nevertheless, in most cases, a considerable redistribution of action effects, is expected in the structure.

Redistribution may be estimated for the whole structure by means of ordinary structural analysis methods, on condition that member characteristics are known. On the other hand, the calculation of the stiffness characteristics of the structural elements is important, due to modification of the dynamic characteristics (fundamental period etc.) of the structure, and thus of the level of a future dynamic loading (e.g. earthquake loads).

To take into account, during the analysis of a R.C. element, the effects of local defects and the deterioration such as cracks, loss of strength or loss of section, is in general a difficult task. In the present article the general principle of a new (modified) stiffness for the damaged region is considered. Such a stiffness modification for the damaged region of the element may appear either to the stiffness versus deflection, mainly for beams and columns (initial value  $EJ$ , new value  $(EJ)'$ ; variation  $\Delta(EJ)$ ,  $E$ =Modulus of Elasticity,  $J$ =moment of inertia), or to the stiffness versus axial shortening, mainly for columns (initial value  $EA$ , new value  $(EA)'$ ; variation  $\Delta(EA)$ ,  $A$ =section), or to the stiffness versus angular deformations, mainly for walls and columns (initial value  $GA$ , new value  $(GA)'$ ; variation  $\Delta(GA)$ ,  $G$ =shear modulus). The first of these three cases, is considered in this article.

Namely, the results of a research project, referring to the problem of modification of the stiffness of a reinforced concrete structure after damage or after repair and/or strengthening, undertaken by the authors in the National Technical University of Athens, are presented. For the accurate calculation of the new stiffness of these structures, an analytical method for the calculation of the equivalent stiffness of the individual structural elements is proposed, based on properly selected models. Although the method presented is general, attention is focused on the columns, which are usually the most sensitive parts of the structure. Columns are considered either damaged, or strengthened with the common method of jacketing. Slip between jacket and columns, is also taken into account. The analysis is performed using the transfer matrix method of linear structural analysis, adequately suitable for the case. The calculations for the problem are performed through a general computer program, especially written for the case, and including all analytical models for the damaged area as well as the interaction between jacket and damaged element in case of repair and/or strengthening. It is to be noted here that linear structural analysis, neglecting nonlinearity, leads to more or less approximate solutions. But it remains a very powerful tool for the designer, for the systematic analysis of structural problems. Especially for the case of slightly damaged members, with non serious inelastic damage, but also for complicated problems, as those described above, where due mainly to the great number of parameters involved-it is not still possible to formulate a general mathematical model of the problem taking into account all parameters of

nonlinearity and leading to numerical results, ready for a practical application.

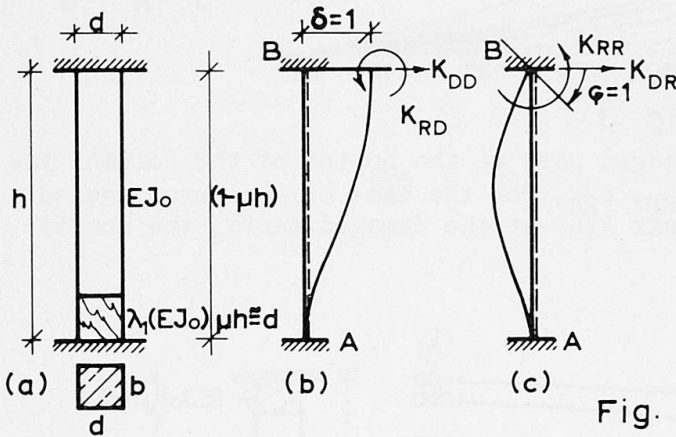
2. STIFFNESS MODIFICATION OF COLUMNS AFTER DAMAGE,

In order to calculate the new stiffness of a damaged column, the damaged and undamaged parts of the member are distinguished. The length of each part is expressed as a percentage  $\mu$  of the total height  $h$  of the column. For the undamaged parts, the geometrical characteristics remain obviously the same, as before damage. For the damaged parts, the modification of these characteristics must be estimated. The most important of them, the stiffness  $(EJ)$  is now a percentage  $\lambda$  of the initial stiffness  $(EJ)$ .

Considering an undamaged column AB of height  $h$ , section height  $d$ , section width  $b$  and stiffness  $EJ_0$ , let the well known stiffness coefficients be:

$K_{0DD}$ ,  $K_{0RD}$  for unitary displacement  $\delta=+1$  at the end B (top) and  $K_{0DR}$ ,  $K_{0RR}$  for unitary rotation  $\phi=+1$  at the end B, as shown on figure 1.

For a damaged column, the elements of the stiffness matrix  $[K]$  can be expressed as percentages  $\rho$  of the equivalent values of the elements of the stiffness matrix for the undamaged column. Using the transfer matrix method, which is adequately suitable for this case of various successive parts composing the whole column, the percentages  $\rho$  are expressed as functions of the parameters  $\lambda, \mu$  of the parts and the ratio  $h/d$ . These expressions have been formulated for the general case of  $n$  successive damaged or undamaged parts, in closed algebraic formulas. Using these formulas for the case of a column damaged only at the bottom A over a length  $\mu \times h$ , the three coefficients  $\rho$  are given on figure 2 as a function of the ratio  $h/d$ , for various values of the parameter  $\lambda$  of the damaged part. Even for  $\lambda=1$ , the coefficients  $\rho$  are different than 1, due to the influence of the shear forces' contribution.



$$\begin{bmatrix} Q \\ M \end{bmatrix} = [K] \begin{bmatrix} \delta \\ \phi \end{bmatrix} = \begin{bmatrix} K_{DD} & K_{DR} \\ K_{RD} & K_{RR} \end{bmatrix} \begin{bmatrix} \delta \\ \phi \end{bmatrix}$$

$$[K] = \begin{bmatrix} \rho_{DD} K_{0DD} & \rho_{DR} K_{0DR} \\ \rho_{RD} K_{0RD} & \rho_{RR} K_{0RR} \end{bmatrix}$$

$$K_{0DD} = \frac{12EJ_0}{h^3} \quad K_{0DR} = -\frac{6EJ_0}{h^2}$$

$$K_{0RD} = \frac{6EJ_0}{h^2} \quad K_{0RR} = -\frac{4EJ_0}{h}$$

$$J_0 = bd^3/12$$

Fig. 1

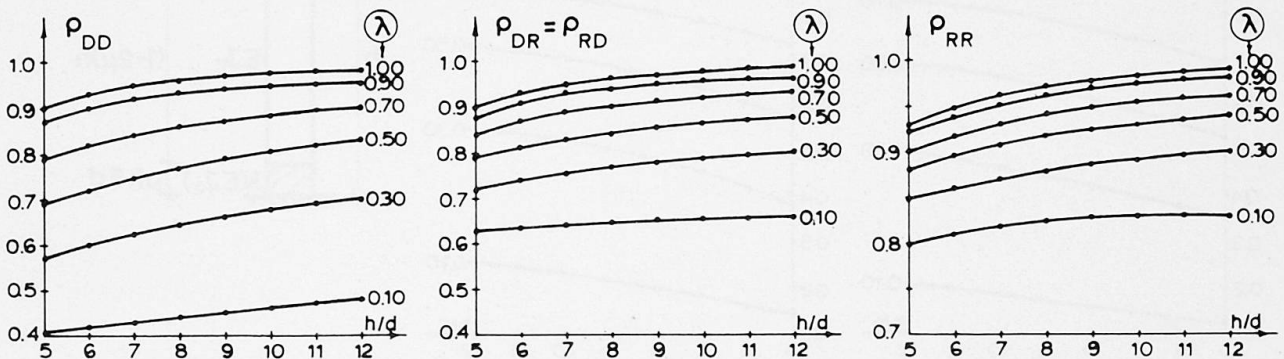


Fig. 2

The conclusion from these formulas and diagrams is that the values of the three coefficients  $\rho$  for each pair of values  $h/d$  and  $\lambda$  are significantly different and thus, it is not possible to assume a constant diminution of the stiffness of the

column, in order to take into account the diminuation  $\lambda$  of the damaged part.

The modification of the column stiffness has a direct influence on the stiffness of the overall structure. As an example the simple frame of the figure 3 is considered. The geometrical characteristics are given on the figure. The two columns BA and CD are damaged at the bottom, with the same stiffness diminuation  $\lambda$ . On fig.3, the variations of moments M, shear forces Q and fundamental period T, are given as a function of the parameter  $\lambda$  and as percentages of the corresponding values of the undamaged structure. Obviously, for  $\lambda=1$ , all diagrams are zero, while for  $\lambda=0$ , they reach the value of a similar frame with joints A and D absolutely free to rotation.

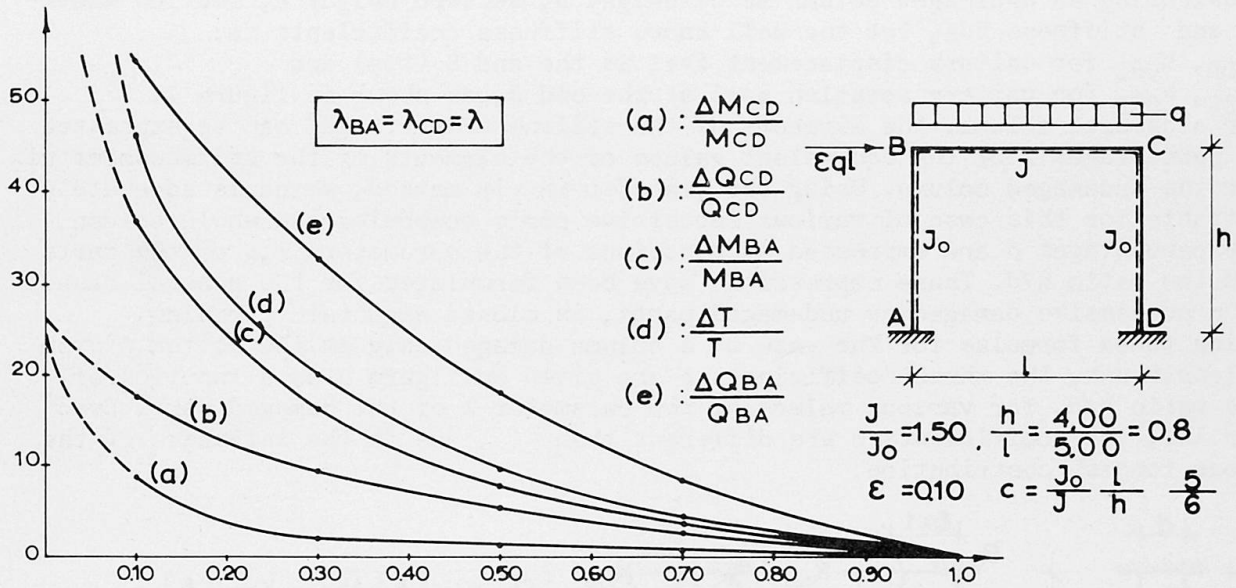


Fig. 3

While for the case considered of a damaged part at the bottom of the column, the coefficients  $\rho$  are three:  $\rho_{DD}, \rho_{DR} = \rho_{RD}, \rho_{RR}$ , for the case of a column damaged at both ends, with the same coefficients  $\lambda, \mu$ , at the damaged parts, the coefficients are two:  $\rho_{DD} = \rho_{DR} = \rho_{RD}, \rho_{RR}$ .

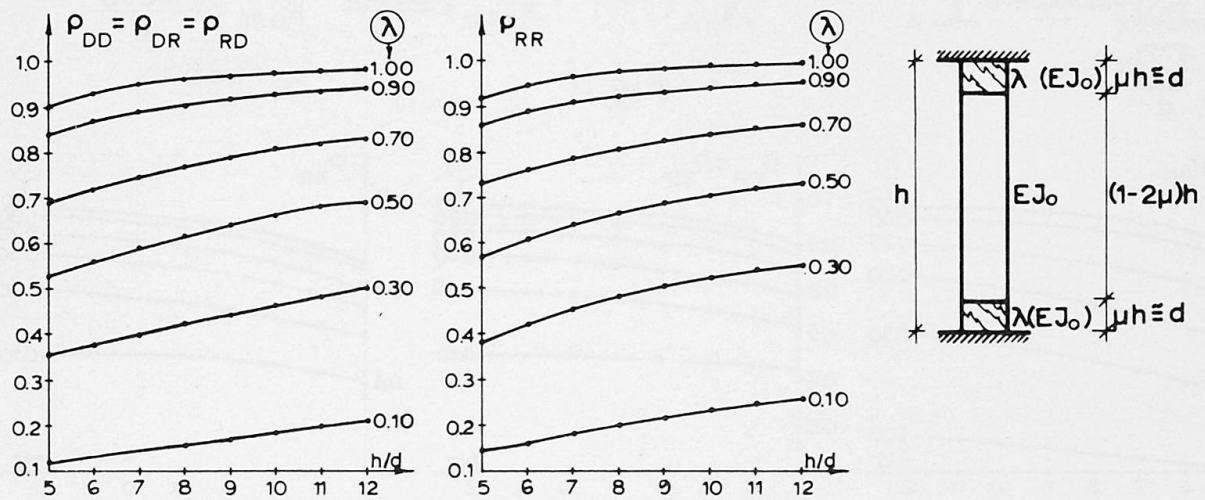


Fig. 4

On figure 4 the variation of the coefficients  $\rho$  as a function of the parameters  $h/d$  and  $\lambda$  for this last case are presented.

When the value of the parameter  $\lambda$  is known, the coefficients  $\rho$  can be calculated

through the aforementioned formulas. But practically, the problem is the estimation of this diminution  $\lambda$  of the stiffness of the damaged part(s). For this estimation an analytical model should be used,

3. ANALYTICAL MODELS FOR THE DAMAGED AREA,

The damage types are classified for various damage levels in groups and four models, one for each group, are used.

The first model describes the case of an horizontal crack of about 1mm width (fig. 5a). This type of damage is mainly due to local defects rather than to insufficient reinforcement. For that case, we assume a damaged length equal to 2 to 3 times of the crack opening on which the steel bars are operating as individual bars built-in the concrete. On condition of sufficient reinforcement, the column in that case reacts as about the undamaged column. As an example. the variation of the three coefficients  $\rho$  of the column are given on figure 6a, as a function of the ratio  $h/d$ . This example has been elaborated for a height of the damaged area  $0,002h$ ,  $\lambda=0,0005$  ( $\lambda$ =moment of inertia of steel bars versus moment of inertia of the whole column section),  $d/\delta=25$  ( $\delta$ =steel bar diameter),  $d'=0,90d$ , and steel to concrete ratio of moduli of elasticity  $n$  equal to 7.

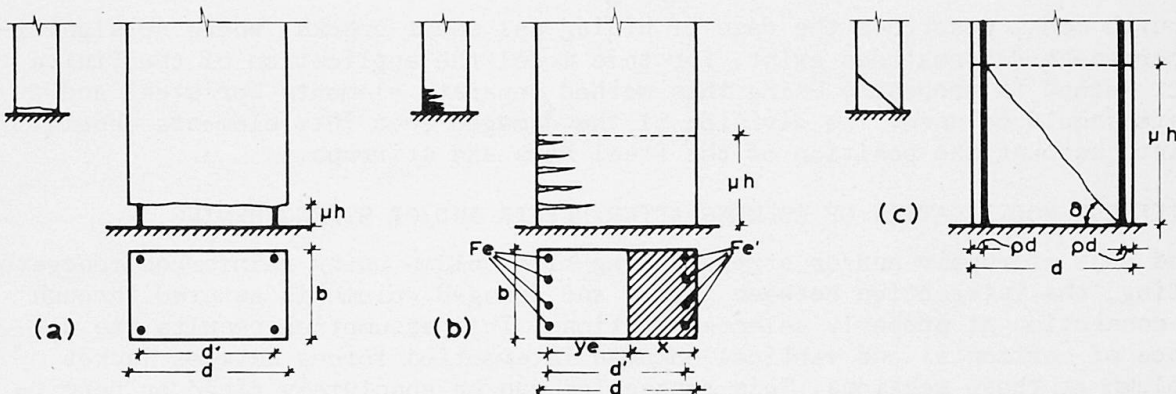


Fig. 5

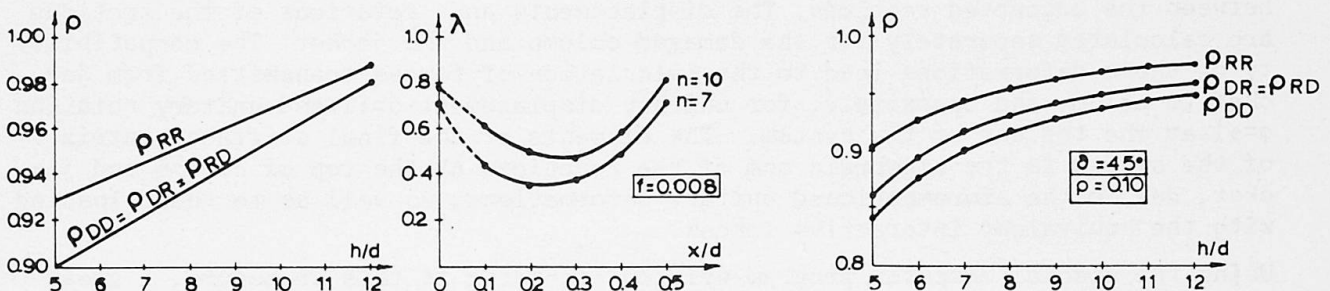


Fig. 6

The second model (fig. 5b), describes the case of frequent and large flexural cracks. For that case, the modification  $\lambda$  of the moment of inertia is calculated as a function of the height  $x$  of the compressive zone of concrete, taking into account all the steel bars. As an example, on figure 6b, the variation of  $\lambda$  is given as a function of the ratio  $x/d$ , for the case of minimum reinforcement  $f=0.008$  and two values of  $n=7$  and  $10$ . Further, for the calculation of the coefficients  $\rho$ , the diagrams of figure 2 can be used,

The third model (fig. 5c), describes the case of a diagonal shear crack of a width about 0,5mm, without permanent deformations. On the same figure the characteristics of the analytical model used are shown. On figure 6c the variation of the three coefficients  $\rho$  as a function of the ratio  $h/d$  are given for a column with a shear crack of the type considered at the bottom, without any other cracks,



The comparison of these figures with figures 2, shows that this case corresponds to a general diminution of the stiffness of the damaged area, equal about to  $\lambda=0,85$ . For this model, all coefficients  $\rho$  are the same for both diagonals of the damaged area. Nevertheless, it is possible that besides the main shear crack, other minor cracks in the damaged area, diminish the stiffness of the concrete. On figure 7, the values of the three coefficients  $\rho$  are given for various values  $\lambda$  of the diminution of the stiffness around the main crack.

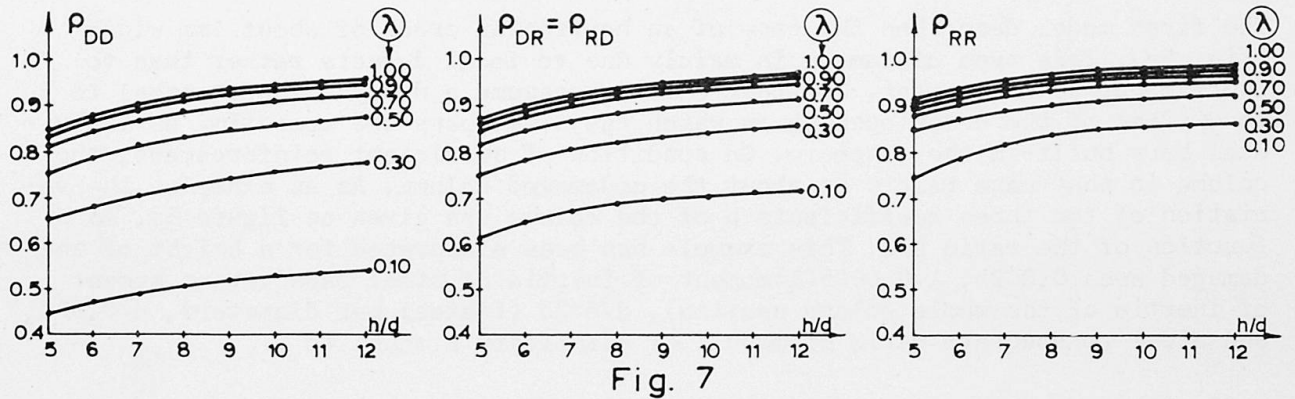


Fig. 7

The fourth model describes the case of bidiagonal shear cracks, where no significant permanent deformations exist. For this model the application of the Finite Element Method is proposed. Using this method separate elements for steel and concrete should be used. The division of the damaged area into elements should take into account the position of the steel bars and stirrups.

#### 4. STIFFNESS MODIFICATION OF COLUMNS AFTER REPAIR AND/OR STRENGTHENING.

For the case of repair and/or strengthening of a column using reinforced concrete jacketing, the interaction between jacket and damaged column is assured through their connection at properly selected sections. This assumption results the appearance of horizontal and vertical unknown interaction forces between jacket and column at these sections. This connection can be absolutely rigid or permitting relative vertical slip, which is expressed as a difference in rotation angle between the connected sections. The displacements and rotations of the sections are calculated separately for the damaged column and the jacket. The compatibility of these deformations lead to the calculation of forces transmitted from jacket to column and oppositely, for unitary displacement  $\delta=+1$  and unitary rotation  $\varphi=+1$  at the top end of the system. The elements of the final stiffness matrix of the system is the algebraic sum of the reactions at the top of column and jacket, due to the aforementioned unitary deformations, as well as to their loading with the equivalent interactive forces.

Using the special computer program written according to this procedure, a great number of cases have been investigated. It is to be noted here that for a jacket-strengthened column the value  $\lambda$  for the damaged column does not play an important role as the jacket mainly contributes to the final stiffness. So, while the differences between the various damage levels described through the equivalent models presented in the last paragraph are important for a damaged column, for the case of a jacket-strengthened column are of minor importance.

On figure 8, the variation of the first of the three coefficients  $\rho$  of the stiffness matrix is given indicatively as a function of the ratio  $h/d$  of the column, for various values of the ratios  $d/b$  of the dimensions of the column section and  $h/t$ , where  $t$  is the thickness of the jacket. Similar diagrams can be given for the other two coefficients  $\rho$ .

Generally speaking, the values of the coefficients  $\rho$  are fragmented upwards to the equivalent value of a full section with dimensions the external dimensions of the jacket (this value is higher than the value calculated with fully rigid

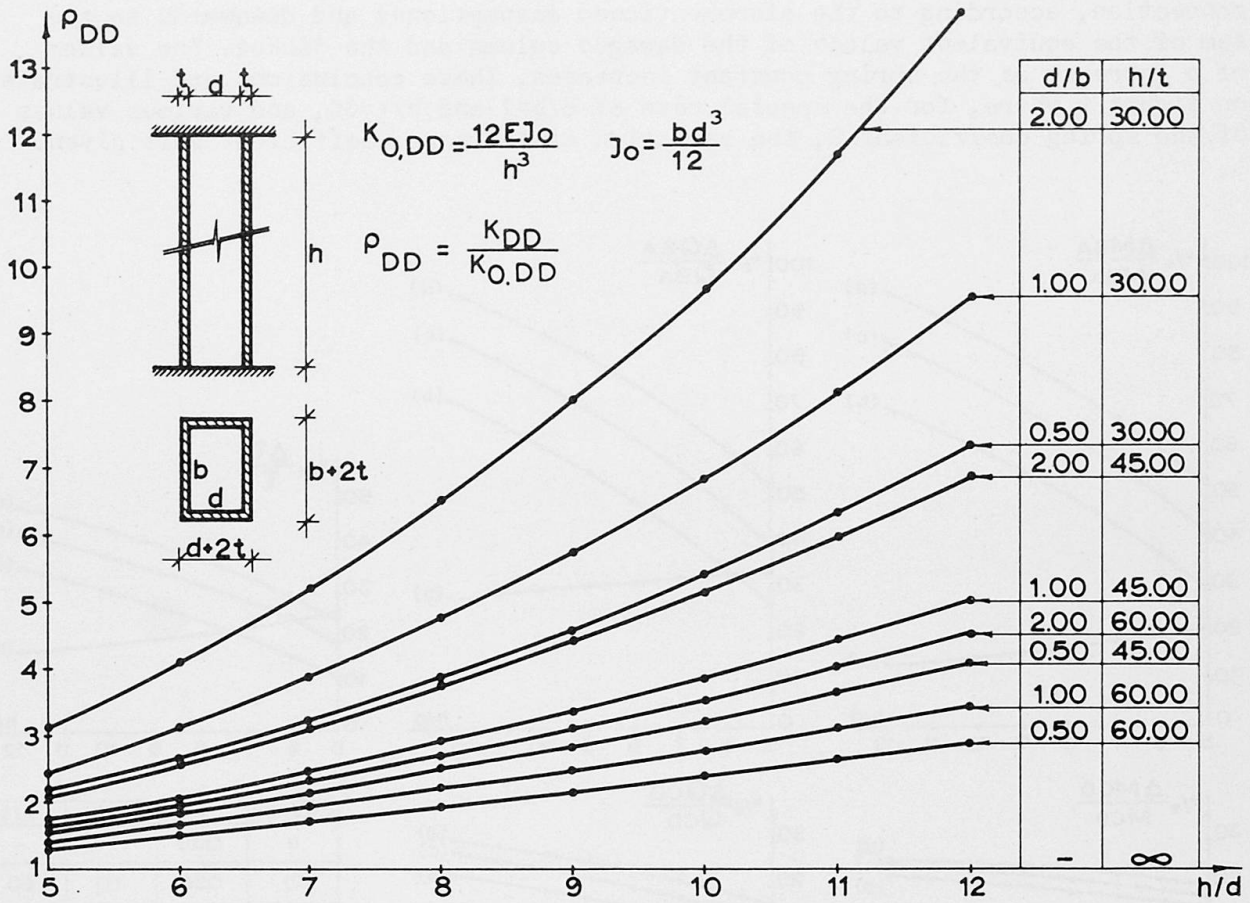


Fig. 8

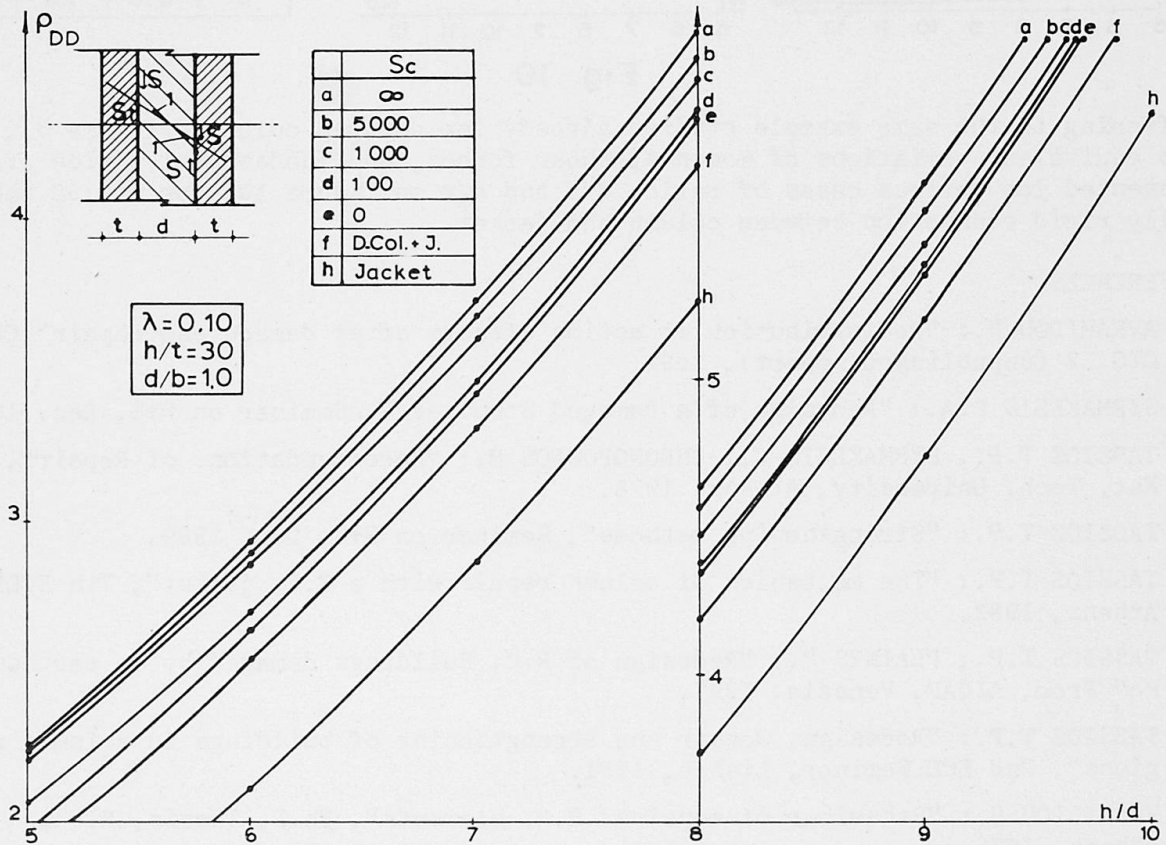


Fig. 9

connection, according to the aforementioned assumptions) and downwards to the sum of the equivalent values of the damaged column and the jacket. The values of  $\rho$  increase as the spring constant increases. These conclusions are illustrated on figure 9 where, for the special case of  $d/b=1$  and  $h/t=30$ , and various values of the spring coefficient  $S$ , the variation of the same coefficient  $\rho$  is given.

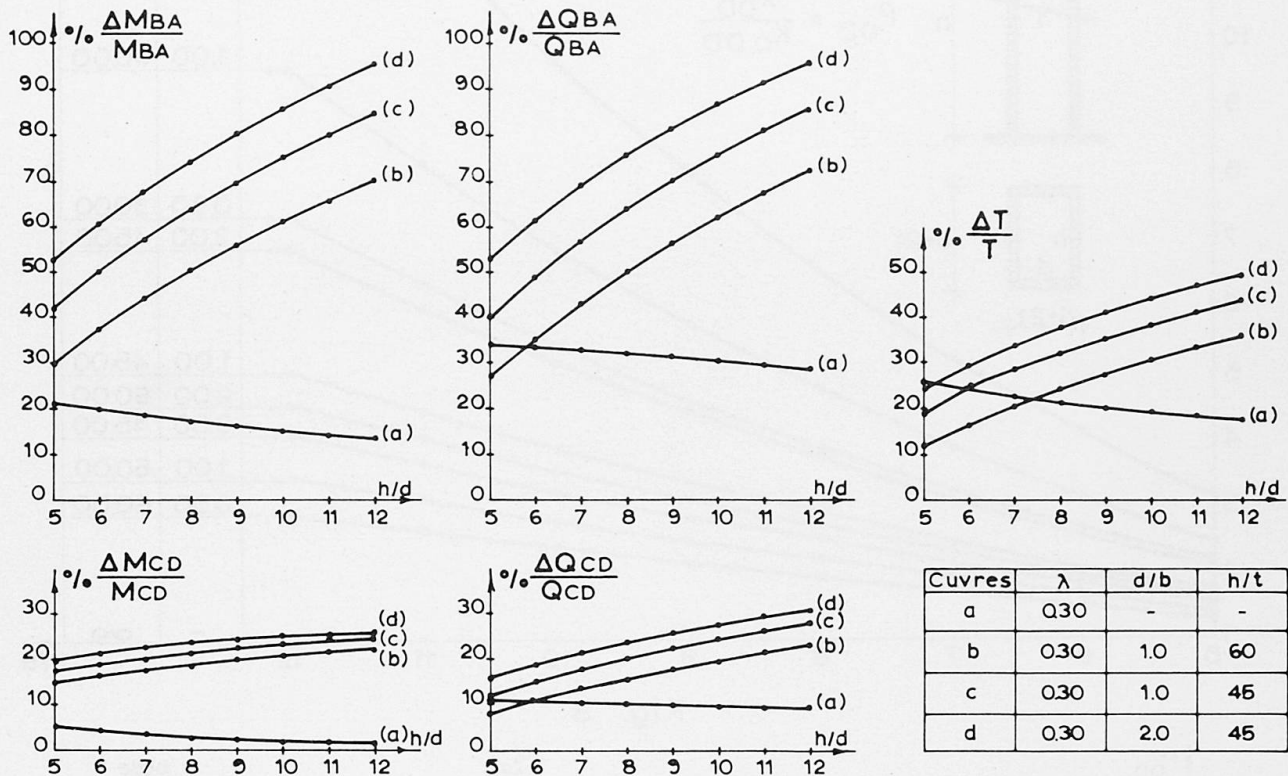


Fig. 10

Referring to the same example studied already for damaged columns (figure 3), the equivalent variations of moments, shear forces, and fundamental period are presented for various cases of ratios  $d/b$  and  $h/t$  on figure 10, for  $\lambda=0,30$  and fully rigid connection between column and jacket.

#### REFERENCES

1. AVRAMIDOU N.: "Redistribution of action effects after damage and repair", CEB/GTG 12 (unpublished report), 1982.
2. SYRMAKEZIS C.A.: "Redesign of a Damaged Structure", Seminar on R+S, Dec. 1980.
3. TASSIOS T.P., SYRMAKEZIS C., CHRONOPOULOS M.: "Recommendations of Repair", Nat. Tech. University, Athens, 1978.
4. TASSIOS T.P.: "Strengthening methods", Seminar on R+S, Dec. 1980.
5. TASSIOS T.P.: "The mechanics of column repair with a R.C. jacket", 7th ECEE Athens, 1982.
6. TASSIOS T.P., PLAINIS P.: "Redesign of R.C. Buildings damaged by an earthquake" Proc. AICAP, Venezia, 1977.
7. TASSIOS T.P.: "Redesign, Repair and Strengthening of buildings in seismic regions", 2nd ECE Seminar, Lisbon, 1981.
8. VASSILIOU G.: "Behaviour of repaired R.C. elements", Ph.D. Thesis, NTU of Athens, 1975.

## Reinforced Concrete Members with Subsequently Bonded Steel Sheets

Eléments en béton armé renforcés ultérieurement par collage d'armature

Stahlbetonbauteile mit nachträglich aufgeklebter Bewehrung

### Marc LADNER

Dr. sc.techn.  
EMPA  
Dübendorf, Switzerland



Born in 1939, Marc Ladner received his diploma as a civil engineer in 1962 and his Dr. sc.techn. degree in 1968 from the Swiss Federal Institute of Technology (ETH) in Zürich. Since 1970, he is working at the Swiss Federal Laboratories for Materials Testing and Research where he is the head of the reinforced concrete structure department.

### SUMMARY

The paper deals with the design of reinforced concrete members, strengthened by subsequently bonded steel sheets. The amount of additional reinforcement is limited for several reasons which are discussed. Moreover, two methods for determining the stress distribution between concrete and external reinforcing steel are summarized, from which practical design rules are drawn.

### RESUME

L'exposé traite du dimensionnement d'éléments en béton armé dont le renforcement ultérieur fait appel à la méthode d'armature collée. Les considérants portent tout d'abord sur la détermination du taux d'armature extérieure pouvant être appliqué à titre de renforcement sur une section existante de béton armé. Il est ensuite fait état de deux procédés pour le calcul des contraintes entre l'acier et le béton. Des conclusions sont tirées pour la pratique.

### ZUSAMMENFASSUNG

Der vorliegende Artikel befasst sich mit der Bemessung von Stahlbetonbauteilen mit nachträglich aufgeklebter Bewehrung. Dabei wird zunächst auf die Ermittlung der Grösse des Bewehrungsanteiles eingegangen, der als äussere Bewehrung auf einen bestehenden Stahlbetonquerschnitt aufgebracht werden kann. Sodann werden kurz zwei Verfahren zur Berechnung der Spannungen zwischen Stahl und Beton gestreift und daraus Folgerungen für die Bemessungspraxis gezogen.



## 1. ASSESSMENT OF THE QUANTITY OF EXTERNALLY BONDED STEEL

### 1.1 Brittleness of Cross Section

In order to avoid a brittle failure of a strengthened reinforced concrete member with externally bonded steel sheets, the total area of reinforcement (Fig. 1) should not exceed an upper limit of

$$\rho_{\text{tot,max}} = \frac{A_{s,\text{tot}}}{A_c} \quad (1)$$

where  $A_{s,\text{tot}} = A_{si} + A_{sa}$  = total area of reinforcement  
 $A_c = bd_1$  = area of concrete.

This limiting value has to be chosen in such a way, that both the inside reinforcement and the externally bonded steel come to yield before the concrete fails by crushing in the compression zone.

On the other hand, neither of the two reinforcements should reach its rupture strain, before the concrete fails in compression. Therefore, the total ratio of the reinforcing steel should be higher than

$$\rho_{\text{tot,min}} = \frac{A_{s,\text{tot}}}{A_c} \quad (2)$$

as a lower limit.

In the following, the expressions for  $\rho_{\text{tot,max}}$  and  $\rho_{\text{tot,min}}$  will be derived under the assumption, that the cross section of a rectangular beam remains plane during bending.

With the notations of Fig. 1, the depth  $x$  of the compression zone can be expressed by

$$x = \frac{f_{si,y} A_{si} + f_{sa,y} A_{sa}}{f_c b k_1} \quad (3)$$

The factor  $k_1$  describes the stress distribution in the concrete compression zone.

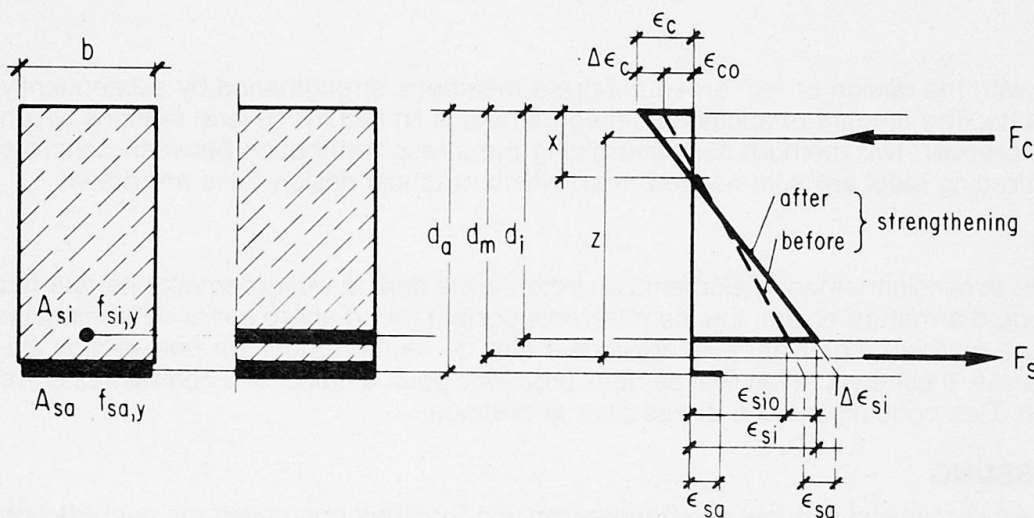


Fig. 1: Notations and dimensions



Using the mean value of the static depth of the cross section

$$d_m = \frac{f_{si,y} A_{si} d_i + f_{sa,y} A_{sa} d_a}{f_{si,y} A_{si} + f_{sa,y} A_{sa}} \quad (4)$$

the ultimate bending moment of the cross section can then be written as

$$M_u = zF_s = (d_m - k_2x)F_s \quad (5)$$

where again  $k_2$  depends on the stress distribution in the concrete compression zone.

With  $x = \xi d_m$  equation (5) can be rewritten as

$$M_u = d_m (1 - k_2\xi)F_s \quad (6)$$

or, after some calculations,

$$M_u \cong d_i \left\{ f_{si,y} A_{si} + \frac{d_a}{d_i} f_{sa,y} A_{sa} \right\} \left\{ 1 - \frac{k_2}{k_1} (\bar{p}_i + \bar{p}_a) \right\} \quad (7)$$

with the notations

$$\bar{p}_i = \frac{f_{si,y} A_{si}}{f_c b d_i} \quad (8)$$

and

$$\bar{p}_a = \frac{f_{sa,y} A_{sa}}{f_c b d_i} \quad (9)$$

When a linear strain distribution is assumed over the cross section, an additional equation for  $x$  can be found

$$x = \frac{d_i (\Delta \epsilon_c + \epsilon_{co})}{\Delta \epsilon_c + \epsilon_{co} + \epsilon_{sio} + \Delta \epsilon_{si}} = \frac{d_i}{1 + \epsilon_{si}/\epsilon_c} \quad (10)$$

The combination of the equations (3) and (10) leads to an expression for the sum of  $\bar{p}_i$  and  $\bar{p}_a$  as a function of  $\epsilon_{si}/\epsilon_c$

$$\bar{p}_i + \bar{p}_a = \frac{k_1}{1 + \epsilon_{si}/\epsilon_c} \quad (11)$$

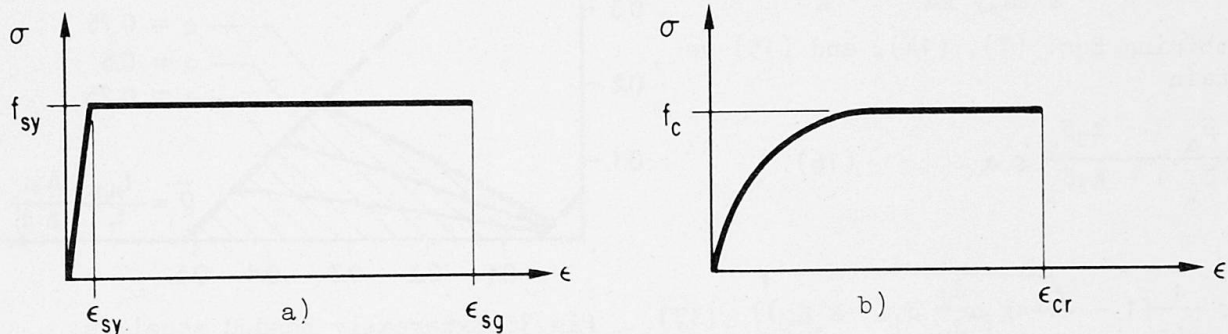


Fig. 2: Idealized  $\sigma$ - $\epsilon$ -diagram for steel (a) and concrete (b)



The  $\sigma$ - $\epsilon$ -diagram for steel can be simplified in a bi-linear form (Fig. 2a). Here,  $\epsilon_{sy}$  denotes the strain, when the yield stress is reached for the first time, and  $\epsilon_{sg}$  is the strain at rupture. On the other hand, the stress-strain curve for concrete is given in Fig. 2b with  $\epsilon_{cr}$  being the strain at rupture.

From the condition

$$\epsilon_{si,y} \ll \epsilon_{si} \ll \epsilon_{si,g}$$

a first set of lower and upper limits for the reinforcement ratio can be obtained

$$\frac{k_1}{1 + \epsilon_{si,g}/\epsilon_{cr}} \ll \bar{\rho}_i + \bar{\rho}_a \ll \frac{k_1}{1 + \epsilon_{si,y}/\epsilon_{cr}} \quad (12)$$

In a similar way, the deformation of the externally bonded steel can also be checked. When  $\epsilon_{sio}$  and  $\epsilon_{co}$  denote the strains of the inner reinforcing steel and of the concrete before strengthening, an additional set of lower and upper limits for the total reinforcing steel area can be established (Eq. 13):

$$\frac{\frac{d_a}{d_i} k_1}{1 + \frac{\epsilon_{sio}}{\epsilon_{cr}} \{1 + (1 + \frac{\epsilon_{co}}{\epsilon_{sio}})(\frac{d_a}{d_i} - 1)\} + \frac{\epsilon_{sa,y}}{\epsilon_{cr}}} \ll \bar{\rho}_i + \bar{\rho}_a \ll \frac{\frac{d_a}{d_i} k_1}{1 + \frac{\epsilon_{sio}}{\epsilon_{cr}} \{1 + (1 + \frac{\epsilon_{co}}{\epsilon_{sio}})(\frac{d_a}{d_i} - 1)\} + \frac{\epsilon_{sa,y}}{\epsilon_{cr}}}$$

Equations (12) and (13) are graphically represented in Fig. 3. For any combination of  $\bar{\rho}_i$  and  $\bar{\rho}_a$  which lays between the limiting straight lines, it is assured that both inner and outer steel will reach the yield stress before the concrete will fail in the compression zone.

1.2 Limitation by  $\Delta M_u$

Some codes or regulations suggest that the increase of the ultimate bending moment  $\Delta M_u$ , due to strengthening, should be limited

$$\frac{\Delta M_u}{M_{uo}} \ll \alpha \quad (14)$$

where  $M_{uo}$  = ultimate bending moment before strengthening (Eq.7,  $A_{sa} = 0$ )  
 $M_u$  = ultimate bending moment after strengthening (Eq.7)  
 $\Delta M_u = d_a f_{sa,y} A_{sa} (1 - k_3 \bar{\rho}_a)$  (15)

Combining Eqs. (7), (14), and (15) we obtain

$$\frac{\frac{d_a}{d_i} \bar{\rho}_a}{\bar{\rho}_i} \frac{1 - k_3 \bar{\rho}_a}{1 - k_3 \bar{\rho}_i} \ll \alpha \quad (16)$$

or

$$\bar{\rho}_a \ll \frac{1}{2k_3} \{1 - \sqrt{1 - 4k_3 \alpha \frac{d_i}{d_a} \bar{\rho}_i (1 - k_3 \bar{\rho}_i)}\} \quad (17)$$

with  $k_3 = k_2 / k_1$  (18)

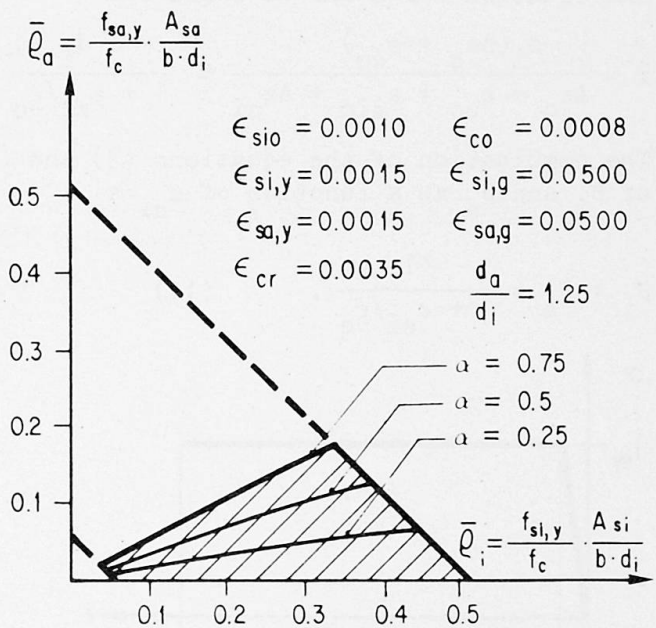


Fig.3: Externally bonded steel vs. internal reinforcement

## 2. LOAD TRANSFER BETWEEN EXTERNALLY BONDED STEEL AND CONCRETE

### 2.1 General Remarks

Although the mathematical models used for describing the load transfer from one material to another throughout an adhesive are of simple nature, the formulas given in the next paragraphs do not show a simple form and may therefore not be applicable in practice. In spite of this fact, the results obtained this way may help to understand some of this process and, together with test results, may lead to some advices for dimensioning and design of the anchorage zone of an additional reinforcement.

### 2.2 Elastic Solution for the Bond Stress Distribution

Let us consider first a concrete prism with bonded steel sheets on two opposite sides (Fig. 4). Assuming that

- the materials concrete, steel, and resin follow Hook's law;
- the resin takes shear stresses only;
- the thicknesses  $t$  and  $d$  as well as the width  $b$  are constant over the total bond length  $l_a$ ;
- the stresses and strains are distributed uniformly over the total cross section (bending effects are neglected)

then, according to [1], the bond stress distribution is given by

$$\tau(x) = \sigma_{so} t \omega \frac{\text{Ch}(\omega x)}{\text{Sh}(\omega l_a)} \quad (19)$$

with

$$\omega^2 = \frac{G}{s} \left( \frac{1}{E_s t} + \frac{2}{E_c d} \right) \quad (20)$$

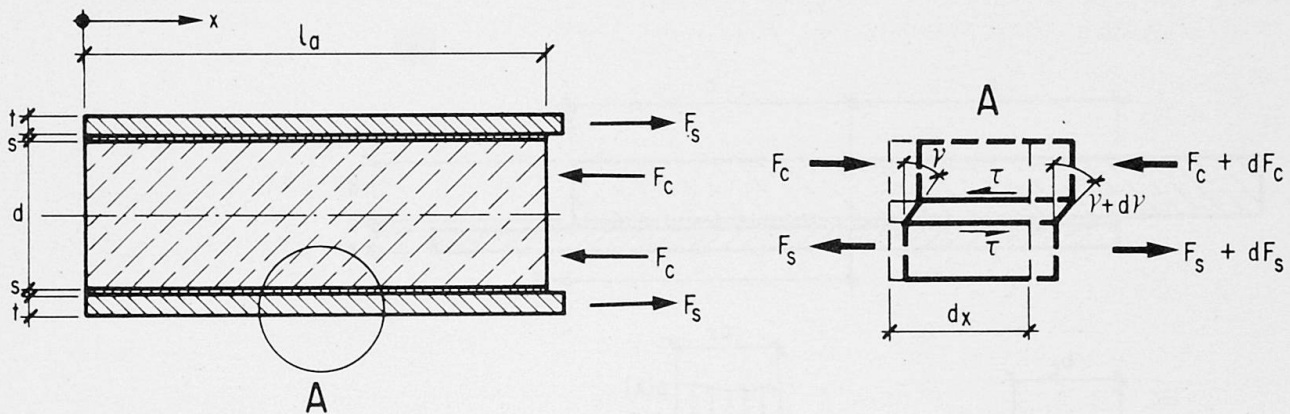


Fig. 4: Concrete prism with bonded steel sheets

The general shape of the bond stress distribution  $\tau(x)$  is shown in Fig. 5. From this, it can be seen clearly, that only a very small part of the total anchorage length  $l_a$  is needed for load transfer. To find the length  $l'$  which is needed for transferring  $k$  percent of the total tensile force  $F_s$  from the steel to the concrete ( $0 \leq k \leq 1$ ) the bond stress  $\tau(x)$  has to be integrated from  $x = x_0$  to  $x = l_a$ :

$$\int_{x_0}^{l_a} \tau b dx = k F_s = k \sigma_{so} b t \quad (21)$$



$$\sigma_{so} t b \left( 1 - \frac{Sh(\omega x_0)}{Sh(\omega l_a)} \right) = k \sigma_{so} b t \quad (22)$$

For  $\omega x_0 > 1$  this expression can be simplified to

$$\frac{e^{\omega x_0}}{e^{\omega l_a}} = 1 - k \quad (23)$$

or

$$x_0 = l_a + \frac{1}{\omega} \ln(1-k) \quad (24)$$

Finally, the effective anchorage length  $l'$  can be written as

$$l' = l_a - x_0 = \frac{-1}{\omega} \ln(1-k) \quad (25)$$

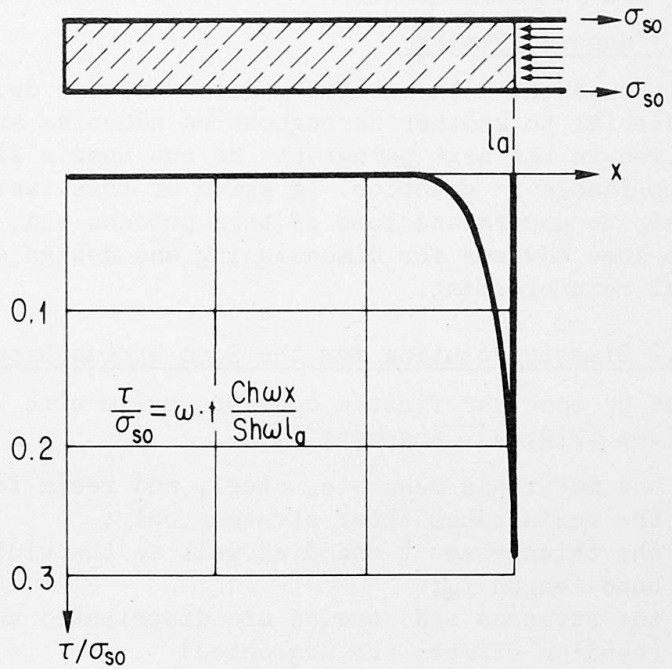


Fig. 5: Bond stress distribution between steel and concrete

### 2.3 Bond and Normal Stress Distribution in a Glued Joint

A very early study about the normal and bond stress distribution  $\sigma$  and  $\tau$  in a glued joint was performed by Goland and Reissner in 1944 [2]. Based on their investigation a more general form of the corresponding differential equations for  $\sigma$  and  $\tau$  will be given in the following (Fig. 6).

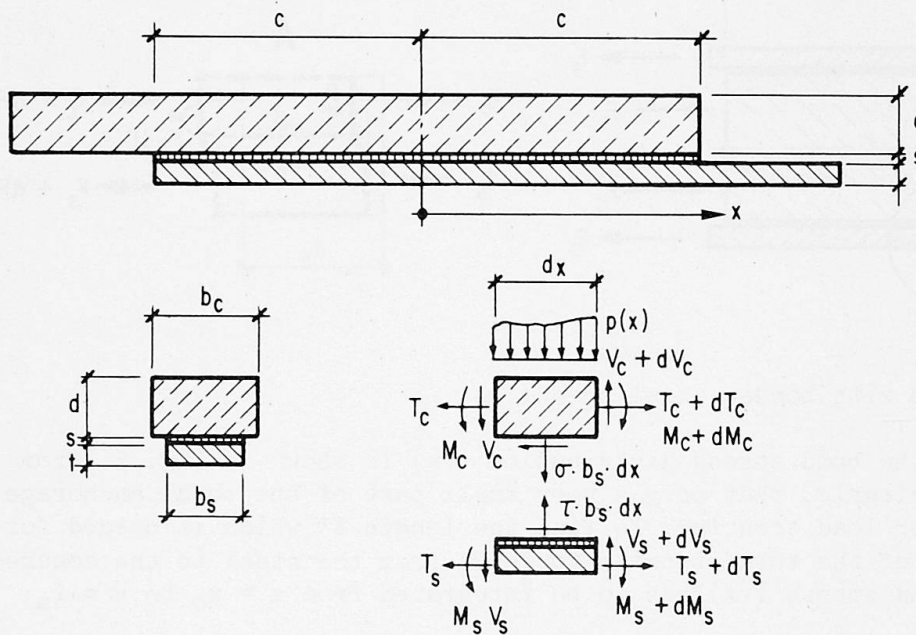


Fig. 6: Notations and dimensions



A first differential equation for  $\tau$  can be established from the conditions of equilibrium and compatibility

$$\frac{d^3\tau}{dx^3} - \frac{4G_a}{E_s} \frac{nb_s t + b_c d}{b_c d t} \frac{d\tau}{dx} + \frac{6G_a}{E_s} \left\{ \frac{nb_s t^2 - b_c d^2}{b_c d^2 t^2} \sigma + \frac{np(x)}{b_c d^2} \right\} = 0 \quad (26)$$

with  $E_s$  = Modulus of elasticity, steel  
 $E_c$  = Modulus of elasticity, concrete  
 $G_a$  = Shear modulus, adhesive  
 $n = E_s/E_c$

In a similar way, a differential equation for  $\sigma$  can be found

$$\frac{d^4\sigma}{dx^4} + \frac{12E_a}{E_s} \frac{b_c d^3 + nb_s t^3}{b_c d^3 t^3} \sigma + \frac{6E_a}{E_s} \frac{b_c d^2 - nb_s t^2}{b_c d^2 t^2} \frac{d\tau}{dx} + \frac{12E_a}{E_c s b_c d^3} p(x) = 0 \quad (27)$$

with  $E_a$  = Modulus of elasticity, adhesive.

Combining the two differential equations (26) and (27) an equation for  $\sigma$  is obtained

$$\frac{d^6\sigma}{dx^6} - B' \frac{d^4\sigma}{dx^4} + C' \frac{d^2\sigma}{dx^2} - D'\sigma + F' = 0 \quad (28)$$

The constants  $B'$ ,  $C'$ ,  $D'$ , and  $F'$  contain all geometric and mechanical properties of the specific problem.

At the beginning of a joint, a compression stress  $\sigma$  is present which should be superimposed to the bond stress  $\tau$ .

For the case, where  $E_s = E_c = E$  ( $n = 1$ ),  $b_s = b_c = b$ ,  $d = t$ , and  $p(x) = 0$ , equation (26) becomes independent of  $\sigma$

$$\frac{d^3\tau}{dx^3} - \frac{8G_a}{E s t} \frac{d\tau}{dx} = 0 \quad (29)$$

and equation (27) is then also independent of  $\tau$

$$\frac{d^4\sigma}{dx^4} + \frac{24E_a}{E s t^3} \sigma = 0 \quad (30)$$

The differential equations (29) and (30) were found and solved by Goland and Reissner in [2].

### 3. CONCLUDING REMARKS

As it can be seen from equation (25), a relatively small amount of the total anchorage length  $l$  is effective for load transfer when all materials involved behave elastically. The total anchorage length  $l_a$  will only be needed when, due to local failure of the bond, the peak value of the bond stress moves towards the unloaded end of the steel sheet. This phenomenon could be seen clearly in test results as reported in [3]. Thus, a redistribution of the bond stresses takes place.



Consider now in more detail the local force flow in the concrete. The concentrated load transfer at the beginning of the anchorage zone can be compared with a nodal point of a truss, where the tension chord is formed by the steel sheet and the compression diagonal member by the concrete. The vertical strut members are usually also represented by the concrete; however, since in ordinary reinforced concrete structures all tensile forces are usually taken by the reinforcing steel, additional "stirrups" should also be provided to equilibrate these vertical strut forces and to bring them up to the compression chord of the truss model (Fig. 7). In this way, a consistent and adequate model is used throughout the whole structure. Test results have shown, that these unfavourable tensile forces may lead to a failure in the concrete (Fig. 8).

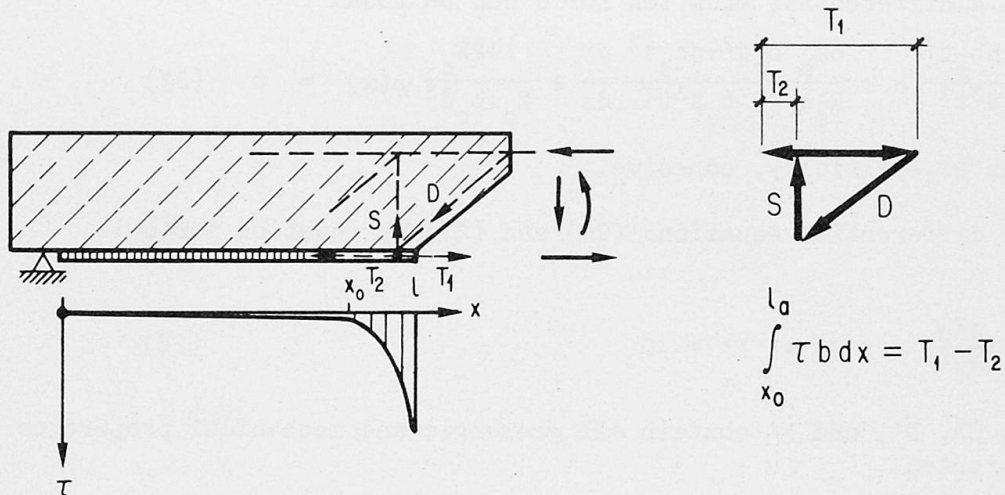


Fig. 7: Truss model

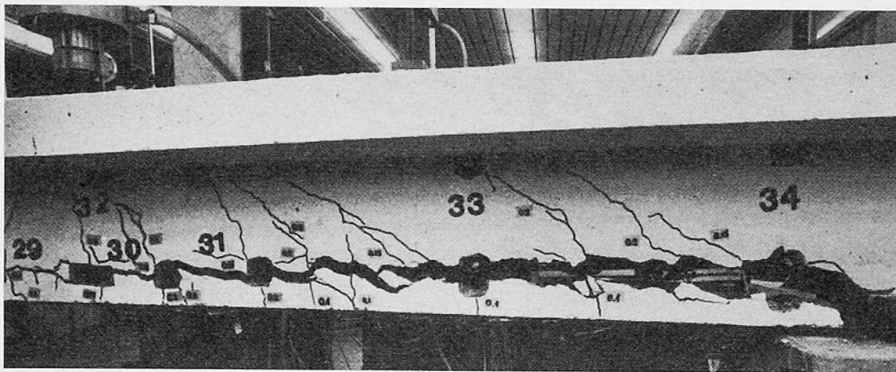


Fig. 8: Failure in a test beam

#### REFERENCES

- [1] BRESSON, J., Nouvelles recherches et applications concernant l'utilisation des collages dans les structures. Béton plaqué. Annales de l'institut technique du bâtiment et des travaux publics, No. 278 (1971), p. 23 ss.
- [2] GOLAND, M.; REISSNER, E., The Stresses in Cemented Joints. Journal of Applied Mechanics, 66 (1944), p. A17 ss.
- [3] LADNER, M.; WEDER, CH., Concrete Structures with Bonded External Reinforcement. Eidgenössische Materialprüfungs- und Versuchsanstalt (EMPA) Dübendorf Report No. 206 (1981).

## Adhésion entre les matériaux traditionnels et les résines époxy

Der Verbund zwischen traditionellen Baustoffen und Epoxidharzen

Adhesive Properties of Epoxy Resins

### Albert H. CARDON

Dr.  
Vrije Univ.  
Bruxelles, Belgique



Albert H. Cardon, (1938). Dr. en Sciences (ULB, 1971). Depuis 1960 assistant à l'U.L.B., puis à la V.U.B. Chargé de cours et ensuite professeur ordinaire à la Faculté des Sciences Appliquées de la Vrije Universiteit Brussel. Responsable de l'unité de mécanique des milieux continus.

### Frans BOULPAEP

Ing.  
Vrije Univ.  
Bruxelles, Belgique



Frans Boulpaep (1953). Ingénieur industriel. Assistant Technique à l'unité de Mécanique des Milieux Continus de la Faculté des Sciences Appliquées de la Vrije Universiteit Brussel (V.U.B.).

### RESUME

Depuis de nombreuses années les résines époxy sont utilisées pour la réparation d'ouvrages de génie civil. Ces résines ont un caractère viscoélastique et présentent dès lors des phénomènes de fluage. Il est fait état de l'influence de la température, de la fréquence et de l'humidité sur ces caractéristiques mécaniques et les conséquences sur l'adhésion et dès lors sur la qualité de la réparation.

### ZUSAMMENFASSUNG

Seit vielen Jahren werden Epoxidharze zu Wiederherstellungsarbeiten im Bauwesen verwendet. Diese Harze sind viskoelastischer Natur und weisen deshalb Kriechphänomene auf. Wir untersuchen den Einfluss von Temperatur, Frequenz und Feuchtigkeit auf diese mechanischen Eigenschaften und die Auswirkungen auf die Adhäsion und so auf die Qualität der Wiederherstellungsarbeiten.

### SUMMARY

For many years, epoxy resins have been used for repairs in civil engineering construction. The resins are viscoelastic and consequently exhibit creep phenomena. The influence of temperature, frequency and the moisture on the mechanical characteristics and the effects on the adhesion properties of the epoxy and finally on the general quality of the repair have been studied.



## INTRODUCTION

L'application relativement facile des résines époxy, sous forme quasi-fluide suivi d'un durcissement rapide, explique en grande partie leur utilisation fréquente dans les problèmes de réfection et réparation d'ouvrages de génie civil. Ils doivent assurer, ou rétablir, des liaisons et transferts de contraintes entre différents matériaux traditionnels tels le béton, la pierre, l'acier, l'aluminium et le bois.

Leur utilisation, bien que généralement en couches minces, suppose de bonnes qualités d'adhésion. Cette adhésion, et le transfert de contraintes réalisé par cette couche époxy, est fonction des caractéristiques de ces résines.

Elles présentent un caractère viscoélastique qui, pour faibles taux de contrainte, peut valablement être considéré comme linéaire. Non seulement des phénomènes de fluage et relaxation vont se manifester, mais la température et l'humidité peuvent fortement influencer leur rigidité.

La fréquence des sollicitations joue également un rôle sur leur comportement mécanique. La rigidité de l'assemblage dans lequel la couche époxy joue un rôle de liaison sera dès lors aussi influencée par ces différents paramètres.

Il est dès lors important de connaître au mieux les propriétés mécaniques globales de ces résines en fonction de la fréquence, de la température et de l'humidité. De connaître ensuite l'influence de cette variation des caractéristiques mécaniques sur l'adhésion et dès lors sur la qualité de la réfection réalisée.

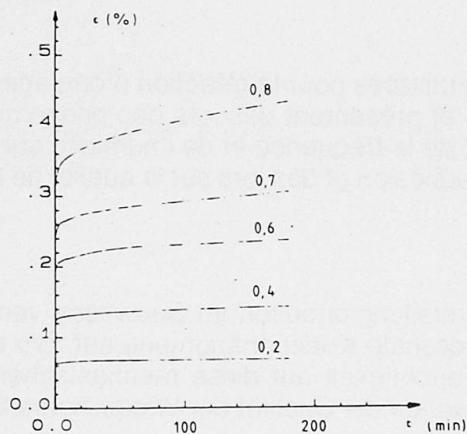
### 1. COMPORTEMENT VISCOELASTIQUE

Pour un matériau élastique lorsque  $\sigma = \sigma_0$  (cte), la déformation est instantanée et constante ; elle vaut  $\epsilon = \sigma_0/E$  (E étant le module d'élasticité).

Lorsque le matériau élastique, pour  $\sigma = \sigma_0 = \text{cte}$ ,  $\epsilon = f^{\text{ion}}(\sigma_0, t)$  et dans l'hypothèse d'un comportement linéaire :  $\epsilon = \sigma_0 k(t)$ .

La déformation varie en fonction du temps et  $k(t)$  est la fonction de fluage.

La figure 1 donne les fonctions de fluage pour une résine époxy utilisée couramment pour des réparations d'ouvrages de génie civil.



Ces courbes sont obtenues à 35°C.

On remarquera que tant que  $\sigma_0 < 0.6 \sigma_{\text{rupture}}$ , on peut les réduire à une courbe de fluage unique  $k(t) = \epsilon/\sigma_0$ .

Pour  $\sigma_0 > 0.6 \sigma_r$  cette réduction n'est plus possible et une modélisation non-linéaire s'impose.

Au lieu de considérer une contrainte imposée, on peut imposer la déformation. Dans ce cas, pour un comportement linéaire, on obtiendra une courbe de relaxation  $r(t) = \sigma/\epsilon_0$ .

Les essais de fluage et de relaxation sont des essais quasi-statiques. L'information qu'elles permettent d'obtenir nécessitera une mesure précise pour les effets quasi-instantanés et les effets à long

terme. Une information équivalente peut s'obtenir en effectuant des essais dynamiques, p. ex.  $\sigma = \sigma_0 \cos \omega t$  avec en comparaison  $\epsilon = \epsilon_0 \cos (\omega t - \delta)$ .

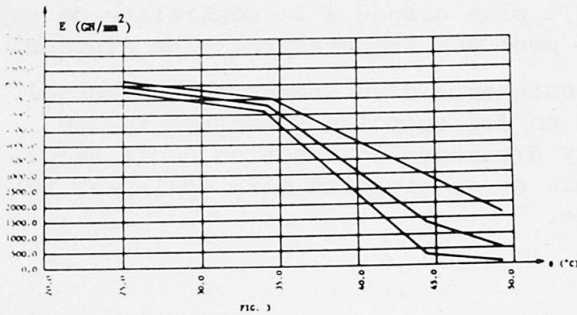
Le module réel du solide élastique parfait  $E$  sera remplacé par un module complexe  $\underline{E} = E_1 + iE_2$  dans lequel  $E_1$  sera une mesure de l'élasticité du matériau et  $E_2$  une mesure de l'amortissement.

Les méthodes classiques dynamiques permettent généralement des mesures de  $E_1$  et  $\text{tg } \delta = E_2/E_1$ .

$E_1$  et  $\text{tg } \delta$  sont fonction de la pulsation  $\omega$ , mais également de la température.

Pour certains matériaux, rhéologiquement simples, une correspondance existe entre la dépendance vis-à-vis de  $\omega$  et celle vis-à-vis de la température. Cette propriété bien connue donne lieu à la construction d'une courbe maîtresse, mieux connu sous le nom du principe W.L.F., (Williams - Landell - Ferry).

Pour des matériaux rhéologiques simples des essais dans une bande de fréquences donnée à différentes températures permettent par translation verticale des résultats d'obtenir les caractéristiques du matériau pour une plus grande gamme de fréquences, ou pour une plus grande gamme de températures.



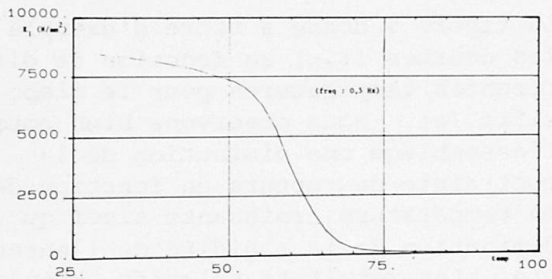
La figure 2 donne  $E_1$  en fonction de la température pour différentes fréquences pour une résine époxy courante. On remarquera que la température de transition (température pivot pour le passage de l'état à grande rigidité vers un état de plus faible rigidité) est d'environ 40°C.

## 2. EQUIPEMENT DE MESURE - TEMPERATURE DE TRANSITION

Nous disposons d'équipements commercialement disponibles permettant d'effectuer des mesures en traction-compression sinusoidale dans une gamme de fréquences 0.1 Hz à 1000 Hz et dans un domaine de variation de températures de -180°C à 250°C. La majorité de nos résultats expérimentaux se situent actuellement entre 0.1 à 10 Hz et de 20°C à 180°C.

Ces domaines de mesure sont suffisants pour la détermination des caractéristiques viscoélastiques des résines époxy que nous étudions.

La température de transition peut évoluer vers des valeurs plus élevées en fonction d'un cycle de recuit de la résine. Elle peut évoluer vers des valeurs plus petites lorsque le degré d'humidité augmente.

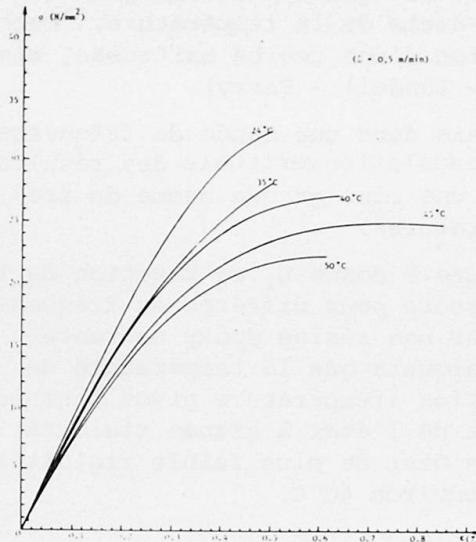


La figure 3 donne  $E_1$  en fonction de la température pour une fréquence de 0.5 Hz pour la résine dont les caractéristiques sans recuit sont données par la figure 2. Lors de cette expérience la résine a subi au préalable un recuit standard (72 heures à 40°C). On remarquera que la température de transition est passée de 40°C aux environs de 60°C.

Une conclusion immédiate s'impose. Afin d'éviter une température de transition basse, environ 40°C, qui est courante, au moins à la surface d'ouvrages de génie civil exposés au soleil, il y a lieu de prévoir une opération de recuit pour agrandir le domaine vitreux.



Si une telle opération de recuit est aisée à effectuer en laboratoire, il semble douteux que la mise en oeuvre des résines époxy pour une réfection sur chantier permette une telle opération contrôlée. Il faut dès lors tenir compte de la valeur de la température de transition sans recuit pour pouvoir juger de la qualité minimale d'une réfection effectuée à l'aide de ces résines.



A titre d'illustration des effets de la température sur la rigidité des résines époxy, la figure 4 donne les courbes contrainte-déformation obtenues à vitesse de déplacement constante pour différentes températures.

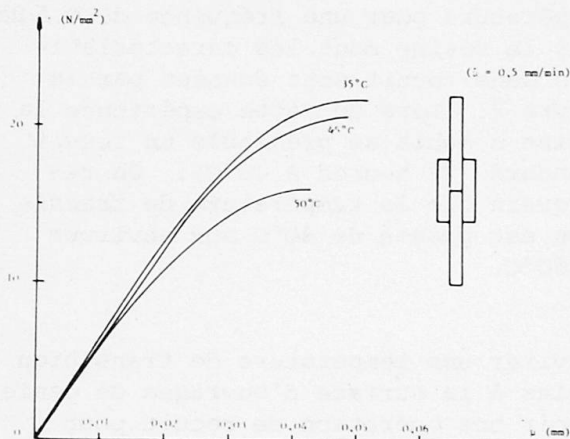
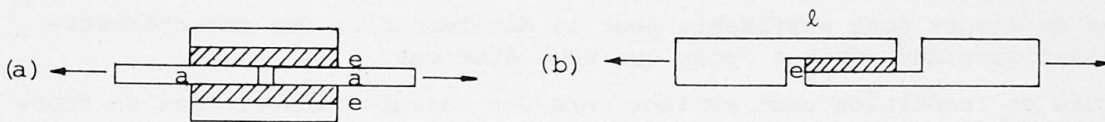
On remarquera que  $\sigma_{\text{maximum}}$  à 50°C est réduit d'environ 1/3 par rapport au  $\sigma_{\text{maximum}}$  à 24°C.

Il apparaît également une déformation maximale plus grande à la contrainte de rupture pour des températures plus élevées.

La résistance d'un ensemble multicouche dont un des composants est une résine époxy diminuera en fonction de la température et sa rigidité sera également réduite.

### 3. ASSEMBLAGE COMPORTANT UNE COUCHE ÉPOXY - ADHÉSION

En vue d'étudier le comportement d'une multicouche, comportant des matériaux traditionnels de génie civil, (pierre, béton, acier, aluminium, bois), et une couche de résine époxy nous avons effectué un grand nombre d'essais de cisaillement sur base de deux types de sollicitation :



La figure 5 donne à titre d'exemple les courbes  $(\tau, \mu)$  en fonction de différentes températures pour le dispositif (a). Nous observons bien pour l'assemblage une diminution de la contrainte de rupture en fonction de la température croissante ainsi qu'une diminution de la rigidité de l'ensemble. Les résultats relatifs obtenus par des essais sur un dispositif de type (b) correspondent à ceux obtenus par le dispositif (a), sauf en ce qui concerne la rigidité d'ensemble qui est plus faible pour (b) que pour (a).

Lors des différents essais que nous avons effectués, nous avons également fait varier les caractéristiques géométriques des surfaces sur lesquelles la résine était appliquée, d'une surface lisse vers une surface rainurée. Nous n'avons pas fait varier les conditions chimiques des surfaces en question.

L'introduction d'une surface rainurée ne donne pas des résultats meilleurs pour le comportement de l'assemblage, par rapport à des surfaces lisses.

Nous essayons actuellement d'introduire un état de surface quantifiable afin de déterminer son influence sur le comportement de l'adhésion et donc de l'assemblage.

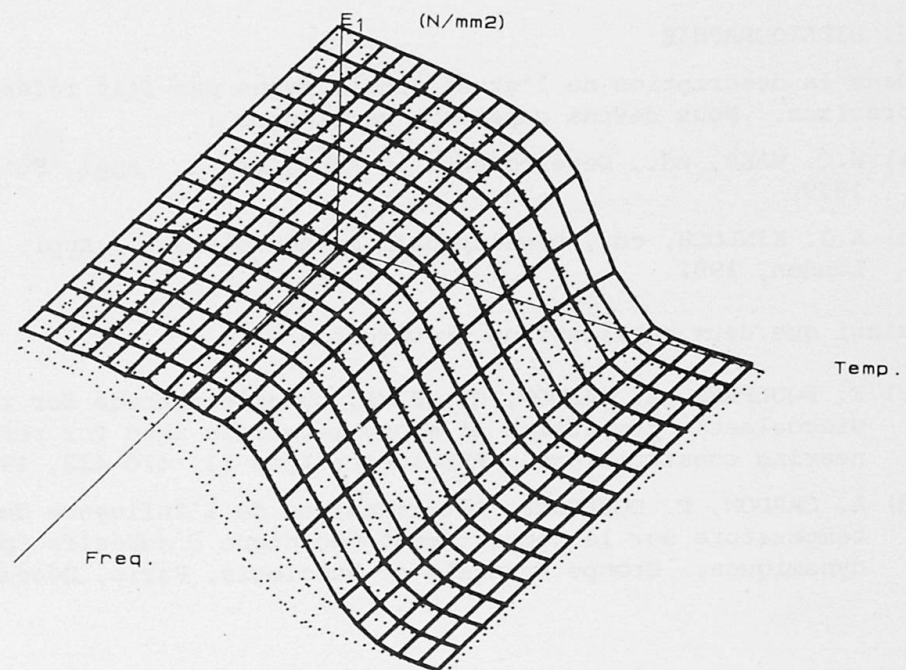
Nous étudions également l'influence de l'épaisseur  $e$  de la couche époxy sur le comportement de l'assemblage du point de vue rigidité et contrainte de rupture.

#### 4. INFLUENCE DE L'HUMIDITE

Si un cycle de recuit permet d'augmenter la température de transition, une augmentation du degré d'humidité a un effet opposé.

La figure 6 donne à titre d'exemple la partie réelle du module complexe  $E_1$ , en fonction de la température et de la fréquence pour deux taux d'humidités.

Nous remarquons un déplacement d'ensemble sensible des surfaces  $E_1(f, \theta)$  vers des plus basses températures lorsque le degré d'humidité augmente.





## 5. MECANISMES DE RUPTURE

Nous effectuons actuellement des essais avec des assemblages comportant différents matériaux reliés par une couche mince de résine époxy, afin d'examiner les différents mécanismes de rupture en fonction des caractéristiques des matériaux de support. La rupture peut se produire dans la couche époxy, dans le matériau de support ou le long de la surface d'adhésion.

Notre objectif est d'établir une correspondance entre le mécanisme de rupture et la nature du matériau de support, y compris son état de surface pour une résine époxy donnée.

## 6. CONCLUSIONS

Si une réfection à l'aide de résines époxy est aisée du point de vue réalisation, la réfection sera fonction du taux de contrainte que cet assemblage devra subir. L'influence de la température et de l'humidité sont importantes et il y a lieu de soigneusement étudier les conditions normales de fonctionnement de l'assemblage afin de choisir la résine adéquate et la préparation de surface nécessaire.

## 7. REMERCIEMENTS

Nous tenons à remercier le Fonds de la Recherche Collective (F.R.F.C.) du Fonds National de la Recherche Scientifique Belge pour le support financier de l'ensemble de ces études.

Nous remercions vivement Mme Myriam BOURLAU pour le soin apporté à la dactylographie et M. Adrien VRIJDAG pour les figures.

## 8. BIBLIOGRAPHIE

Dans la description de l'étude nous n'avons pas fait référence à des publications précises. Nous devons cependant mentionner :

- a) W.C. WAKE, ed., Developments in Adhesives 1. Appl. Science Publishers, London, 1979.
- b) A.J. KINLOCH, ed., Developments in Adhesives 2. Appl. Science Publishers, London, 1981.

ainsi que deux publications précédentes :

- c) F. BOULPAEP, A. CARDON, Cl. HIEL, Dynamic methods for the determination of the viscoelastic properties of epoxy materials used for refectons of civil engineering constructions. Rheologica Acta 21, 420-422, 1982.
- d) A. CARDON, F. BOULPAEP, Détermination de l'influence de l'humidité et de la température sur le comportement mécanique d'adhésifs époxy par des méthodes dynamiques. Groupe Français de Rhéologie, Paris, Décembre 1982.

## Non-linear Analysis and Strengthening of a Reinforced Concrete Building

Calcul du renforcement d'un bâtiment au moyen de l'analyse non-linéaire

Nicht-lineare Analyse für die Bemessung der Verstärkung von Stahlbetonbauten

### Ester CANTÙ

Researcher  
University of Pavia  
Pavia, Italy



Ester Cantù, born in 1952, graduated in Civil Engineering at the University of Pavia. Her research field concerns the non-linear analysis of R.C. members and the cyclic behaviour of plain and reinforced masonry elements in load-bearing brickwork.

### Aldo CAUVIN

Associate Professor  
University of Pavia  
Pavia, Italy



Aldo Cauvin, born 1939, graduated in Civil Engineering at the Milan Institute of Technology (Politecnico). His research work deals mainly with the problem of non-linear analysis of R.C. structures; he also works as a consultant in the field of structural engineering.

### SUMMARY

Severe disorders appearing in a reinforced concrete framed building led to the necessity of determining its safety level. This aim was achieved both with experimental tests and with numerical analyses, linear and non-linear. Non-linear analysis proved to be very useful in determining the moment redistribution capability of the structure and realistic values of displacements.

### RESUME

Les dommages assez graves apparus dans une structure à cadres en béton armé ont nécessité la détermination de son niveau de sécurité. Des essais et des analyses numériques linéaires et non-linéaires ont été réalisés. L'analyse non-linéaire a permis de déterminer la capacité de redistribution des moments à l'intérieur de la structure, ainsi que de calculer les valeurs réalistes de déplacements.

### ZUSAMMENFASSUNG

Das Auftreten von schweren Schäden in einer Konstruktion aus Stahlbeton mit Rahmencharakter macht die Bestimmung ihres Sicherheitsniveaus notwendig. Zu diesem Zwecke wurden experimentelle Untersuchungen sowie numerische Analysen linearer und nicht-linearer Art durchgeführt. Die nicht-lineare Analyse erwies sich als äusserst nützlich um die Umlagerungskapazität der Konstruktion und die auftretenden Verschiebungen zu bestimmen.



## 1. INTRODUCTION

One of the fields in which non-linear analysis of structures is most useful is certainly the evaluation of the degree of safety of existing damaged r.c. buildings.

In fact, in these cases it is important to obtain a realistic image of the distribution of action effects and displacements, so that decisions concerning repairs can be taken according to the "true" behaviour of the structure. Repairs of damaged buildings are extremely costly; if the redistribution of action effects is well known, through non-linear analysis, the added margin of safety permitted by structural ductility can be understood and sometimes exploited, and the amount of repairs necessary to restore an adequate safety level can be reduced.

Besides, non-linear analysis permits to determine realistic values of displacements at service load level.

In the following paragraphs the investigations concerning a university building, in which severe disorders were produced by poor design and execution are described. The importance of the application of non-linear analysis in understanding the structural behaviour is emphasized.

## 2. USE OF NON LINEAR ANALYSIS IN ASSESSING THE SAFETY AND SERVICEABILITY OF EXISTING R.C. STRUCTURES

As it is well known, the analysis of r.c. structures at ultimate limit state is performed in a rather conventional and unrealistic way if linear analysis is used. In fact the critical sections of the structure are verified if

$$M_{act d} \leq M_{yu}$$

where  $M_{yu}$  = yielding moment of the section

and  $M_{act d}$  = acting design moment from linear elastic analysis.

This procedure is on the safe side in most cases and is normally used to design new structures, but has the following shortcomings:

- The acting moments are computed disregarding the redistribution produced by cracking and plastic behaviour of reinforced concrete. Therefore there is a contradiction in the fact that, while the yielding moment is calculated considering non-linear constitutive laws of materials, the acting moment is computed assuming that the behaviour of elements made of the same materials is perfectly linear.
- The ultimate limit state which is conventionally adopted is a "first yield" limit state, that is no plastic rotation of critical sections is permitted, while the ultimate limit state as defined by modern codes, such as the CEB Model Code [1] corresponds to the reaching of either a failure mechanism or the rotation capacity in a critical section, thus fully exploiting the available plastic redistribution, which can be very high in ductile structures.

As a consequence, non-linear analysis need be performed to assess the behaviour of a given structure in a realistic way.

## 3. EXAMPLE STRUCTURE - DESIGN CRITERIA - EXTENT AND NATURE OF DAMAGE

The aforesaid considerations were applied to the case of a recently built r.c. building, where damages occurred due to excessive deflections (Figs.1 and 2). The building is schematically shown in Fig.3: it is composed of 3 floors, the ground floor being used as lecture-hall. The others were partitioned in order to be used as studies and laboratories.

The floors, 15 meters square, are orthogonal grids of r.c. beams. These beams were designed as simply supported, despite the fact that no discontinuities exist between the beams and their supporting columns.



Fig.1 Typical floor

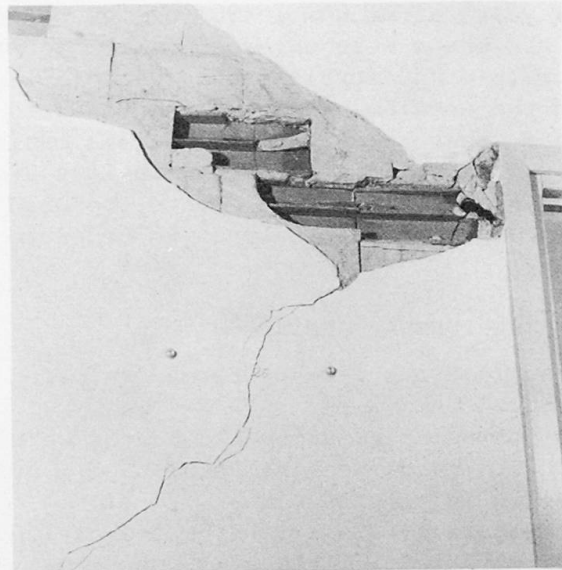


Fig.2 Cracking in partitions

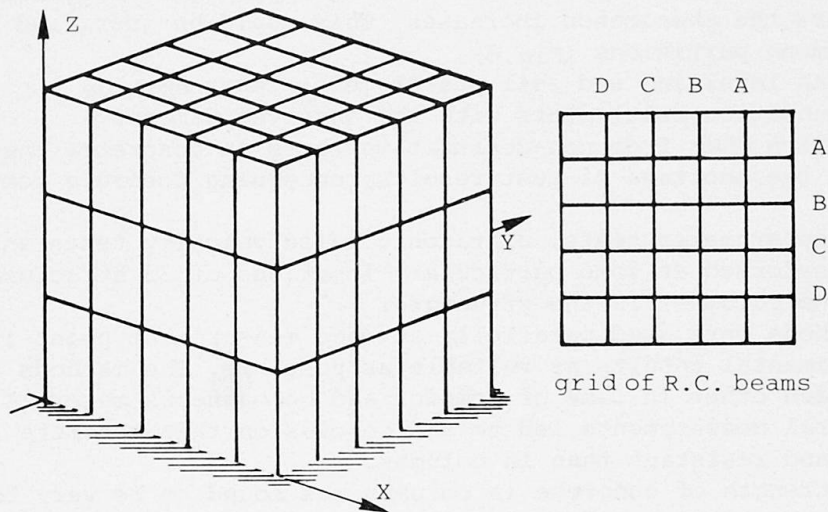


Fig.3 Simplified topology of the structure

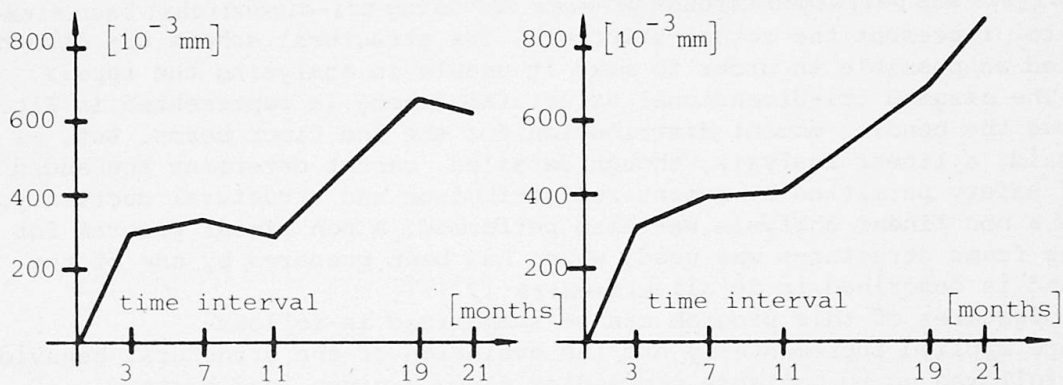


Fig.4 Gauge length variation across two cracks (versus time)



Few years after completion of the building large and increasing deflections of the beams were observed, which led to cracking in partitions (Fig.2). A group of 30 strain-gauge lengths were chosen across the cracks in partitions and the opening of cracks was measured and plotted versus time. Fig.4 shows some typical diagrams making clear the increasing trend of the deformation, if seasonal variations are suitably taken into account. The increase in damage led to the need of accurate experimental measurements and computational analyses in order to assess the safety conditions.

#### 4. EXPERIMENTAL CHECKS

Investigations were performed in order to ascertain the reasons of the observed behaviour.

The following experimental checks were carried out:

- strain-gauge measurements;
- levelling of the slabs;
- penetrometer tests of the foundation soil;
- non-destructive tests on concrete.

The conclusions drawn from there are summarized here.

The mentioned strain-gauge measurements across cracks were carried on and showed two different trends. At some locations the opening of cracks seems to decrease, at others the phenomenon increases. This could be justified by stress redistribution among partitions (Fig.4).

The results of slab levelling and soil penetrometer tests exclude all connections of foundation settlements with the observed damages.

Essential information came from non-destructive tests on concrete, that were made necessary by the shortage of test results concerning concrete compressive strength.

Surface hardness sclerometer tests, ultrasonic pulse velocity tests and pull-out tests were performed at some particular locations of 33 structural elements (beams and columns) in the structure.

Those testing methods were used parallelly at each measurement point in order to make the experimental results as reliable as possible. The methods are consistent with each other in case of compact and homogeneous material.

All the experimental measurements led to the conclusion that concrete in beams was more compact and resistant than in columns.

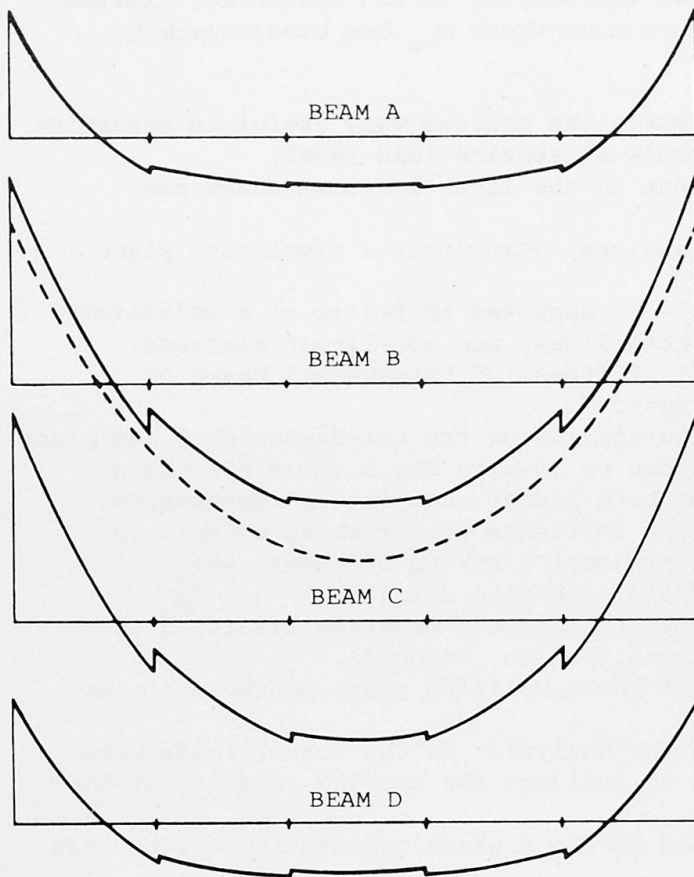
The compressive strength of concrete in columns was found to be very low, therefore in the computations a 12 MPa design compressive strength was assumed, coinciding with the minimum allowed by C.E.B. Model Code |1|.

#### 5. LINEAR AND NON-LINEAR ANALYSES

Linear analysis was performed through program SAP using tri-dimensional beam elements in order to represent the actual structure. The structural scheme was chosen as detailed as possible in order to make it usable in analyzing the repair effects. The assumed tri-dimensional structural scheme is represented in Fig. 3. Fig.5 shows the bending moment distribution for the 2nd floor beams. But, as already said, a linear analysis, though detailed, cannot determine the added margin of safety permitted by moment redistribution and structural ductility. Therefore a non linear analysis was also performed. A non linear program for r.c. plane frame structures was used, which has been prepared by one of the authors and is described in detail elsewhere |2||3|.

The basic features of this program can be summarized as follows:

- Loads are applied incrementally and the evolution of the structural behaviour can be followed up to collapse proceeding along a given load history.
- Non linear effects can be simulated:
  - a) Cracking and "tension stiffening"



length  $\dashv$  1 m  
 moments  $\dashv$  100 kN.m  
 — 3-D linear analysis  
 - - - 2-D linear analysis

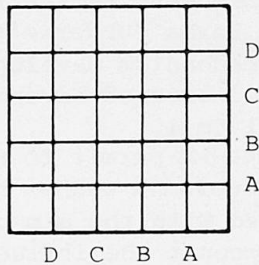


Fig.5 Tri-dimensional linear analysis: bending moments acting on 4 beams of 2nd floor grid

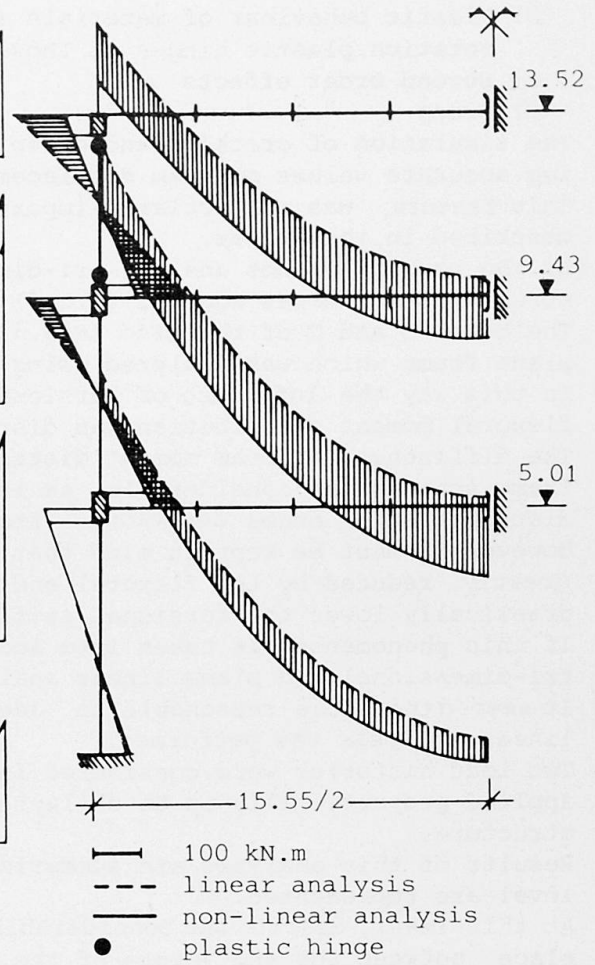


Fig.6 Linear and non-linear plane analysis: bending moments acting on the model structure

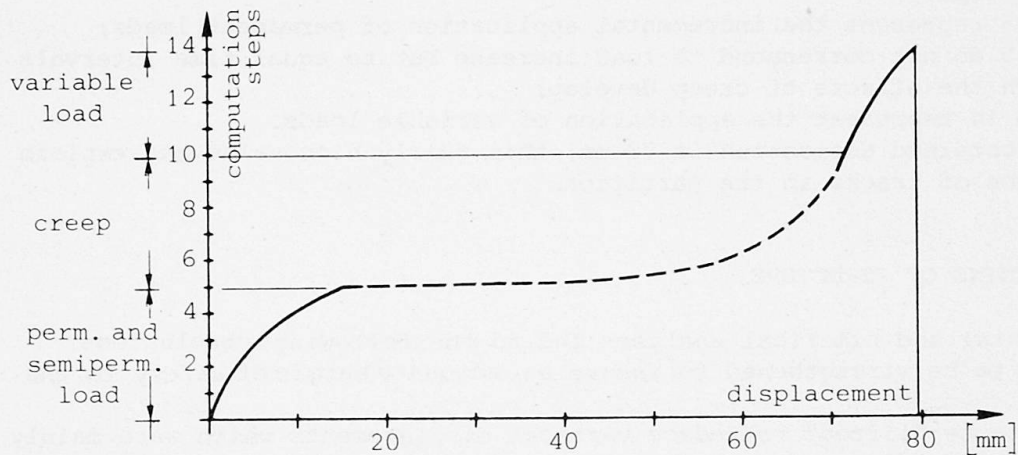


Fig.7 Evolution of vertical displacement at mid-span of a 2nd floor beam



- b) Plastic behaviour of materials (by introducing strain hardening, limited rotation plastic hinges in those sections where  $M_{yu}$  has been exceeded).
- c) Second order effects
- d) Creep

The simulation of cracking and creep makes the program very useful in determining accurate values of beam displacements at service load level.

This feature was particularly important in the investigations which are described in this paper.

As the program cannot analyze tri-dimensional structures, a simplified plane structural scheme was adopted (Fig.6).

The beams B and C of the grid (Fig.3) were supposed to belong to a multistory plane frame which was analyzed using both linear and non-linear analysis.

In this way the influence of torsional stiffness of transversal beams on flexural moment distribution was disregarded.

The differences in beam moment distribution, using the tri-dimensional and plane frame schemes are considerable, as it can be seen in Fig.5, where the moment distribution in beams deriving from both linear analyses is represented.

However it must be kept in mind that the influence of torsional moments is greatly reduced by the flexural and torsional cracking of beams, which drastically lower the torsional stiffness. See also ref. |4|.

If this phenomenon is taken into account the moment diagrams resulting from tri-dimensional and plane linear analyses tend to coincide.

It seemed therefore reasonable to adopt the simplified plane scheme when non linear analysis was performed.

Two load histories were considered in the analysis. In the former, loads were applied proportionally up to collapse to evaluate the bearing capacity of the structure.

Results of this analysis are summarized in Fig.6 where moments at service load level are represented.

At this level, despite the considerable moment redistribution which has taken place between the end joints of the beams (underreinforced) and the midspan sections (overreinforced) a failure mechanism develops in the columns of the top floor. Therefore loads cannot be increased beyond this level and the safety coefficient  $\gamma_f$  is approximately equal to 1.

The available structural ductility does not permit to reach an adequate margin of safety and the need to strengthen the columns cannot be avoided.

The latter load history was considered with the aim of computing accurate values of beam displacements, taking into account the influence of creep.

First permanent and semipermanent loads were applied; then creep was simulated using the procedure described in |3|; at last variable loads were applied incrementally up to service load level.

The values of vertical deflections are represented in Fig.7, in function of the computation steps:

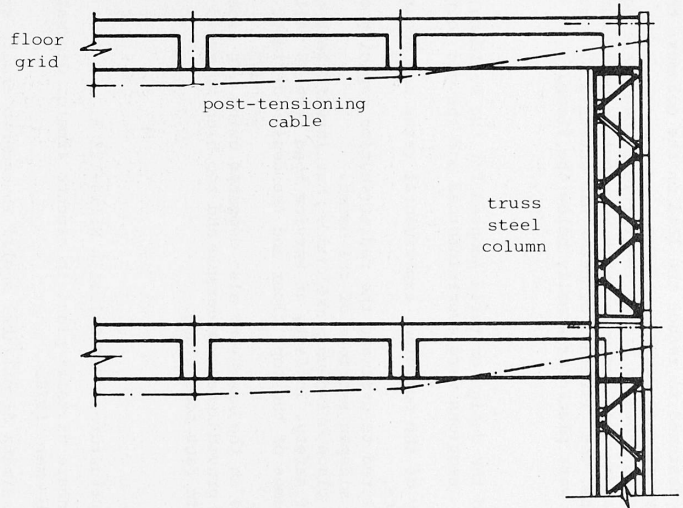
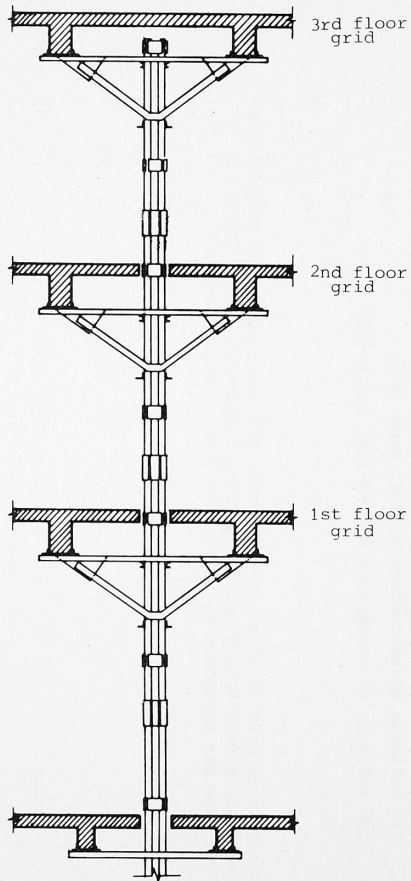
- steps 1 to 5 represent the incremental application of permanent loads;
- steps 6 to 9 do not correspond to load increase but to equal time intervals during which the effects of creep develop;
- steps 10 to 14 represent the application of variable loads.

The maximum obtained deflection is 79 mm; this fairly high value may explain the formation of cracks in the partitions.

## 6. STRENGTHENING OF STRUCTURE

The experimental and numerical analyses led to the following conclusions.

- Columns had to be strengthened to insure an adequate margin of safety to the structure.
- Beams had to be "lifted" to reduce vertical displacements which were mainly responsible for the formation of cracks in partitions.



△ Fig.9 Final strengthening scheme (truss steel columns and post-tensioning cables)

◁ Fig.8 Temporary strengthening scheme to support grid beams



A temporary support was first designed to reduce the load on the columns; the scheme of this support is represented on Fig.8.

The final strengthening scheme is shown on Fig.9: the vertical load bearing function was committed to truss steel columns which were put in place surrounding of the existing columns. The "lifting" of beams was obtained by post tensioning steel cables which were placed externally below the floor.

#### 7. CONCLUSIONS

The previous paragraphs showed the design criteria adopted for the building: as a consequence the mid-span sections were overreinforced and the end joints underreinforced.

To assess the degree of safety of the building, experimental tests and accurate linear analyses were inadequate.

Only non linear analysis permitted to evaluate the redistribution capacity of the structure between end and midspan sections of the beams.

The redistribution which took place is indeed considerable, but insufficient to guarantee an adequate level of safety. In fact, at service load level a failure mechanism develops in the columns of the top floor and the design ultimate limit state cannot be reached.

Maximum vertical displacements in the beams were also computed using non linear analysis. These displacements proved to be considerable and too high to avoid the damages in partitions, which in fact took place.

#### REFERENCES

1. CEB, Model Code for R.C. Structures. CEB Bulletin N.124-125 E.
2. CAUVIN A., Analisi non lineare di telai piani in cemento armato. Giornale del Genio Civile, Jan - Feb - Mar 1978.
3. CAUVIN A., Verifica approssimata di pilastri snelli in cemento armato appartenenti a telai a nodi spostabili. Industria Italiana del Cemento, Sept 1979.
4. ACI Special Publication 18, Torsion of Structural Concrete. ACI Detroit, 1968.
5. Lectures of CEB Course, Non Linear Analysis and Design of R.C. and prestressed Structures. Pavia, 1981.
6. CEB Bulletin d'Information N. 134, Rome 1979.
7. CEB Bulletin d'Information N. 153-154, Paris 1982.

*The authors wish to thank Prof.G.Macchi for his support and suggestions.  
The final strengthening was designed by F.Angrisano and P.Crosti.  
This work was sponsored by C.N.R. (National Research Council).*

## Redistribution of Action-Effects on Repaired R.C. Frames

Redistribution des sollicitations dans les ossatures en béton armé restaurées

Wiederverteilung der Beanspruchung bei restaurierten Rahmentragwerken aus Stahlbeton

### **Nina AVRAMIDOU**

Professor  
Univ. of Florence  
Florence, Italy



N. Avramidou, born 1942, received her Architect degree at the University of Florence, Italy. Member of Task Group 12 of CEB. Member of a «Coordinate Italian experimental research» group of CNR on repair problems.

### **SUMMARY**

Some of the results of an extensive parametric study on the expected redistribution of forces in repaired/strengthened R.C. frames are presented. The principal aim of this endeavour is the estimation of the order of magnitude of the redistribution on different R.C. frames, after combined damages as well as various interventions. Some temporary conclusions concerning the re-design of damaged frames are included.

### **RESUME**

L'article présente quelques résultats d'une étude paramétrique concernant la redistribution des effets des actions dans les ossatures des constructions en béton armé réparées ou renforcées. Le but de l'étude est de déterminer l'ordre de grandeur de la redistribution des sollicitations dans les ossatures de constructions typiques pour différentes techniques d'intervention et pour des dommages combinés. Des conclusions sont présentées pour le calcul des ossatures endommagées.

### **ZUSAMMENFASSUNG**

Es werden einige Ergebnisse einer weitgehenden parametrischen Studie angegeben, die die Wiederverteilung der Beanspruchung bei restaurierten und verstärkten Rahmentragwerken aus Stahlbeton behandeln. Die Untersuchung wurde unternommen, um die Größenordnung solcher Wiederverteilungen auf typische Rahmentragwerke durch kombinierte Schäden und verschiedene Eingriffe zu untersuchen, und zu einer vorläufigen Schlussfolgerung was die Neuberechnung der beschädigten Rahmen anbetrifft, zu kommen.



## 1. GENERAL REMARKS

The paper deals with the problems of assessment of damaged existing R.C. buildings (damages due to vertical loads as well as to earthquakes) and of re-design of such structures repaired and/or strengthened by various techniques.

In order to make decisions regarding assessment of damaged R.C. structures and remedial steps of interventions a considerable amount of data concerning pathology image and the residual structural characteristics, after damage, is needed. On the basis of such an information a new structural analysis of the whole building is needed, in order to evaluate the redistribution of all action effects.

First of all, we must notice the different ways to take damage into account, in the different computational procedures used. For instance, structural damage may be viewed as a decreased value of the flexural stiffness (EJ), or of the shear stiffness (GA), or of the axial stiffness (EA) in particular cross-sections; also a combined damage may be viewed taking into account contemporarily the reduction of the flexural as well as the shear and axial stiffnesses. This approach can be used in a linear static and dynamic analysis.

The second available approach is to consider the structural damage by means of a degrading stiffness beam model in a pre-determined loading and unloading hysteretic path. Clearly, the first available approach may be viewed as a naive approach leading to very simple computations; on the other hand, the latter is much more complicated and requires to define a realistic degrading-stiffness model, what is nowadays an object of many researches in this field of investigation.

Clearly, these approaches may not be directly compared due to the different types of analysis: the former is linear, while the latter is nonlinear. So the first approach can be used to investigate an already-damaged frame subjected to a new loading condition, within the elastic range. The non linear analysis is better suited for a " damage in progress " frame, subjected to strong static or (more often) dynamic actions.

Both the afore-presented methods have been used, in order to evaluate the redistribution of action effects after different damage degrees.

Depending of estimated or calculated bearing capacity values of the damaged structures, on emergency needs, on cost-benefit considerations, etc, several means of interventions may be adopted in order to restore or increase the capacity-ratio value of a building element or of a whole building.

Enlarged sections of repaired (strengthened columns beams or walls), infilled or braced R.C. frames etc may exhibit considerably higher stiffnesses after repair and/or strengthening. Therefore, appropriate redistribution of action-effects has to be taken into consideration, relating with vertical as well as horizontal loads.

## 2. REDISTRIBUTION OF ACTION-EFFECTS AFTER DAMAGE

### 2.1. Procedure of investigation.

The sample frames used in this parametric study are representatives of common R.C. frames for low - medium - and high-rise buildings. Each sample frame has been investigated, by a linear analysis, for many possible degrees of damages, starting from only one damaged sub-element up to the formation of a mechanism. The progressive damage state as well as the number and position of damaged sub-elements have been formed by another more sophisticated analysis of these sample frames based on a simple acceleration response spectrum (load-time history) of the same absolute values and on degrading-stiffness models in a predetermined loading and unloading hysteretic path.

In particular, sample plane R.C. frames (simple 3 - 5 - and 10 - storeys, 2 bays frames) have been used and static (for vertical loads) as well as a response spectrum dynamic analysis (for earthquake loads), according to the existing Ita-



lian Earthquake Resistant Code, has been developed in order to study such combined stiffness modification effects on the redistribution of action effects on damaged R.C. frames, (see Fig. 1).

Horizontal loads could have been considered by means of a static analysis, too; nevertheless it is particularly significant the increasing of the fundamental period in the damaged frame. This leads to smaller values of the accelerations, to be read in the input spectrum, and hence fairly decreased inertia loads are computed. This must be taken into account when comparing the output stresses in the dynamic analysis.

## 2.2. Evaluation of the output results

In order to evaluate the overall behaviour between the original and the damaged frames, as well as the order of magnitude of redistribution of action effects expected on such frames, it can be attempted comparing the following set of data by computations of the two structures:

- Fundamental periods or frequencies, which show the change of dynamic flexibility of the frame;

- Any norm of the generalized stress/strain or displacement vectors; particularly:  
 $\|S\| = \max$  absolute value of the  $S$  components (stress-strain or nodal displacements)

$\|S\|_2 =$  Euclidean norm, just as above.

The  $^2$  significant components must be restricted to the most interesting data.

In the present paper for the presentation of some of the output results the method of the Euclidean norms of the computed bending moments, shear and axial forces was computed.

So, for columns as well as for beams the Euclidean norms of the computed action-effects of the whole column line as well as of the whole bay are presented:

$$R = \sqrt{R_1^2}$$

where  $R_1$  denotes the maximum of the top/bottom value of  $R$  in an element of a column  $^1$  line or of a bay ( $R$  means bending moment or shear load or axial load).

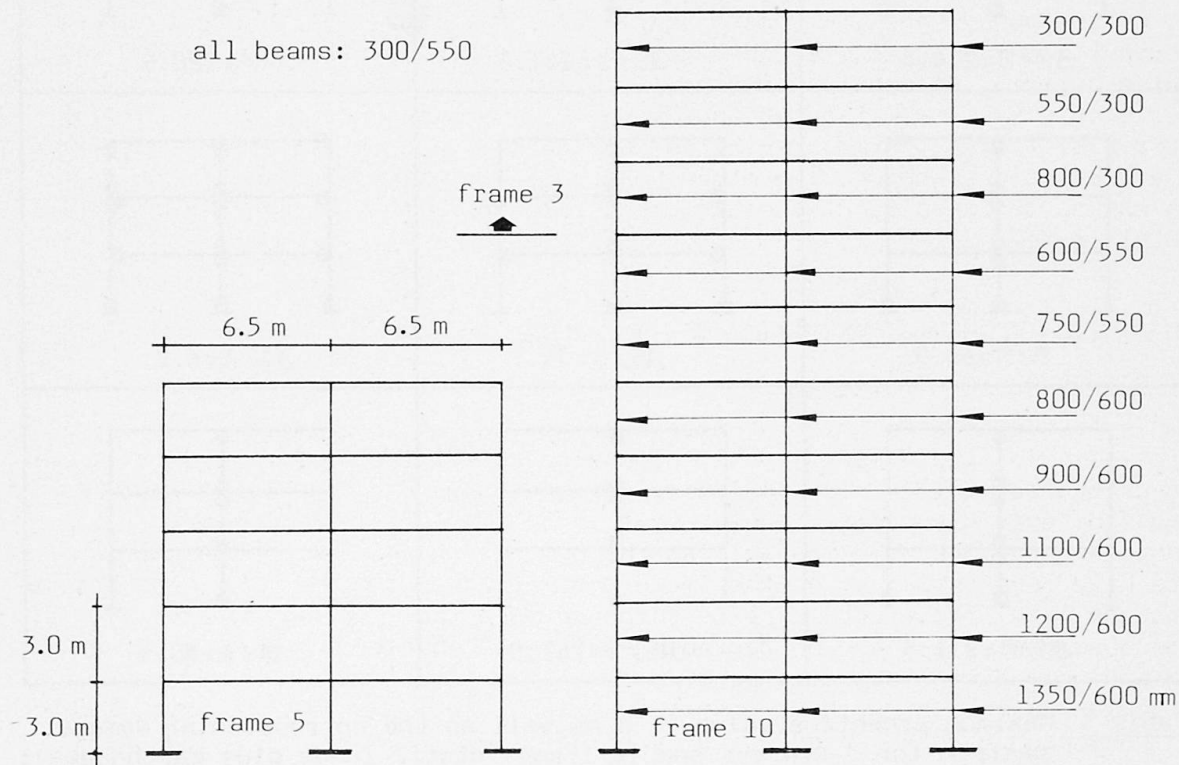


Fig. 1 Sample plane frames; low-, medium, and high rise

Percentage of stress increasing or decreasing (bend. mom., shear and axial force), is computed for " damage cases ", corresponding to various damaged sub-elements; some results are summarized on table 1.

On reference [2] a regression analysis has been developed in order to estimate the order of magnitude of such redistributions and in order to come to some temporary conclusions for civil engineering practice, as far as the "re-design" of damaged frames is concerned.

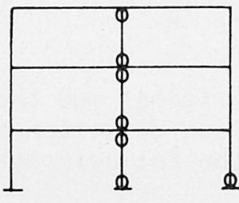
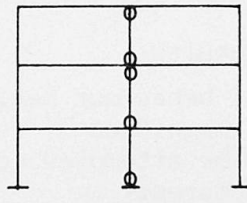
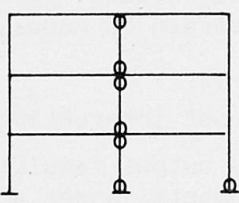
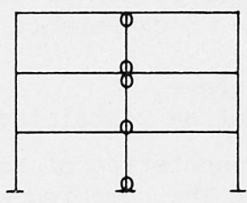
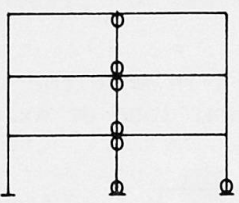
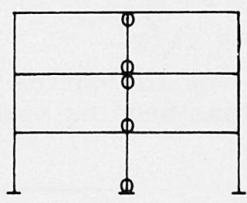
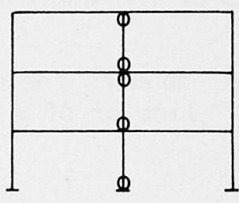
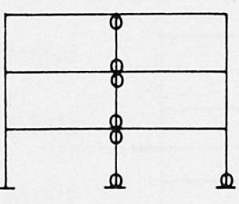
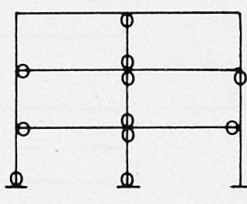
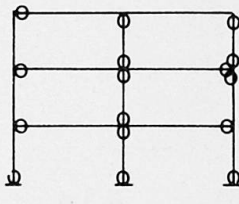
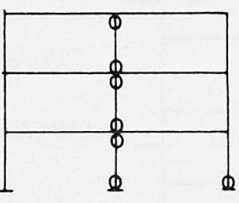
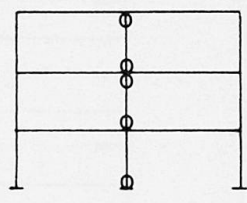
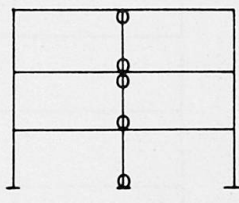
1 <sup>st</sup> B	 $\Delta M/M=145.1$	 $\Delta S/S=61.8$	
2 <sup>nd</sup> B	 $\Delta M/M=126.0$	 $\Delta S/S=61.8$	B: Bending moment S: Shear force A: Axial force
1 <sup>st</sup> CL	 $\Delta M/M=274.4$	 $\Delta S/S=241.5$	 $\Delta A/A=80.5$
2 <sup>nd</sup> CL	 $M/M=61.9$	 $\Delta S/S=34.7$	 $\Delta A/A=6.2$
3 <sup>rd</sup> CL	 $\Delta M/M=231.3$	 $\Delta S/S=241.5$	 $\Delta A/A=80.5$

Table 1 Maximum percentage value of R as well as the corresponding damage pattern for 3-storeys sample frame (static loads plus earthquake);  $\Delta E/E=0.9-0.99$ ; B: bay; CL: column line

### 2.3 Provisional conclusions

A detailed evaluation of percent value ( $\Delta R/R$ ) in redistributed action-effects shows that the effects are not concentrated by the damaged subelements: rather high percent changes in stresses are also in distant beams and columns. For instance, the stresses in the upper beam may be compared, due to the lower damages.

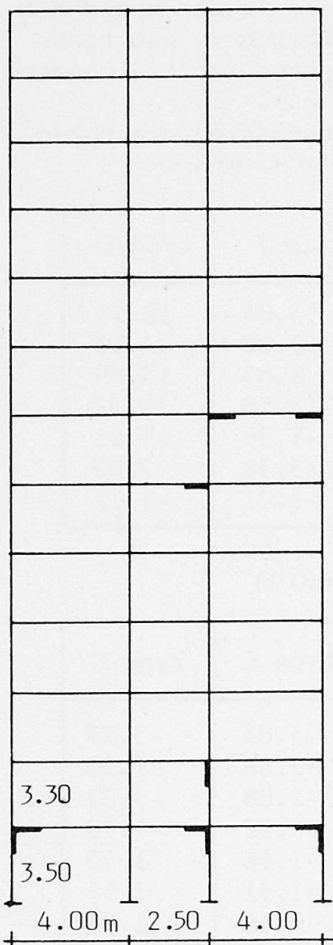
From the analysis and the results of the above extensive investigation it becomes evident that the redistribution of all action-effects of the studied R.C. frames after combined damage is practically negligible for up to 50% damages ( $\Delta E/E=0.50$ ). For damages more than 90% ( $\Delta E/E \div 0.90$ ) bending and shear loads redistribution is high. Also, the redistribution of action-effects for beams is considerably lower than for columns and it has to be taken into account for heavier damages. (i.e.  $\Delta E/E > 0.75$ ).

Another interesting general result of the above numerical analysis of various damaged R.C. frames is that natural period values are considerably higher for heavy damages (i.e.  $\Delta E/E > 0.75$ ) than for the original state; also the decrease is more drastic and effective for high than for low-rise buildings. This has to be taken into account in the case earthquake resistance analysis is needed for the damaged frame.

Finally, the higher the frame the lower the redistribution, the more damaged subelements the less the redistribution.

## 3. REDISTRIBUTION OF ACTION-EFFECTS AFTER REPAIR AND/OR STRENGTHENING

### 3.1 Procedure of investigation



In what follows, different types of interventions are examined, concerning tow-dimensional R.C. frames subjected to vertical and horizontal loads, in order to study the stiffness modification effects and the order of magnitude of redistribution of action effects on these repaired and/or strengthened frames. In particular, vertical loads have been taken into account by a static analysis, while horizontal (seismic) actions have been computed by means of a dynamic response-spectrum analysis, according to Italian Earthquake Resistante Code.

Three different frames have been investigated in order to cover different types of frames, i.e. a fairly high multi-story frame (12-storeys 3 bays), a middle rise frame (8-storeys 3 bays), and finally a low rise frame (3-storeys 12 bays). In Fig. 2 the general arrangement and the damaged sub-elements of high rise frame are presented.

It should be noted that such frames are not abstract and regularly shaped frames, but they are indeed practical examples of existing structures needing different interventions.

The different types of interventions taken into account are described in details in following:

Intervention type A: R.C. jackets (100 mm width), monolithic sections.

Intervention type B: The same as above, except than collaboration may not be assumed.

Intervention type C: Local replacement of damaged concrete and steel ("equal sections" method) see ref. [5].

Intervention type D: Bracing elements were introduced in a bay of the frame in all storeys.

Fig. 2 Sample frame C



- Intervention type E: Infill R.C. walls (100 mm width) were introduced in a bay (the largest one) of the frame in all storeys.
- Intervention type F: R.C. jackets (100 mm width) on all base floor columns, monolithic sections.
- Intervention type G: R.C. jackets (100 mm width) on all base and first floor columns, monolithic sections.

For interventions type A, B, and C only the damaged sub-elements (see Fig. 2) were repaired/strengthened. The bracing elements were normal "X"-type light steel elements; the infilling elements have been treated as four-node isoparametric finite elements, connected to the frame nodes (only 3th bay strengthened).

For low-rise 3-storeys 12-bays R.C. sample frame, different cases of strengthening were taken into account:

St-1 (strengthening case 1): 7 infilling elements were introduced per storey in all storeys.

St-2 (strengthening case 2): 3 infilling elements were introduced just as above

St-3 (strengthening case 3): 1 infilling elements were introduced just as above

### 3.2 Evaluation of the output results

Three different set of data have been considered for comparison of different stiffening systems, that is: periods, stresses and displacements.

As concern stresses, the output results were summarized in the same way adopted for the damaged frames (see 2.2).

### 3.3 Provisional conclusions

As long as redistribution of action effects is concerned, there is no marked difference between the middle-rise and the high-rise frames, although it has to be noted that strengthening of these low frames may lead to increased inertia loads due to decreased natural period values.

On tables 2,3 and 4 percent values of stress increasing or decreasing are shown, referred to high-rise frame (for all different types of intervention).

Element	type A	type B	type C	type D	type E	type F	type G
1st CL	-0.98	-0.77	-1.04	-23.32	-28.35	13.04	18.15
2nd CL	-1.92	-1.90	-1.62	-25.81	-30.47	8.82	14.99
3rd CL	4.71	3.35	1.93	-41.37	-52.58	8.55	13.89
4th CL	3.31	3.09	1.16	-66.31	-76.57	13.19	18.52
1st B	3.32	2.78	2.17	-11.09	-14.39	-5.35	-5.66
2nd B	11.80	9.96	8.62	-6.26	12.79	-3.38	-2.09
3rd B	4.12	3.84	2.53	-66.10	-66.85	-3.71	-5.22

Table 2 Percent values of bending moment increasing or decreasing

Element	type A	type B	type C	type D	type E	type F	type G
1st B	2.20	1.75	1.45	-6.51	-8.10	-3.03	-3.77
2nd B	6.29	5.28	5.08	-4.43	8.08	-2.86	-1.53
3rd B	2.68	2.55	1.81	-40.83	-39.56	-2.08	-3.02
1st CL	1.75	1.75	1.44	-14.84	-16.22	-1.22	-1.78
2nd CL	-1.10	-1.41	-0.83	-19.72	-22.49	-1.56	1.43
3rd CL	3.95	4.54	2.50	-41.32	-53.16	-1.31	1.53
4th CL	3.36	3.27	2.04	-76.35	-84.22	-0.68	-1.91

Table 3 Percent values of shear force increasing or decreasing



Element	type A	type B	type C	type D	type E	type F	type G
1st CL	0.44	1.02	0.25	-2.38	-2.77	-0.44	-0.38
2nd CL	0.43	0.24	0.12	-2.23	-9.22	1.20	2.05
3rd CL	1.22	0.66	0.57	3.37	-26.55	0.57	2.53
4th CL	0.39	0.23	-0.02	13.34	-29.08	-0.61	-0.43

Table 4 Percent values of axial force increasing or decreasing

It is obvious that comparison between different repairs or different structural stiffening are meaningful; it shall therefore attempt to compare type A, B, C results on one hand, and type D, E or F, G results on the other.

Concerning the first three types of repair, it could be noted that final aim is always the increasing of the sub-element stiffness, but in the cases A, B the geometric properties are changed, where in the case C the material property only is altered. Clearly, up-grading material results in linear strengthening of the section, as long as the Young modulus increases. The R.C. jackets, on the other hand, provide greatest benefits as long as cubic increasing of the section properties is achieved. Finally, it should be notice that the local strengthening generally causes an increasing of the stress values in terms of bending, shear and axial stresses at the extreme points, as could be easily shown by furtherly working out the presented results.

So, a complete survey of the upgraded structural behaviour ought to take into account other types of the results, also, just as the natural frequencies of the frame (which shows somehow a certain degree of dynamic stiffness) and its nodal displacements. Furthermore, the resulting behaviors under static and dynamic loads are significantly different, and the final benefits ought to be found in the final load condition ( static plus earthquake). This means that in the static analysis some effects may be non-positive, but this agrees with the final aim of the structural project, wich is to make the frame seismic-resistance.

The comparison between strengthening type D and E ( i.e. bracing or infilling elements) is a rather complex matter to be discussed here. Shortly, a considerable reduction of the action-effects may be expected (as much as 75%) on columns as well as for beams. A significant exception is given by elements next to the stiffned bay; this may be easily explained by the fact that the node rotations and translations are strongly reduced if such nodes are connected by a shear element, so that bending moments and other stresses increase, just as by a rigid external link.

For strenthening type F and G (i.e. jackets covering the entire height of the lower floors) the redistribution of the action-effects is considerable only for bending moments on columns (approx. 10+20% higher moments); for the beams of the frame the redistribution is negligible.

Two different probles arise for the foundations of type D and E strengthened frames; the use of bracing elements requires careful check and calculations of the load bearing capacity of the footings of columns adjacent to the braced bay, due to because of the increase of their axial load; one the other hand, the use of infilling elements requires a new heavy fondation.

Fairly significant values are shows on table 5, where the percentange of decreasing periods are recorded for the different cases and for the different periods. In the slender frames (frame C and B), the stiffening effects are "heavier" on the first period, while low rise frame (frame A) shows increasing advantages in the following periods. This accounts for a quite different behavior of different slenderness frames subjected to horizontal actions. Furthermore, the percentage plot in case A-Stl seems to be rather "flat", what may suggest that a "limit stiffening has been reached.

On the basis of these results, it should be emphasized that the period reduction



Frame	1st mode	2nd mode	3rd mode
A- St-1	12.0%	17.1%	18.5%
A- St-2	17.3%	21.1%	31.1%
A- St-3	27.3%	34.5%	48.1%
B-b	63.5%	48.5%	43.8%
B-p	55.7%	36.3%	33.8%
C-b	74.9%	55.9%	45.3%
C-p	68.7%	43.3%	31.9%

Slend. ratio	1st p.lower.
3.0 ÷ 4.0	0.25 ÷ 0.35
0.3 ÷ 0.4	0.60
0.2 ÷ 0.3	0.70

Table 6 Slenderness ratio and 1st period lowering

Table 5 Percentage of decreasing periods, assuming unstiffening values as 100%

may characterize a stiffening project. While the final aim of such an approach may be to include the period lowering (stiffened frame 1st period/unstiffened frame 1st period) in the seismic code for stiffened frames, some trial values can be nevertheless recorded here, as table 6 shows.

#### 4. FURTHER REMARKS

As it becomes evident from the results of the above extensive investigations, the redistribution of action-effects after interventions is considerably lower than case of damages.

The change in stiffness of the repaired/strengthened elements leads to a redistribution of action effects also in distant sections; as a consequence, some non-damaged areas might need a certain strengthening or, most probably, the action effects taken into account on building components to be repair/strengthened should be increased accordingly.

Also, due to differential creep between the existing "old" element and the additional "young" ones in case of R.C. jackets of columns (enlarged sections of walls, ecc), an additional redistribution of action-effects has to be taken into consideration.

#### BIBLIOGRAPHY

1. GREEK RECOMMENDATIONS for repair concrete structures. NTU of Athens, 1978
2. AVRAMIDOU N., CHRONOPOULOS M., A Parametric Study on the Redistribution of Action-Effects on Damaged R.C. Frames. Proceeding of Florence Constructions Institute, March 1982
3. GRAZZINI S., Redistribution of Action-Effects on R.C. Structures. Diploma Thesis, Institute of Constructions, Florence, March 1983
4. MELE M., Repair, Strengthening and Seismic Adjustment of R.C. Buildings Existing in Seismic Areas. L'Industria Italiana del Cemento, No. 11/1981
5. AVRAMIDOU N., FEI C., An Investigation of Mechanical Behaviour of Repaired R.C. Frames under Severe Repeated Loads. 7 W.C.E.E., Istanbul, 1980

## Concrete Columns Submitted to Cyclic Biaxial Bending

Colonnes en béton soumises à une flexion cyclique biaxiale

Stahlbetonstützen unter zweiachsialer zyklischer Biegebeanspruchung

### Claudio CECCOLI

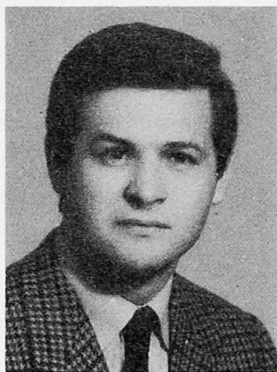
Prof.  
Ist. Tecn. delle Costruz.  
Bologna, Italy



Born in 1942, received his degree in Civil Engineering from Bologna University in 1965. Professor, he is now carrying out research activities in Structural Engineering. He is a member of CNR Committees.

### Maurizio MERLI

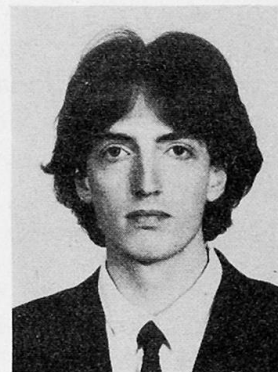
Assoc. Prof.  
Ist. Tecn. delle Costruz.  
Bologna, Italy



Born in 1946, received his degree in Civil Engineering from Bologna University in 1971. Professor associato, he teaches Tecnica delle fondazioni and is carrying out research activities in Structural Engineering.

### Secondo BIANCHI

Civil Engineer  
Univ. of Bologna  
Bologna, Italy



Born in 1957, received his degree in Civil Engineering from Bologna University in 1982. He is carrying out research in Structural Engineering.

## SUMMARY

This paper describes a theoretical evaluation of the fatigue strength behaviour of concrete plastic hinges, subjected to a constant axial load and cyclicly varying biaxial bending, with controlled curvatures. The low cycle fatigue strength is evaluated taking into account the «spalling» of concrete, the damage around cracks and the instability of compression bars. Various numerical examples are reported.

## RESUME

L'article traite d'un procédé analytique pour l'évaluation de la résistance à la fatigue des rotules plastiques en béton, sujettes à un effort normal et à une flexion biaxiale, avec déformations imposées. La résistance à la fatigue est évaluée en considérant l'épaufrure du béton, l'endommagement tout autour des fissures et l'instabilité des barres comprimées. Différents exemples numériques sont présentés.

## ZUSAMMENFASSUNG

Der Beitrag beschreibt ein analytisches Bemessungsverfahren für die Erfassung der Ermüdungsfestigkeit plastischer Betongelenke unter zyklischer Belastung mit Normalkraft und zweiachsialer Biegung. Der Widerstand wird unter Berücksichtigung der Abspaltung der Betonüberdeckung, der Schädigung in den Rissbereichen und der Instabilität der Druckbewehrung bestimmt. Es werden verschiedene Zahlenbeispiele gegeben.



## 1. INTRODUCTION

Referring to frames with sidesway it is well known that, in presence of seismic loads, columns must be considered among the most seriously involved structural elements. Because the seismic wave-directions are widely variable, it is necessary to consider the columns subjected to biaxial bending, cyclically varying during ground motion.

In general, because it is not economical to design columns in elastic range, it is advisable to make them able to absorb and dissipate seismic energy by ductile behaviour. If we examine the behaviour of a column in elasto-plastic range, it is evident that its performance relies on low cycle fatigue strength of plastic hinges which develop near the joints.

A high ductility factor for monotonic loads, i.e. a high ratio of ultimate curvature ( $\chi_{ult}$ ) to yielding curvature ( $\chi_y$ ), is not sufficient to assure that a structure can survive to exceptional seismic actions and, as a consequence, to cyclic loads. As a matter of fact it is well known that high ductility factor means good capacity to dissipate seismic energy during one cycle of loading, but it is not implied that, after many loading cycles, the energy dissipation capacity is still satisfactory. The performing of the ductile behaviour for sufficient numbers of cycles is necessary.

This problem seems very important for the definition of the validity of the well known structural models of hysteretic behaviour (for example Takeda model), and for the determination of the "residual safety" of a concrete building which survived to an earthquake.

This research concerns an analytical study of concrete beam-column elements, subjected to imposed cyclic curvatures; in addition this paper contains the stress-strain curves for the longitudinal reinforcement, which first reaches the yielding point. Then we examine the monotonic ductility variation according to the variation of neutral axis slope, to different steel contents, to various axial load levels, to different distribution of longitudinal steel bars and to some ratios  $\chi_{max}/\chi_{ult}$ . For the same parameters we have also determined the number of cycles before failure. On the basis of the above-mentioned results we have drawn the so-called low strength fatigue curves. This paper ends with some remarks about the behaviour of concrete elements subjected to complex imposed loading histories.

In the references we recall only the notes strictly relating to these subjects; in particular we refer to the note by Ceccoli-Benedetti-Bianchi [13] where you can find the fundamental criteria adopted for a preliminary analytical development.

## 2. DESCRIPTION OF THE PROCEDURE

This study has been developed choosing: (a) appropriate constitutive laws for steel and concrete, (b) geometric features of sections, (c) loading histories.

With reference to point (a), for steel we have substantially employed the well known constitutive law proposed by Ramberg and Osgood [1], in the form suggested by Goldberg and Richard [3] and modified by Giuffrè and Pinto [5] (Fig. 1a). The adopted model allows to take into account the "Bauschinger effect", but not the strain-hardening. The concrete envelope stress-strain curve is the one suggested by Kent and Park [6], but in the modified version by Okamoto. Starting from this model we have introduced some modifications, apportioned by the same Kent and Park, to consider the confinement of concrete by the hoops.

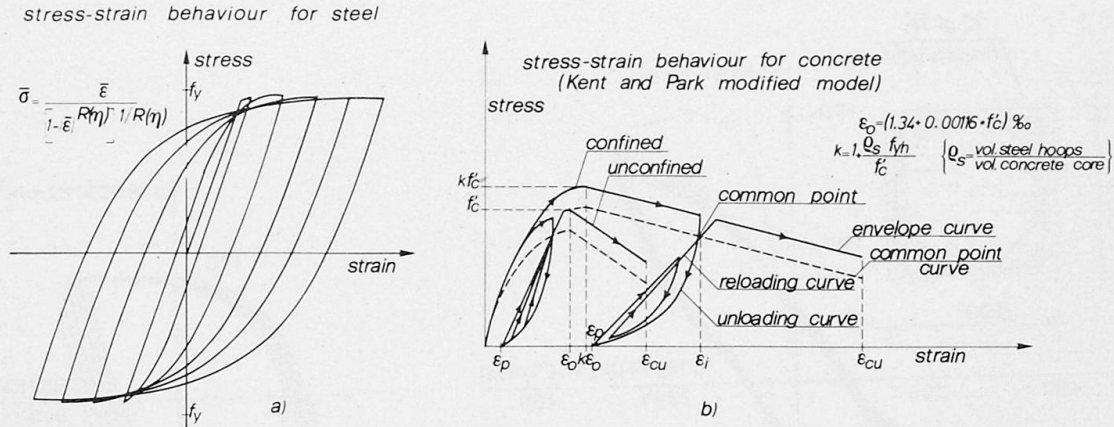


Fig. 1

The unloading branches begin on the before stated envelope curve and, with parabolic law, reach the residual plastic strain according to Karsan and Jirsa [4]; the reloading is imposed by a linear branch, passing through the "common point". The ultimate strain of the confined concrete, according to Corley [11], Bo and De Stefano [9], has been assumed as 7‰; the concrete spalling begins when a compressive strain of 3‰ is reached. The concrete damage, following the reversal strain, strictly connected to the shear transfer, has been introduced considering a progressive reduction of the envelope curve amplitude up to 5%, for each deformation cycle.

The value of the buckling load of the compressed bars, no more continuously bound, is evaluated considering the length of bond slip gradually increasing, according to Tassios and Yannopoulos [10]. At the end of bond slip length the bar is assumed partially clamped; the constraint is furnished by the elastic subgrade corresponding to the still intact concrete. The critical load is defined on the basis of the Shanley theory [2] and we consider the post-buckling of the bars.

Referring to point (c) we notice that, univocal references lacking, the variation of impressed curvatures has been considered of the sinusoidal type, with amplitude less than  $\chi_{ult}$ . We have also checked some different curvature variations, about which we are dealing at point 5.

On the basis of the previously described assumption, the hysteretic loops of plastic hinges may be determined by incremental procedure. At each step of impressed curvature, the equilibrium is reached by iterative loops for the cross section, decomposed in elemental areas. The behaviour of the plastic hinge under biaxial bending has been analyzed considering several slopes of the neutral axis. The amplitude of the bending moment connected to each curvature value, has been determined vectorially adding the moment components having directions coinciding with neutral axis and its normal (<sup>1</sup>).

### 3. DETAILED ANALYSIS OF THE BEHAVIOUR OF A PLASTIC-HINGE

Figure 2a shows the  $M-\chi$  plot for a plastic hinge (whose section is represented in

(<sup>1</sup>) The code developed by the Authors is implemented on the Digital VAX 11/780 of C.C.I.B. (Bologna), Engineering School.

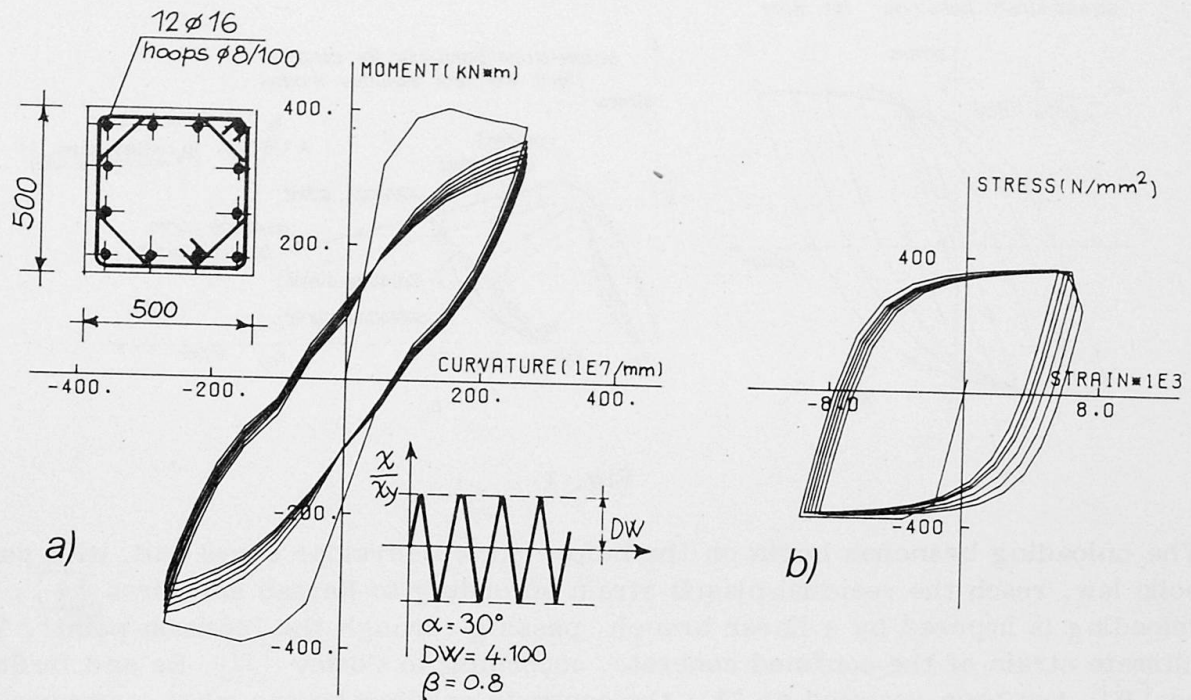


Fig. 2

the same figure) subjected to biaxial bending, with  $\alpha = 30^\circ$  and  $N = 0.2 bhf'_c$  ( $f'_c = 25 \text{ N/mm}^2$ ). The maximum curvature reached at each cycle is  $0.8 \chi_{ult}$ . Figure 2b shows the  $\sigma$ - $\epsilon$  plot for the bar which first reaches the yielding point.

The  $M$ - $\chi$  plot, at first linear as materials are stressed in the elastic range <sup>(2)</sup>, shows a pronounced decay of load carrying capacity when steel is yielded. Spalling stops the increase of the resisting moment and, because of the triangular shape of the compressive zone, the decrease of the moment carrying capacity is gradual. After the first quarter of cycle, the bending moment decreases according to the decreasing of the curvature; at this stage the  $M$ - $\chi$  plot is essentially governed by the steel in tension, because, during unloading, the concrete load carrying capacity is quickly lost.

When bending moment changes sign, at a first stage moment capacity is high because concrete in the previous tensioned zone is reloaded and steel in the previous compressed zone is unloaded. Subsequent decreasing stiffness follows from spalling and softening of  $\sigma$ - $\epsilon$  curve of concrete.

The  $M$ - $\chi$  plot shows a slight pinching which is characteristic of plastic hinges subjected to "moderate" axial load. According to Park and Paulay [7], this is due to the fact that the section is completely cracked. The equilibrium of internal forces is assured by the compressive stresses which, owing to steel hysteresis, are applied to the reinforcing bars still subjected to positive strains.

The second cycle of the imposed curvatures shows a clear softening of the resisting moment due to the lower answer of the compressed concrete, to the spalling and to the progressive damage. During the subsequent cycles we note an increasing re-

<sup>(2)</sup> The step from intact section to cracked section does not appear because of the small number of points selected in each loading cycle.

duction of the maximum moment owing to the buckling of the compressed bars, as it appears on  $\sigma$ - $\epsilon$  plot.

#### 4. ANALYSIS OF THE NUMERICAL RESULTS

The geometrical and mechanical characteristics of the plastic hinges we have examined are described in table 1. Preliminarily we have studied the behaviour of the various plastic hinges under gradually increasing controlled curvature.

Table 1

Unit	$b \times h$ (mm $\times$ mm)	$f'_c$ (N/mm <sup>2</sup> )	$f_y$ (N/mm <sup>2</sup> )	$n$	$\phi_{sl}$	$\rho_{sl}$	$d_{sh}$	$\phi_{sh}$	$\rho_{sh}$
1	300 $\times$ 300	25	380	3	12	1.00	100	8	1.20
2	300 $\times$ 300	25	380	3	14	1.37	100	8	1.20
3	300 $\times$ 300	25	380	4	12	1.51	100	8	1.24
4	300 $\times$ 300	25	380	4	14	2.05	100	8	0.95
5	300 $\times$ 300	25	380	4/5	14	1.19	100	8	0.95
6	500 $\times$ 500	25	380	4	16	0.96	100	8	0.73

$n$  = number of longitudinal bars along each side;  $\phi_{sl}$  = longitudinal bar diameter;  $\rho_{sl}$  = % of longitudinal reinforcement;  $d_{sh}$  = hoop spacing;  $\phi_{sh}$  = hoop diameter;  $\rho_{sh}$  = % of transverse reinforcement.

Figs. 3 and 4 show the  $M$ - $\chi$  plots for unit 2 and 5 under axial load equal to  $0.2 bhf'_c$ . For unit 2 we note a progressive reduction of maximum bending-moment and ultimate curvatures when  $\alpha$  increases: both the phenomena are related to the trapezoidal or triangular shape of the compressed zone, and the consequent reduction of internal lever arm. When  $\alpha = 0$  (simple bending) the spalling is much more evident than when  $\alpha \neq 0$  (biaxial bending); in fact the damaged concrete part in the former case is much more noticeable than in the latter. For unit 5 the  $M$ - $\chi$  plots are strongly influenced by the side ratio and, as foreseen, the less stiffness the more ductility.

In fig. 5, relating to unit 1, we show the number of cycles preceding failure and the ductility factor when the slope  $\alpha$  of neutral axis is varying. Increasing  $\alpha$ , the ductility decreases, but the worsening of behaviour during seismic loads is only apparent because, at the same time, the number of cycles increases. The reduction of the ductility factor is essentially connected to a quicker reduction of  $\chi_{ult}$  com-

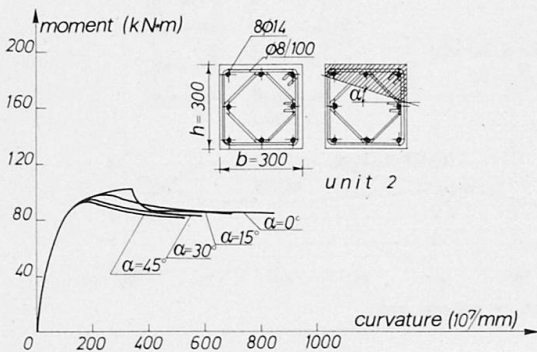


Fig. 3

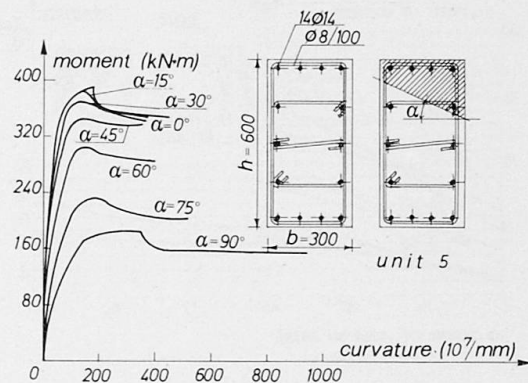


Fig. 4

pared with  $\chi_y$ . In other words the reduction of  $\chi_y$  versus the increment of  $\alpha$  is due to the triangular shape of the compressed zone, but the reduction of  $\chi_{ult}$  is more pronounced because, in addition to the above mentioned triangularization, we also have the reduced efficiency of compressed concrete, whose stress-path follows the failing branch. The increment of number of cycles preceding failure is related to the gradual buckling of the compressed bars.

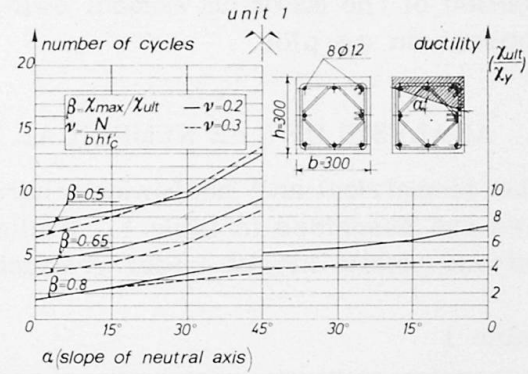


Fig. 5

When the axial load increases, monotonic ductility factor decreases, but not always when dealing with cyclic loads. For  $\beta = (\chi_{max}/\chi_{ult}) \leq 0.5$  and  $\alpha > 15^\circ$  the fatigue strength increases because the increment of axial load reduces the negative influence on the triangular shape of compressed zone. When  $\alpha \leq 15^\circ$  the triangularization of the compressed zone is not important and for  $\beta > 0.5$  from the beginning we have an extended spalling; at this moment a remarkable lowering of the neutral axis is necessary, but beyond a certain level the widening of the compressed zone does not counterbalance the loss of the cover concrete and we have an increment of the compressive strains. Similar trends are evident for the remaining units.

It may be interesting to notice that increasing the number of bars along each side, when  $\alpha < 15^\circ$ , we have an increase of the number of cycles preceding failure (fig. 6). The plots relating to unit 5 (fig. 7), taking into account the particular shape of the section, are slightly different, but it is confirmed that generally, when ductility reduces, we have an increment of the number of cycles before failure and vice-versa.

The results of the numerical developments can be handled to draw the so-called fatigue curves; these curves, concerning unit 1 and for different  $\alpha$  values, are shown in fig. 8. Considering our forcibly limited analysis, the fatigue curves must be considered indicative only, but it is clear that, with adequate experimental tests, they will be useful to evaluate the ductility factor necessary during an earthquake with a fixed number of deformation cycles. About the subject it is worthwhile no-

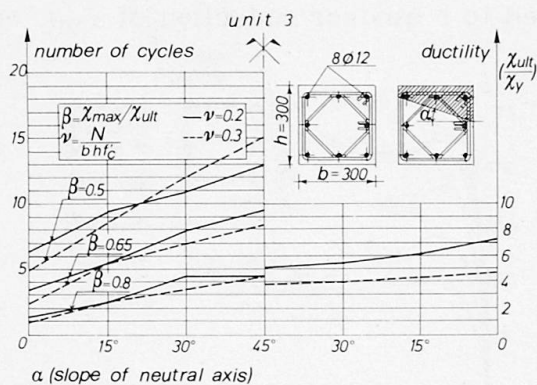


Fig. 6

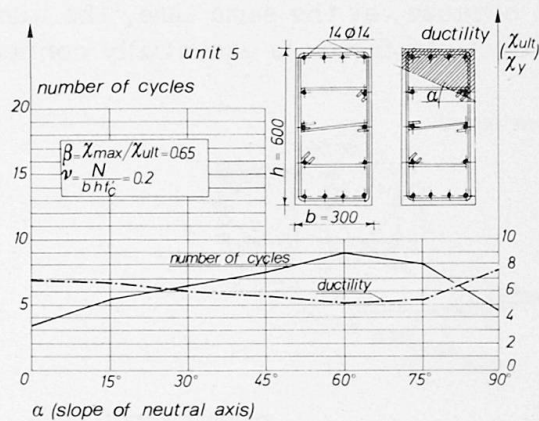


Fig. 7



ting that the drawn curves, taking into account the percentual damage imposed for each cycle, do not admit an asymptote and however, with the same ductility factor, the number of cycles substained under biaxial bending is always higher.

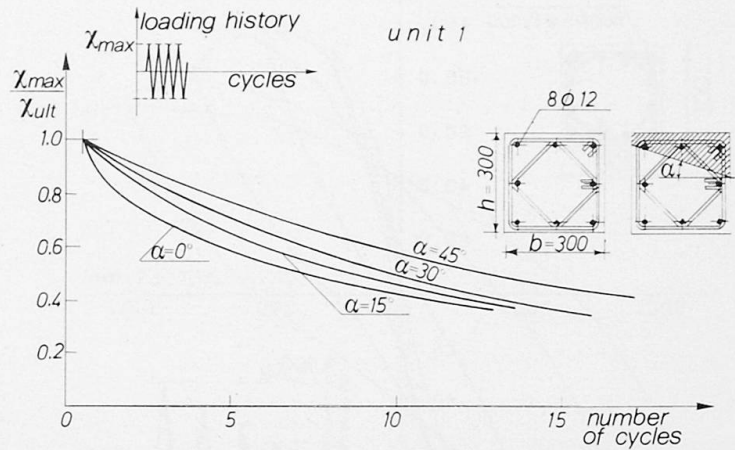


Fig. 8

### 5. IMPRESSED CURVATURES WITH A LAW NOT SIMPLY SINUSOIDAL

Referring to Bertero's considerations [8], we have analyzed, as an exemplification, loading histories able to define with greater reliability the static vicissitudes connected to the development of seismic phenomena.

In fig. 9 we have drawn the  $M-\chi$  and  $\sigma-\epsilon$  plots for a plastic hinge subjected to a loading history characterized by maximum amplitudes different in the two directions; in brief the seismic effect is superimposed to an initial curvature due to the permanent loads. When  $\alpha = 45^\circ$  we get 10 cycles against 13 which we find for a sinusoidal loading history with an amplitude equal to half the sum of the maximum excursions; when  $\alpha$  increases we have a slight efficiency loss of the low cycle fatigue strength.

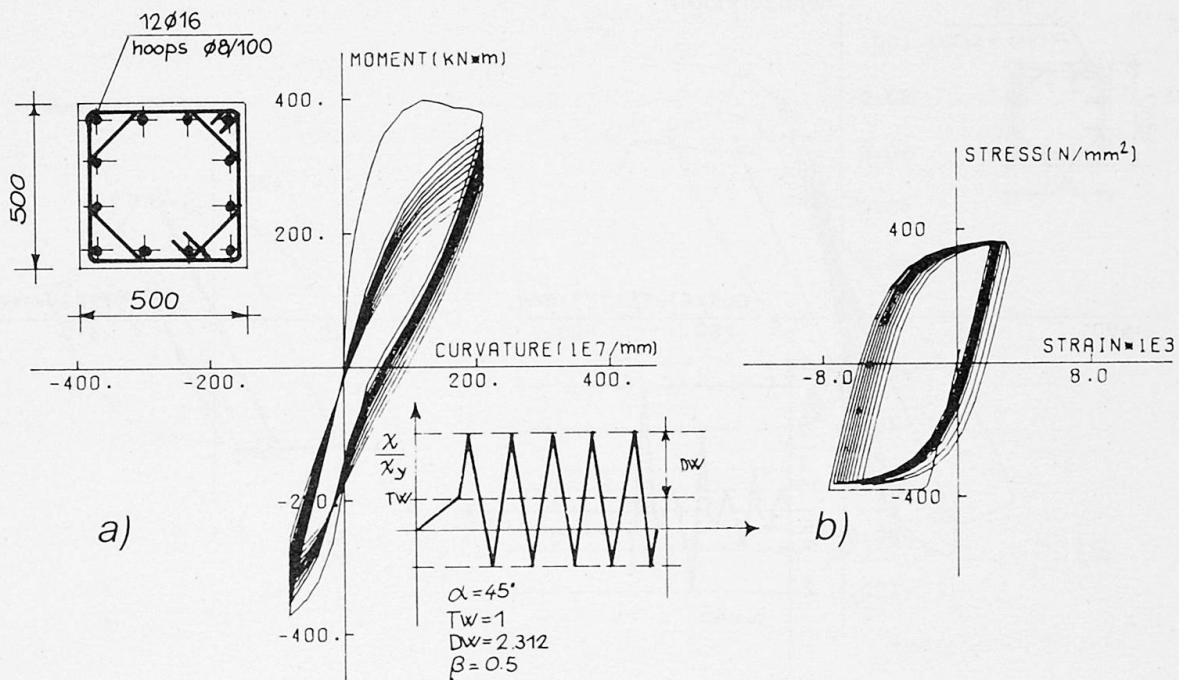


Fig. 9

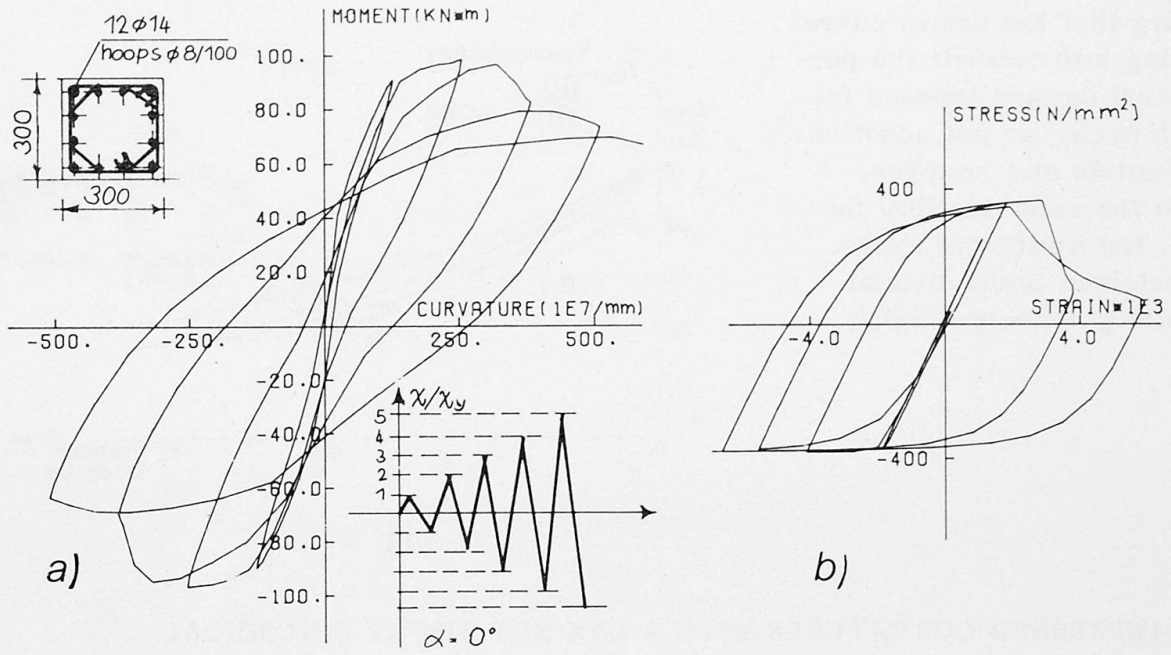


Fig. 10

In fig. 10 we consider loading histories varying according to a sinusoidal law with a gradually increasing amplitude. The number of cycles before failure results independent of  $\alpha$ ; when  $\alpha = 0$  we however note a widening of hysteresis loops, probably due to a more efficient contribution of the compressed bars which are distant from the neutral axis.

The plots in fig. 11, referring to cyclic sinusoidal curvatures gradually increasing

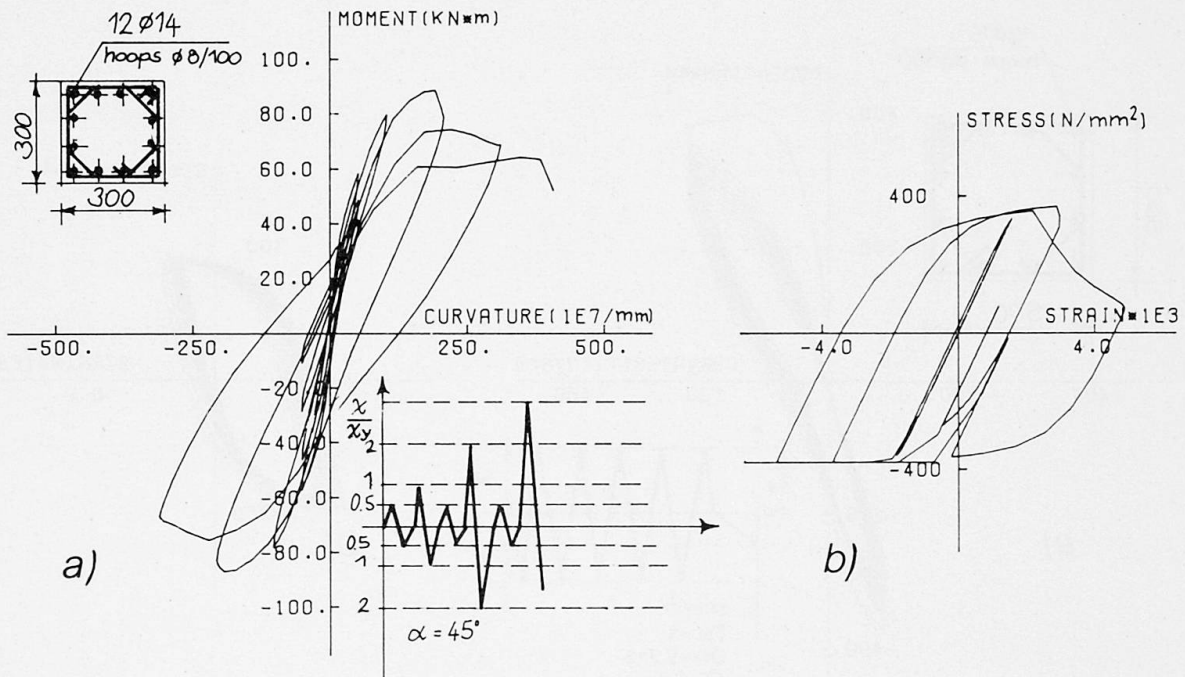


Fig. 11



and alternate to cyclic sinusoidal curvatures with a low amplitude, are difficult to comment in a few words.

## 6. SUGGESTIONS TO FURTHER RESEARCHES

We consider it very interesting to develop the study to draw the low strength fatigue curves referring to a large number of plastic hinges with different geometrical and mechanical properties. When we deal with loading histories of variable amplitude the problem is difficult and so it is necessary to introduce different criteria of study.

However on the one side some experimental checks of the results and, on the other side, refinements of the techniques of numerical simulation are necessary, particularly referring to shear influence and post-buckling of compressed bars.

ACKNOWLEDGEMENTS: The Authors are much indebted to Professor P. Pozzati, Director of the Institute of "Tecnica delle costruzioni", Bologna, Engineering School, for his advice and encouragement.

## REFERENCES

1. RAMBERG W., OSGOOD W.R., Description of stress-strain curves by three parameters. Technical Note 902, National Advisory Committee for Aeronautics, July 1943.
2. SHANLEY F.R., Strength of Materials. McGraw-Hill, New York, 1957.
3. GOLDBERG H., RICHARD W., Analysis of nonlinear structures. Journal of Structural Division, ASCE, August 1963.
4. KARSAN I.D., JIRSA J.O., Behaviour of concrete under compression loadings. Journal of the Structural Division, ASCE, December 1969.
5. GIUFFRE' A., PINTO P.E., Il comportamento del cemento armato per sollecitazioni cicliche di forte intensità. Giornale del Genio Civile, maggio 1970.
6. KENT D.C., PARK R., Flexural members with confined concrete. Journal of the structural division, ASCE, July 1971.
7. PARK R., PAULAY T., Reinforced Concrete Structures. J. Wiley and Sons, New York, 1975.
8. BERTERO V.V., Seismic behaviour of structural concrete linear elements (beams, columns), and their connections. Proceedings 14th Symposium AICAP/CEB, Structural Concrete under Seismic Actions, Rome, May 1979.
9. BO G.M., De STEFANO A., Il calcestruzzo leggero strutturale nell'edilizia in zona sismica. L'Industria Italiana del Cemento, marzo 1980.
10. TASSIOS T., YANNOPOULOS P., Analytical studies on reinforced concrete members under cyclic loading based on bond stress slip relationship. ACI Journal, May-June 1981.
11. PARK R., PRIESTLEY J.N., GILL W.D., Ductility of square-confined concrete columns. Journal of the Structural Division, ASCE, April 1982.
12. CECCOLI C., BENEDETTI A., Richiami sulla duttilità delle strutture di c.a. e questioni applicative. Proceedings 14th Symposium ANIAI, Bologna, luglio 1982.
13. CECCOLI C., BENEDETTI A., BIANCHI S., Contributo all'analisi teorica del comportamento a fatica oligociclica di conci di trave di c.a. doppiamente armati pressoinflessi. Proceedings 13rd Symposium CTE, Verona, settembre 1982.

Leere Seite  
Blank page  
Page vide

## Strength of Steel Frame Structures in Fire

Résistance au feu des structures en acier

Feuerwiderstand von Stahlkonstruktionen

### Shunsuke BABA

Assoc. Prof.  
Nagoya Univ.  
Nagoya, Japan



Shunsuke Baba, born 1949, received his degree of Dr. Eng. in 1977 at Nagoya Univ. by thesis titled «On the Structural Safety based on Extremum Theory». He has worked at Dep. of Geotech. Eng. as Assoc. Prof. for 4 years, now has a deep interest in the problem of structural behaviour in high temperature environments.

### Toshiya YAMAMOTO

Eng.  
Sumitomo Heavy Ind.  
Tokyo, Japan



Toshiya Yamamoto, born 1959, received his Master degree in 1983 at Nagoya University.

### SUMMARY

The strength of steel frame structures during and after a fire are evaluated using a finite element thermo-visco-elastoplastic analysis based on the original experimental data. Strengthening of the post-fire structure is also described.

### RESUME

La résistance des structures en acier pendant et après un incendie est évaluée sur la base de l'analyse thermo-visco-élastoplastique des éléments finis. Le renforcement de la structure après un incendie est aussi décrit.

### ZUSAMMENFASSUNG

Der Feuerwiderstand von Stahlkonstruktionen wird mit Hilfe einer auf Finiter Elemente beruhenden Analyse berechnet. Die Verstärkung von Konstruktionen nach einer Feuereinwirkung wird ebenfalls beschrieben.



## 1. INTRODUCTION

In the case that a steel frame structure is exposed by fire, a strength of the structure decreases during the time fire is spreading. After the fire has been extinguished, a strength of structure called "post-fire strength" is less than the initial design strength before fire, which is called "pre-fire strength".

First, decrease of the strength during fire is calculated by a numerical analysis based on the original test data obtained by the authors. Decrease of the strength is evaluated by a decrease of "degree of safety for the structural collapse".

Second, the relationship between "fire spreading time" and post-fire strength is provided, where the fire spreading time implies total time (counted by minutes) from an outbreak of the fire until a start of fire extinguishing operations.

Third, strengthening of the post-fire structure is performed so as to recover the initial (pre-fire) strength.

## 2. NUMERICAL CALCULATION

### 2.1 Thermo-Visco-Elastoplastic Behavior

At an early stage of fire, when the temperature is less than 300 degrees C, deformation of a steel frame structure is caused by a combination of elastic, plastic and thermal strains. When the temperature reaches the 400s, creep strain holds a part of total deformation, and in the 500s - 600s, half of the total deformation is caused by the creep strain. Therefore effect of the creep needs to be included in the numerical analysis of structures in fire.

Steel material in high temperature is assumed here to behave as a thermo-visco-elastoplastic body. It implies that the behavior of steel is described as an independent superposition of a thermo-elastoplastic and a creep behaviors [1].

### 2.2 Constitutive Relations

For a thermo-visco-elastoplastic body it is assumed that the strain increment  $de_{ij}$  can be represented in the form of the sum of elastic, plastic, thermal and creep strain increments, i.e.,  $de_{ij}^E$ ,  $de_{ij}^P$ ,  $de_{ij}^T$ ,  $de_{ij}^C$ , as

$$de_{ij} = de_{ij}^E + de_{ij}^P + de_{ij}^T + de_{ij}^C \quad [1]$$

in which each strain increment is described as

$$\begin{aligned} de_{ij}^E &= [(1+p)/E] ds_{ij} - (p/E) ds_{kk} \delta_{ij}, \quad E = E(T, \dot{\epsilon}) \\ de_{ij}^P &= \Lambda_p s_{ij}^* \\ de_{ij}^T &= a dT \delta_{ij} \\ de_{ij}^C &= \dot{\epsilon}_{ij}^C dt \end{aligned} \quad [2]$$

where  $E$  is elastic modulus (a function of temperature  $T$  and equivalent strain rate  $\dot{\epsilon}$ );  $p$ , Poisson's ratio;  $\delta_{ij}$ , Dirac's delta;  $a$ , coefficient of thermal expansion;  $T$ , temperature; and  $s_{ij}^*$ , stress deviator.

Plastic strain increment  $de_{ij}^P$  is described as a product of positive scalar function  $\Lambda_p$  and normal to yield surface  $\partial f / \partial s_{ij}$ , by assuming an associated flow rule; where  $f$  is a yield surface. Now the material is a structural steel, and von Mises yield criterion can be applied to the yield surface  $f$ , that is,  $f$  is described as follows by assuming an isotropic strain-hardening;

$$f = \left( \frac{3}{2} s_{ij}^* s_{ij}^* \right)^{1/2} - \bar{s}_y(T, \bar{\epsilon}^P, \dot{\epsilon}) \quad [3]$$



$\bar{e}^P$  but also by temperature  $T$  and equivalent strain rate  $\dot{\bar{e}}$ . Using Prager's consistency condition  $df=0$  to Eq.[3], we get

$$df = \frac{3}{2\bar{s}_y} s_{ij}^* ds_{ij}^* - \frac{\partial \bar{s}_y}{\partial T} dT - \frac{\partial \bar{s}_y}{\partial \bar{e}^P} d\bar{e}^P - \frac{\partial \bar{s}_y}{\partial \dot{\bar{e}}} d\dot{\bar{e}} = 0$$

and by introducing the relations such as

$$s_{ij}^* ds_{ij}^* = \frac{2}{3} \bar{s}_y d\bar{s}_y, \quad d\bar{e}^P = \frac{2}{3} \Lambda_p \bar{s}_y$$

the following relation is finally obtained;

$$d\bar{s}_y - \frac{\partial \bar{s}_y}{\partial T} dT - \frac{\partial \bar{s}_y}{\partial \bar{e}^P} \frac{2}{3} \Lambda_p \bar{s}_y - \frac{\partial \bar{s}_y}{\partial \dot{\bar{e}}} d\dot{\bar{e}} = 0$$

Undefined positive scalar  $\Lambda_p$  in Eq.[2] is thus determined as follows [2].

$$\Lambda_p = (d\bar{s}_y - \frac{\partial \bar{s}_y}{\partial T} dT - \frac{\partial \bar{s}_y}{\partial \dot{\bar{e}}} d\dot{\bar{e}}) / (\frac{2}{3} \bar{s}_y \frac{\partial \bar{s}_y}{\partial \bar{e}^P}) \quad [4]$$

Creep strain increment  $de_{ij}^C$  is represented approximately as a product of creep strain rate  $\dot{e}_{ij}^C$  and time increment  $dt$  as shown in Eq.[2] (see Ref. [3]). Creep strain rate  $\dot{e}_{ij}^C$  is described in the following convenient style, by using an equivalent creep strain rate  $\dot{\bar{e}}^C$  [4];

$$\dot{e}_{ij}^C = \Lambda_c s_{ij}^*, \quad \Lambda_c = \frac{3}{2\bar{s}} \dot{\bar{e}}^C(T, \bar{s}) \quad [5]$$

in which  $\dot{\bar{e}}^C$  is a function of temperature  $T$  and stress level represented by an equivalent stress  $\bar{s}$ .

### 2.3 Material Properties

As described in 2.2, elastic modulus  $E$ , equivalent yield stress  $\bar{s}_y$  and equivalent creep strain rate  $\dot{\bar{e}}$  are treated here as functions of temperature  $T$ , equivalent plastic strain  $\bar{e}^P$ , equivalent strain rate  $\dot{\bar{e}}$  and equivalent stress  $\bar{s}$ . These functions are determined by a series of strain-controlled high-temperature tension tests and stress-controlled high-temperature creep tests organized by the authors [5]. The test specimens are cut from a web of rolled H-beam made by SS41 steel whose nominal tensile strength is 41 kg/mm<sup>2</sup> (4.02 MPa).

### 2.4 Heat Transfer Analysis [7]

Temperature distribution in the section of non-protected steel frame members are calculated by two-dimensional finite element analysis. Standard temperature-time curve specified for the fire resistance test [6] is used in the calculations, and the heat transfer from heat source to the member is given by a radiation and a convection.

### 2.5 Structural Analysis [7]

Three-nodes seven-degrees-of-freedom beam-element is used on the basis of the simplest assumptions such as

- small deformation
- in-plane deformation
- Bernoulli-Euler's assumption.

Original Newton-Raphson technique is used for a convergence of iterative calculations.



### 3. NUMERICAL RESULTS

One-story one-span steel frame structure with fixed ends as shown in Fig.1 is exposed by fire. The cross-section of the frame member is represented in Fig.1, where the boundary conditions on radiation and convection are also indicated. Uniform load  $q_{i0}$  is applied to a horizontal member of the frame; the magnitude is determined to be 60% of an elastic limit load (first yield load)  $q_{y0}$ , for which the yield region occurs at someplace of the members at the first time. The definitions on these loads are also denoted in Fig.1.

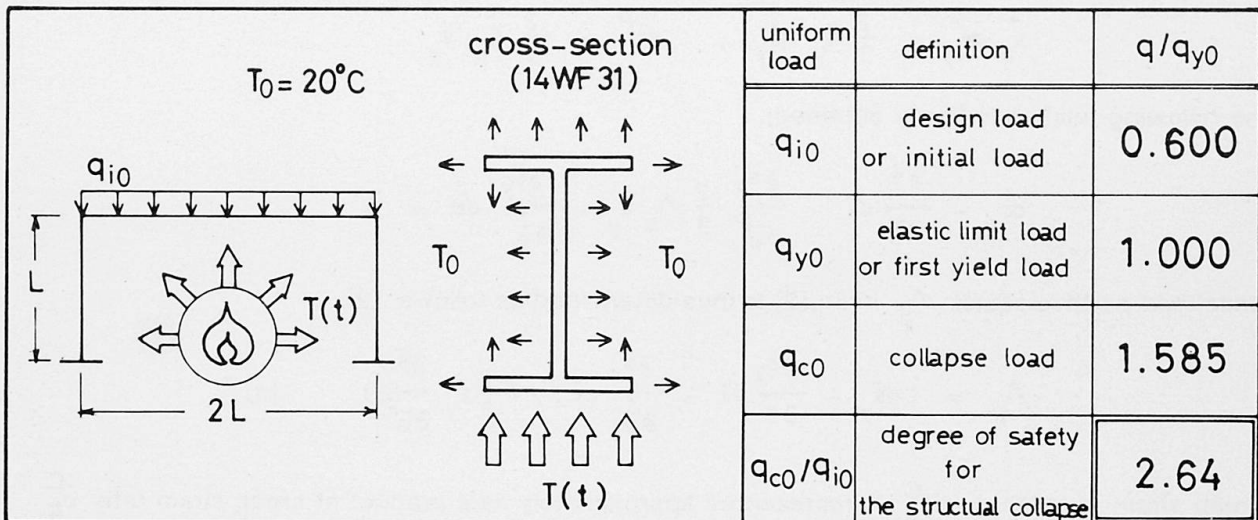


Fig.1 Dimensions of Steel Frame Structure and Definitions of Initial Uniform Loads  $q_0$ .

Thermo-visco-elastoplastic analysis is applied to the structure, and the following calculations are conducted;

(1) Progress of deformation and reduction of strength during fire:

a) Vertical displacement  $d_v$  at the center of horizontal member is shown in Fig.2(a) and horizontal displacement  $d_h$  at the corner is shown in Fig.2(b), where the fire spreading time  $t_f$  is taken as the abscissa.

b) Load-displacement ( $d_v$ ) curves are shown in Fig.3(a). Using the results, degrees of safety for the structural collapse are indicated in Table 1(a) in the case that fire spreading times  $t_f$  are 10, 20, 25 and 30 minutes, where they are defined as the ratios of collapse loads  $q$  at  $t_f=10, 20, 25$  and 30 minutes to the initial design load  $q_{i0}$ .

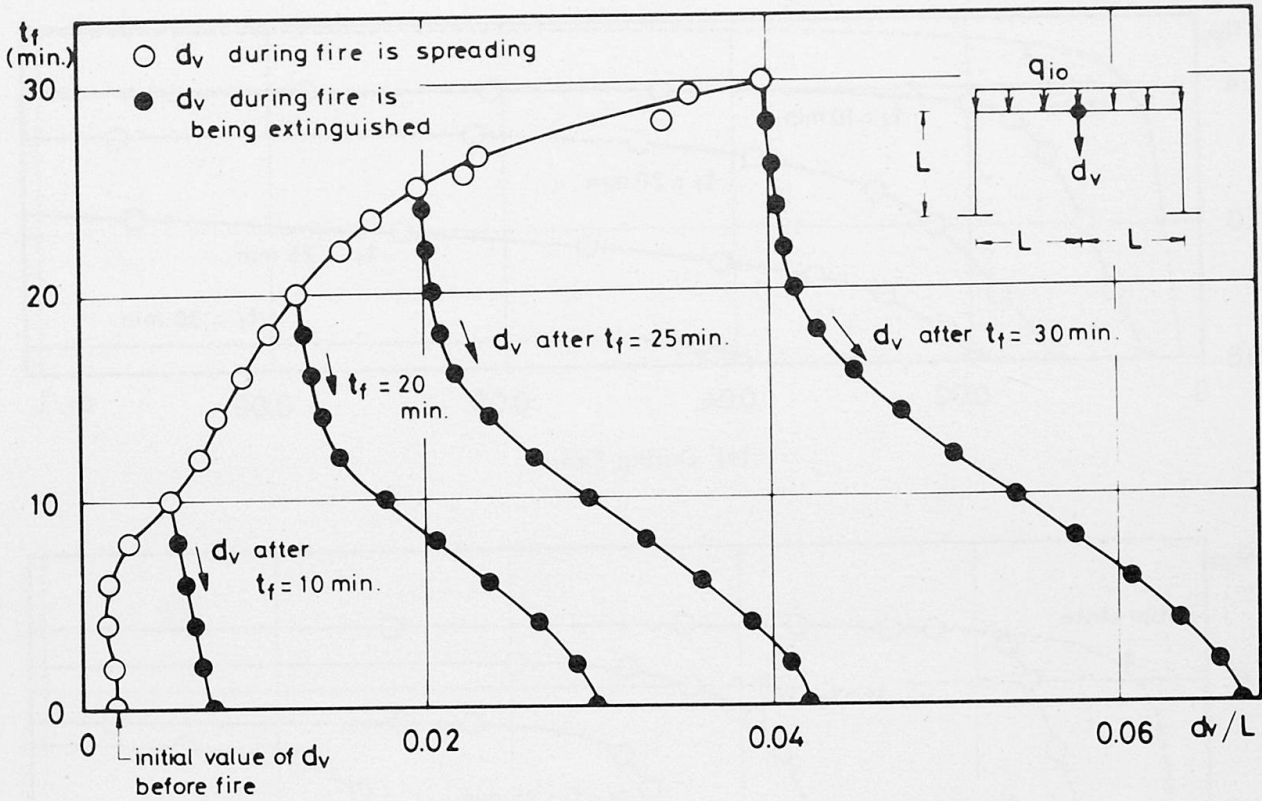
(2) Further progress of deformation and recovery of strength after fire:

a) Displacements  $d_v$  and  $d_h$  during the time fire is being extinguished are shown in Fig.2(a) and (b), respectively, where the ordinate ( $t_e$ ) has an opposite direction to the original ordinate ( $t_f$ ). The time necessary for fire extinguishing [ $t_e$ ] is assumed to be equal to the fire spreading time  $t_f$ , i.e.,  $t_e = t_f$ .

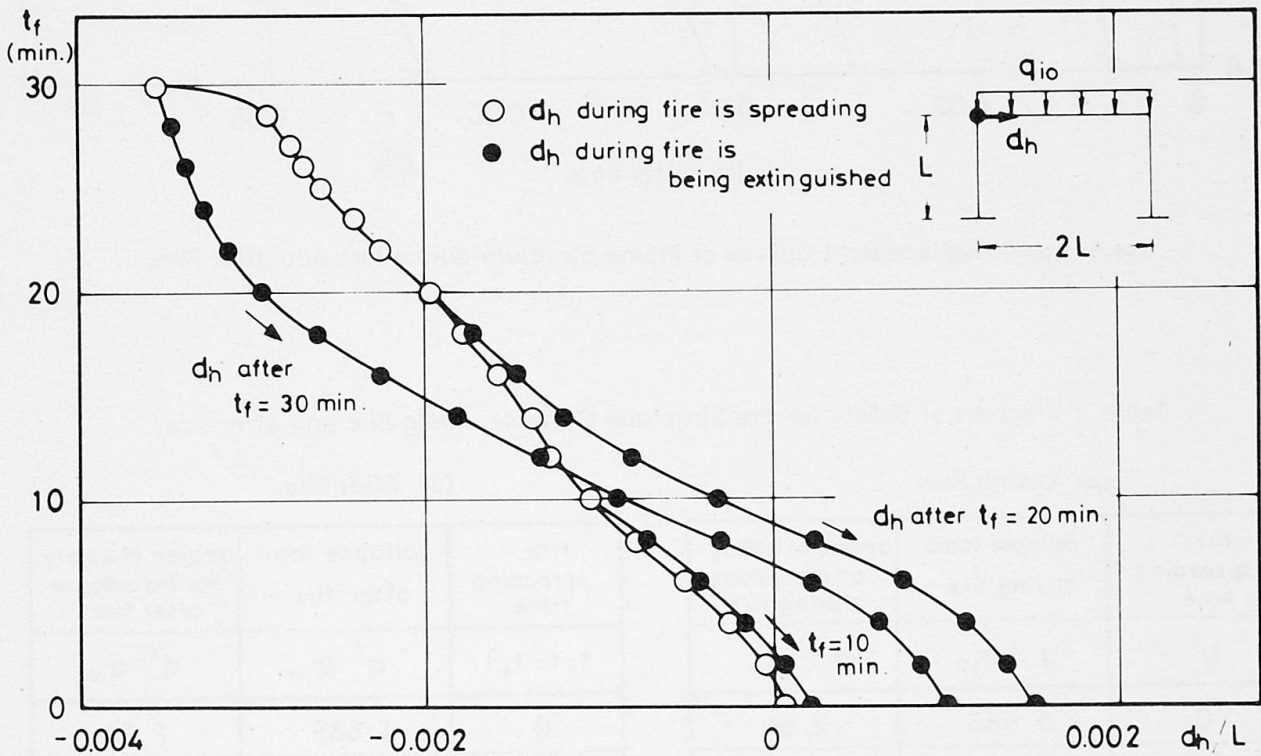
b) Load-displacement ( $d_v$ ) curves are shown in Fig.3(b). Using the results, degrees of safety in the case of  $t_f = t_e = 10, 20, 25$  and 30 minutes are indicated in Table 1(b), where the degrees of safety are defined as the ratios of collapse loads  $q^*$  at  $t_e = 10, 20, 25$  and 30 minutes to the initial design load  $q_{i0}$ .

(3) Strengthening of post-fire structure:

a) Lengths of strengthening plates, necessary for a recovery of the initial strength after fire, are indicated in Table 2.

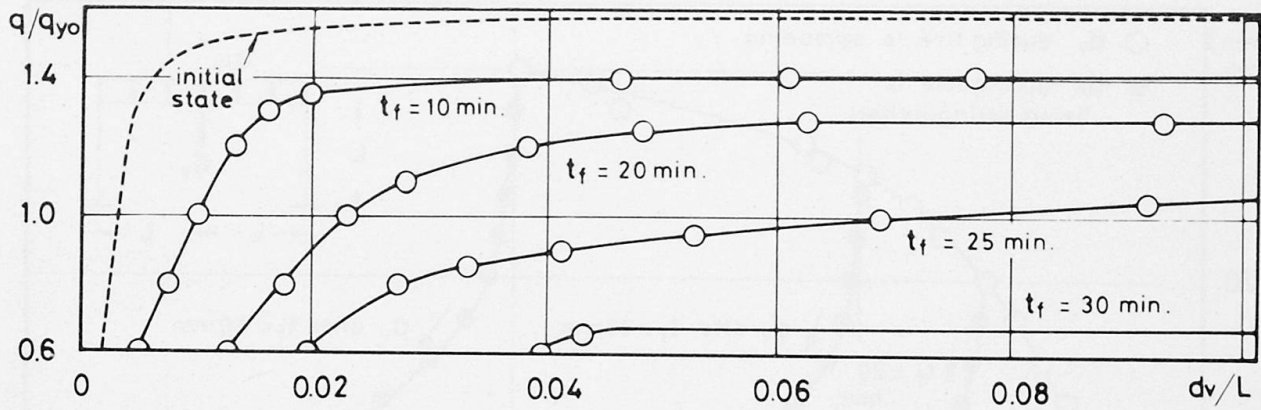


(a) Vertical Displacements ( $d_v$ ) at Center.

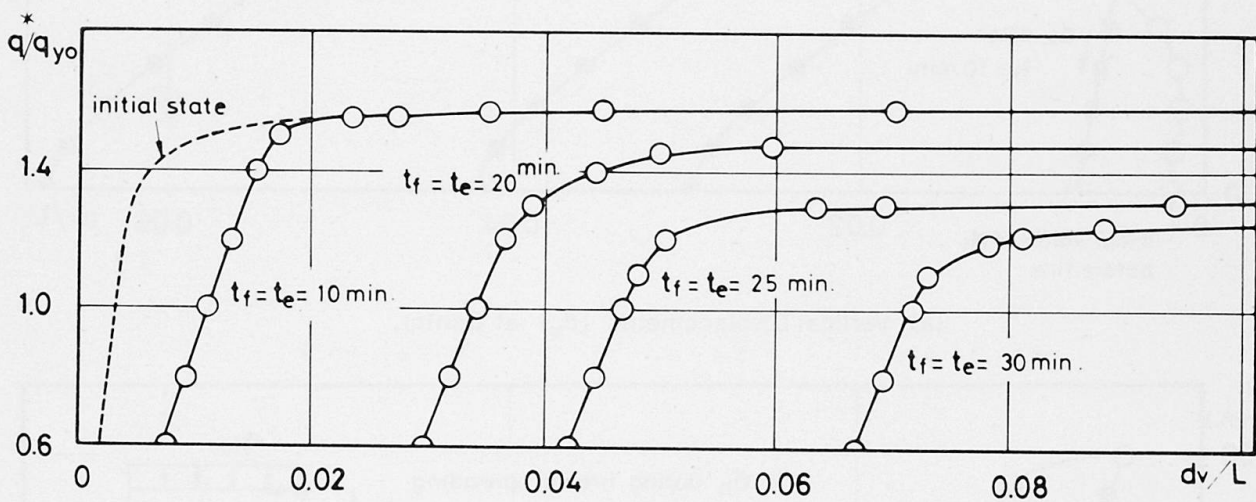


(b) Horizontal Displacements ( $d_h$ ) at Corner.

Fig.2 Time-Displacement Curves of Frame Structure during Time that Fire is Spreading and that Fire is Being Extinguished.



(a) During Fire.



(b) After Fire.

Fig.3 Load-Displacement Curves of Frame Structure during Fire and after Fire.

Table 1 Degrees of Safety for the Structural Collapse during Fire and after Fire.

(a) During Fire.

fire spreading time	collapse load during fire	degree of safety for the collapse during fire
$t_f$	$q / q_{y0}$	$q / q_{i0}$
0	1.585	2.64
10	1.420	2.37
20	1.290	2.15
25	1.050	1.75
30	0.685	1.14

(b) After Fire.

fire spreading time	collapse load after fire	degree of safety for the collapse after fire
$t_f (= t_e)$	$q^* / q_{y0}$	$q^* / q_{i0}$
0	1.585	2.64
10	1.585	2.64
20	1.470	2.45
25	1.320	2.20
30	1.250	2.08

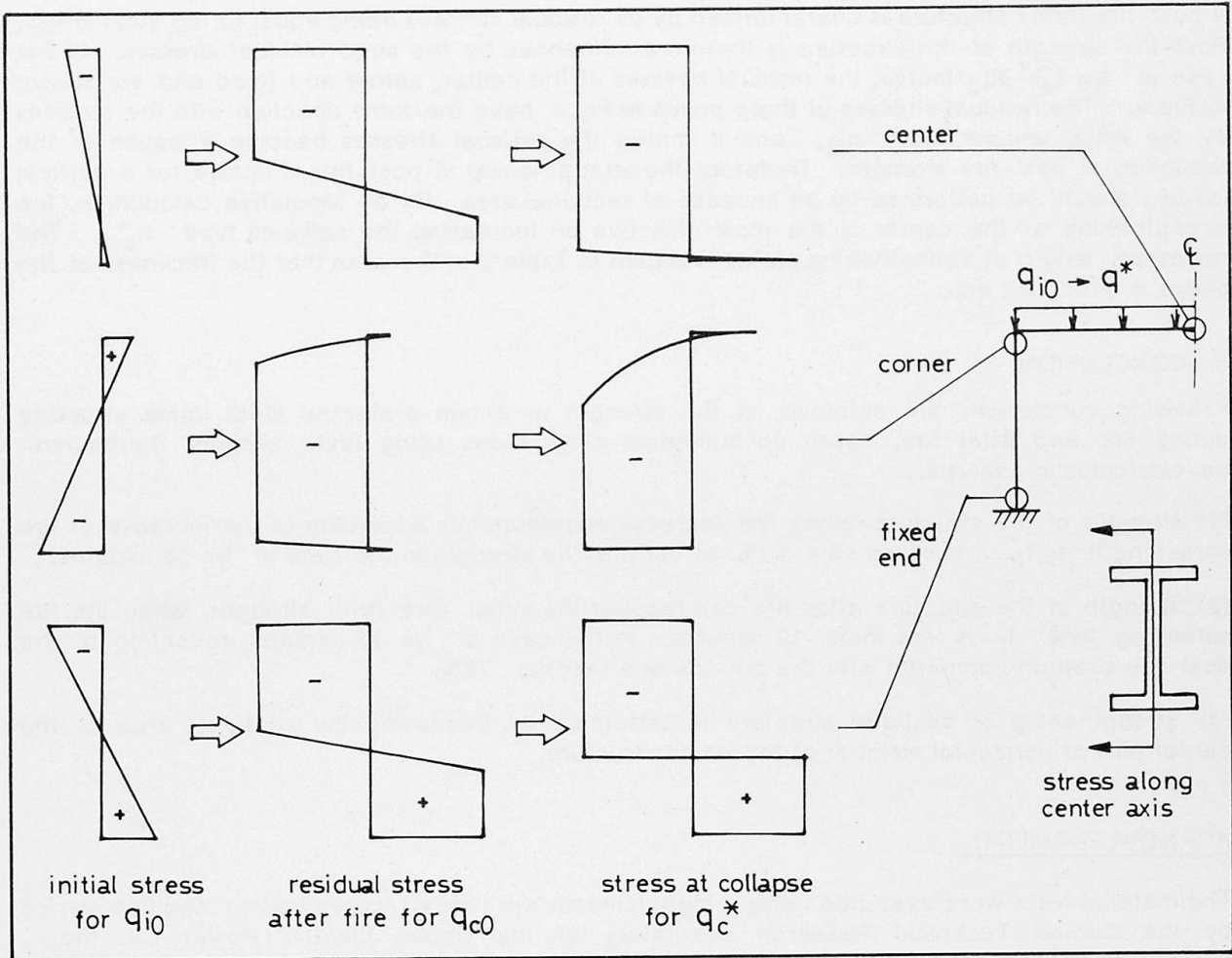


Fig.4 Residual Stresses in H-Section of Frame Structure after Fire ( $T_f = T_e = 30$  minutes).

Table 2 Lengths of Strengthening Plates and Recovery of Strength for the Structural Collapse due to the Strengthening.

fire spreading time	length of strengthening plates	collapse load after strengthening
$t_f (= t_e)$	$c (l = cL)$	$q^*/q_{y0}$
0	0	1.585
10	0	1.585
20	3/32	1.600
25	5/32	1.605
30	9/32	1.595

The diagram shows a frame structure with a strengthened corner. The original section is a 14 WF 31. The strengthening is applied to the corner with a length  $l = cL$ . The thickness of the strengthening plate is  $t$ , and the distance from the corner to the end of the plate is  $\frac{t}{6} \approx 2$  mm.



A post-fire frame structure is characterized by its residual stresses being equal to the yield stress. Post-fire strength of the structure is therefore influenced by the large residual stresses. In the case of  $t_f = t_e = 30$  minutes, the residual stresses at the center, corner and fixed end are shown in Fig.4. The residual stresses of three points in Fig.4 have the same direction with the stresses by the initial uniform load  $q_{i0}$ , and it implies the residual stresses become a cause of the reduction of post-fire strength. Therefore the strengthening of post-fire structure for a vertical loading should be performed by an increase of sectional area. By an simulative calculation, the strengthening at the center is the most effective on increasing the collapse load  $q_c^*$ . The necessary length of strengthening plates is shown in Table 2 in the case that the thickness of the plates is fixed as 2 mm.

#### 4. CONCLUSION

Following conclusions are obtained on the strength of a non-protected steel frame structure during fire and after fire, based on numerical calculations using finite element thermo-visco-elastoplastic analysis.

- (1) Strength of the structure during fire decrease acceleratingly according to the increase of fire spreading time  $t_f$ . It reaches only 43% of the pre-fire strength in the case of  $t_f = 30$  minutes.
- (2) Strength of the structure after fire can recover the initial (pre-fire) strength, when the fire spreading time  $t_f$  is less than 10 minutes. In the case of  $t_f = 30$  minutes, reduction of the post-fire strength compared with the pre-fire one reaches 79%.
- (3) Strengthening of post-fire structure is performed by increasing the sectional area of the center part of horizontal member of the frame structure.

#### ACKNOWLEDGMENTS

The material tests were executed using a high-temperature tension/creep testing machine owned by the Central Technical Research Laboratory of the Chubu Electric Power Co. Inc.. Computations were carried out on FACOM M-200 in the Nagoya University Computer Center.

#### REFERENCES

1. YAGAWA, M. and MIYAZAKI, N. : Present State of Creep Analysis Using Finite Element Method (in Japanese), J. JSME, 79, 1976, pp.532-538.
2. JSTM ed. : Fundamentals of Solid Mechanics (in Japanese), Daily Industrial Newspaper, 1980, p.263.
3. ZIENKIEWICZ, O.C. and CORMEAU, I.C. : Visco-Plasticity—Plasticity and Creep in Elastic Solids—A Unified Numerical Solution Approach, IJNME, 8, 1974, pp.821-845.
4. MROZ, Z. : Mathematical Models of Inelastic Material Behaviour, Solid Mechanics Div., Univ. of Waterloo, 1973, p.160.
5. YAMAMOTO, T. : Study on the Behavior of Steel Frame Structure in Fire Environments (in Japanese), M.Thesis, Nagoya Univ., 1983.
6. BS476 : Fire Tests on Building Materials and Structures, British Standards Institutions, London, 1972.
7. BABA, S. and KAJITA, T. : Out-of-Plane Deformation of Steel Frame in Fire, Proc. 1st. Int. Conf., Computing in Civil Eng., New York, 1981, pp.343-358.

## Structural Design Considerations in Strengthening of Timber Buildings

Calcul de structures et consolidation de constructions en bois

Statistische Berechnungsmethoden zur Verstärkung von Holzbauten

### S.K. MALHOTRA

Professor  
Techn. Univ. of Nova Scotia  
Halifax, NS, Canada



S.K. Malhotra received his Ph.D. from the Technical University of Nova Scotia, Halifax, Canada. He has been involved with teaching and research in timber engineering, and has published numerous papers. He holds many appointments on technical committees of professional, research and design code development organizations.

### SUMMARY

Factors affecting the serviceability of timber buildings are reviewed. Also, various aspects of evaluation and upgrading of such buildings are outlined. Structural design considerations in strengthening of timber buildings are discussed briefly. Some examples of strengthening of existing buildings for continued or different use are given. Reliability-based design procedures, which provide a unified approach for structural design standards for various materials, are examined, as they relate to the strengthening of buildings.

### RESUME

Les facteurs affectant la serviciabilité de constructions en bois sont passés en revue. Divers aspects de l'évaluation et de la rénovation ainsi que quelques considérations sur le calcul de structures pour des constructions en bois sont exposés. Quelques exemples de consolidation de bâtiments existants en vue du même ou d'un nouvel usage sont présentés. Des méthodes de calcul, basées sur la sécurité et permettant une approche unifiée des normes de calcul de structures pour différents matériaux, sont examinées, en rapport avec la consolidation de bâtiments.

### ZUSAMMENFASSUNG

Einflussgrößen auf die Gebrauchsfähigkeit von Holzbauten werden behandelt. Weiter werden Ansichten über die Bewertung und Verbesserung solcher Bauten, wie auch statistische Berechnungsmethoden zu deren Verstärkung diskutiert. Beispiele der Verstärkung von bestehenden Bauten für dieselbe oder eine andersartige Nutzung werden angegeben. Für verschiedene Materialien werden zusammenhängende, auf Zuverlässigkeitsanalysen basierende Bemessungsregeln für die Verstärkung von Bauten behandelt.



## 1. INTRODUCTION

The reasons for rehabilitation or strengthening of existing buildings can be many, such as: change in the use of building; change in the applicable design code requirements; deterioration of structural members or fastenings; damage to building elements as a result of fire, earthquake, or other like occurrence; historic; aesthetic; etc. As part of the process of strengthening of existing buildings, it is imperative to conduct a detailed structural and materials evaluation. A proper evaluation requires a good understanding of the quality and properties of the materials in the building and of the factors that influence these properties.

This paper provides, very briefly, some highlights of technical aspects of evaluation and structural design considerations in strengthening of timber buildings.

## 2. FACTORS AFFECTING SERVICEABILITY OF TIMBER BUILDINGS

The task of strengthening of existing timber buildings requires a comprehensive understanding of various factors on the safety and serviceability of these buildings. The foremost of these factors is the total load a building must carry, including not anticipated or non-so-apparent loads in design, such as those of piping, heating/cooling attachments to the structural members, ponding, etc.

Another important factor is the influence of duration of load on material properties. It is well recognized [5, 6, 14] that wood members can sustain short-duration loads of higher magnitude in relation to design loads of normal duration, Fig. 1. To take into account the effect of duration of load, design code [5] and design specification [14] for wood construction classify loads into six categories

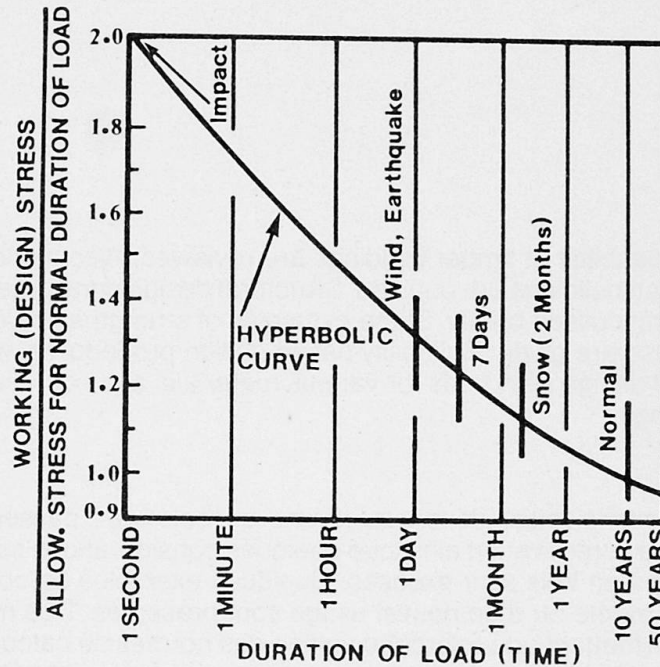


Fig. 1 Relationship Between Design Stress and Duration of Load

according to their duration and provide adjustment factors for use in design for these categories: instantaneous (impact), 1 day (wind, earthquake), 7 days, 2 months (snow), normal (10 years) and continuous (more than 10 years).

Other factors that should be considered are moisture, weather, temperature, chemicals, creep, decay, damage by insects and marine organisms, and fire [1]. Moisture has significant effect on the strength and other properties of wood. Furthermore, free water in wood promotes decay, checking, peeling of paint coatings, loosening of fastenings and corrosion of fasteners. Timber buildings exposed to weather may be subjected to cyclic effect of wetting and drying, which may cause checking in wood. Wood can be attacked by fungi, insects or marine organisms, shortening the useful life of timber buildings. Application of preservative treatment and implementation of proper construction details can enhance the durability of the building [20].

The loss of load-carrying capacity of timber members under the action of fire is the result of two causes, that is the formation of charcoal in the outside portion of the member and the weakening of a thin layer immediately beneath the charcoal. In heavy timber construction, fire resistance is provided by massive wood member sizes and avoidance of concealed spaces in which fire may originate and spread undetected. After fire damage, surface char can be removed by sand-blasting and then the load-carrying capacity of the residual section can be determined [9, 18, 19].

### 3. CONSIDERATIONS IN EVALUATION AND STRENGTHENING OF TIMBER BUILDINGS

The first step in assessment of the condition of an existing timber building, is a comprehensive visual examination of all building components including fastenings. This inspection also involves species identification of wood members and determination of the extent of deterioration or damage. Many types of equipments and techniques are available for use in the inspection.

Structural evaluation of timber construction requires estimating the load-carrying capacity of: structural components that show sign of deterioration or distress; structural members that will be affected by the strengthening; structural members that are expected to carry increased loading; structural or non-structural components that are affected by earthquake or similar types of hazard loads. There are three basic methods of evaluating structural components and structural systems: (i) Engineering and scientific judgement based on known past performance; (ii) Load tests; and (iii) Engineering analysis. The type of method suitable to a particular building depends on the condition of the building and the nature of the project. Some case histories of strength evaluation of structural wood members and of timber buildings are given in [4, 7, 10, 12].

Strengthening or upgrading of structural systems can be done either by strengthening individual structural members or by adding new structural components. The use of combinations of the two approaches is rather common. For example, a timber column can be strengthened with timber. The strength of such a built-up member can be determined with the aid of efficiency curves like the ones shown in Fig. 2. This figure provides the variation of strength of built-up column to that of equivalent solid column for different bolt spacings for column cross section shown on the graph. Equivalent solid column is taken as a column of same overall dimensions as those of the built-up column. Efficiency curves can be developed for different types and sizes of built-up columns, based on the research by Malhotra and Van Dyer [11].

A building may appear to have performed satisfactorily over the years, but current building code requirements particularly for earthquake loads may require extensive structural modifications. In structural systems for withstanding lateral forces due to wind or seismic ground motion, it is important to consider the manner in which the lateral forces are to be transferred to the foundation of the structure.

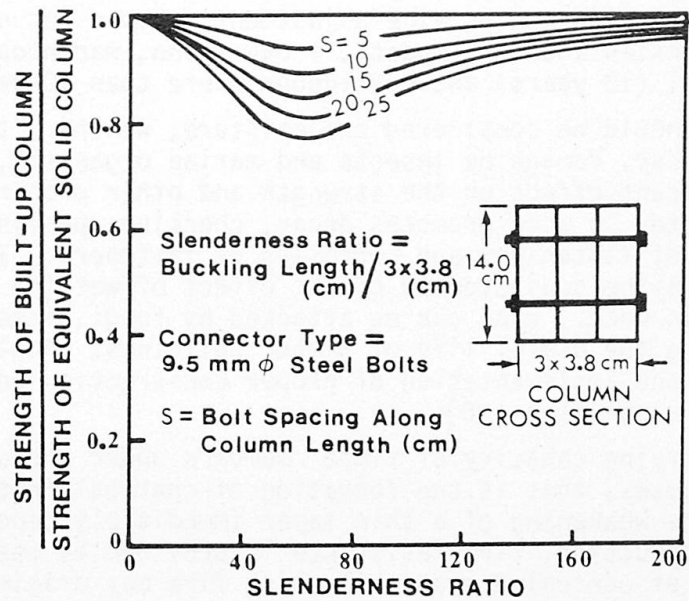


Fig. 2 Efficiency of Bolted Built-Up Timber Columns With Respect to Equivalent Solid Columns, For Various Bolt Spacings

Each structural member must have adequate strength to resist the applied forces as well as be able to transfer these forces to the adjoining elements. Thus, particular attention has to be given to design structural connections so as to ensure integrity of the structure.

There are two basic types of structural systems for resisting forces. In the first system, the lateral forces are resisted by moment connections or knee-braces, Fig. 3. The forces are transferred to the ground through trusses (or girders) and columns. The trusses are designed for forces by the lateral as well as gravity loads and the columns for combined bending and axial loads. The second structural

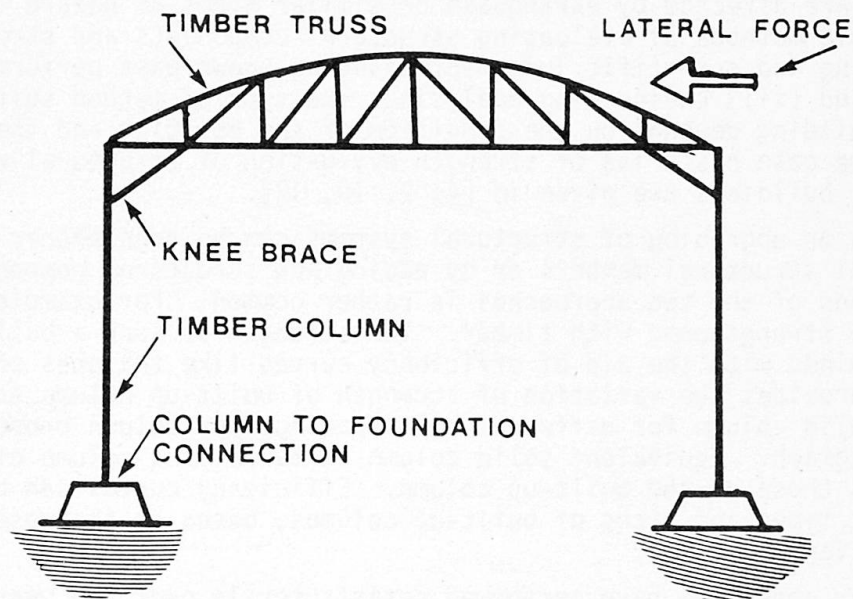


Fig. 3 Knee-Braced Truss Bent - A Structural System to Resist Lateral Forces

arrangement for resisting lateral forces, is shearwall and diaphragm system. A shearwall or diaphragm is plate-type structural element capable of transmitting forces in its own plane. Shearwalls and diaphragms are very effective structural wood systems for resisting lateral forces. Figure 4 shows shearwall and diaphragm action in the distribution of lateral forces on a simple leox-like building. If floors, walls and roofs in a building are to function as structural diaphragm or shearwall, they must be designed adequately to fulfill that role. Care is to be given to adequately reinforce openings in shearwalls and diaphragms with framing members and connections. Diaphragms must be suitably connected to the shearwalls and the entire structure be fastened securely to the foundations to resist uplift forces.

In many instances of rehabilitation or strengthening of buildings, composite structures made of different materials are often encountered. Limit states design, a probabilistic design approach currently under development in Canada, offers a unified procedure for all civil engineering structural standards and thus, simplifies the design and evaluation of composite structures. It also provides a means of incorporating reliability into the investigation of the structure's limit states. A brief description of limit states design, particularly as applied to timber structures, is given in [13].

#### 4. EXAMPLES OF REPAIR, REHABILITATION AND STRENGTHENING OF BUILDINGS

There are numerous methods of repair of timber buildings, such as: replacement of decayed parts; structural damage repair by using mechanical fasteners like clamps, metal bands, bolts, etc.; repair of structural damage by epoxy and other types of adhesives. Some examples of repairs of timber structures are given in [2, 3, 7, 15, 16, 17, 21].

There are many examples and case histories of recent rehabilitation and strengthening of timber buildings, as listed in various publications on the subject. Some examples are illustrated in [4]. The Butler Square Building in Minneapolis, Minnesota, U.S.A., is an excellent example of a warehouse type building into eight

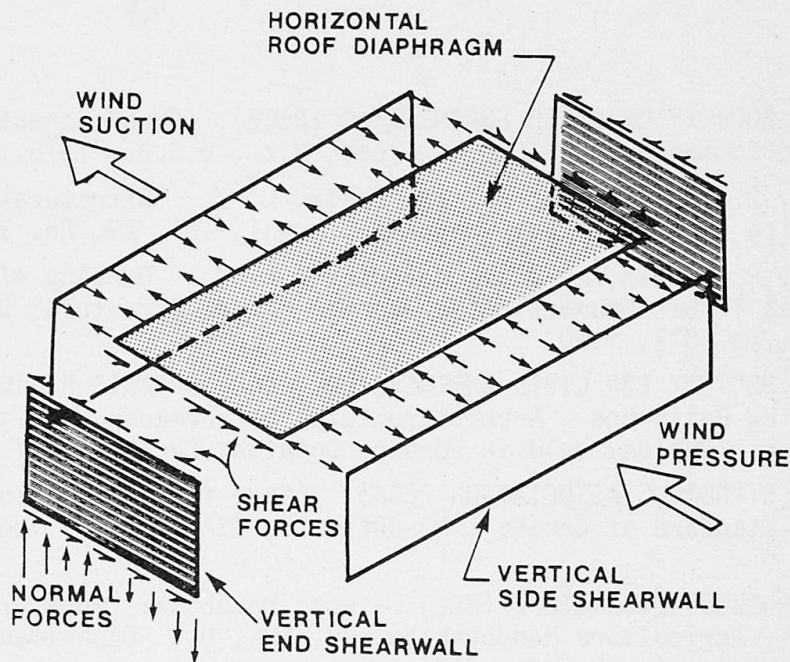


Fig. 4 Shearwall and Diaphragm Action in a Simple Building Subjected to Wind Load



floors of office and retail space [8]. It has been awarded an Honour Award by the Minnesota Society of Architects. The remodelling was accomplished by using heavy timber flooring, solid timber joists and beams of two solid timber pieces bolted together. Exterior bearing wall of masonry provided the major lateral stability of the building. The massiveness of the building (about 46450 square metres) was considered undesirable for its intended use and consequently the concept of atrium was utilized to provide an openness to the interior space.

## 5. CONCLUSIONS

Wood, a renewable resource, has many inherent advantages for construction applications. It can be used in wide varieties of creative ways for buildings that are not only functional but have aesthetic appeal as well. Many timber buildings of today are innovative structural systems. Examples and case histories of recent rehabilitation or strengthening of timber buildings indicate the versatility of wood as material of construction.

There can be many reasons for rehabilitation or strengthening of existing buildings. Some aspects of evaluation, including factors affecting the serviceability of timber buildings, were reviewed in the paper. Various structural design considerations in strengthening of timber buildings were discussed briefly. With scientific evaluation and investigation and with engineering design, timber buildings can be strengthened to provide many years of very satisfactory performance and durable service life.

## 6. ACKNOWLEDGEMENTS

The author would like to acknowledge the financial assistance provided by the Natural Sciences and Engineering Research Council for some of the projects discussed in this paper. Appreciation is extended to all individuals, in particular to Dr. G. G. Meyerhof, Dr. G. Finke and Mr. R.A.G. Ritchie, with whom he had many valuable discussions related to various aspects of the subject matter dealt with in the paper.

## REFERENCES

1. AMERICAN SOCIETY OF CIVIL ENGINEERING (ASCE). "Wood Structures - A Design Guide and Commentary", ASCE, New York, N.Y., U.S.A., 1975.
2. AVENT, R. P., SANDERS, P. H., and EMKIN, L. Z. "Structural Repair of Heavy Timber with Epoxy", Forest Products Journal, Vol. 29, No. 3, 1979.
3. AVENT, T. P., EMKIN, L. Z., and SANDERS, P. H. "Banding of Structural Repairs at Timber Connections", Journal of the Structural Division, ASCE, Vol. 106, No. ST1, 1980.
4. CANADIAN SOCIETY FOR CIVIL ENGINEERING (CSCE) ONTARIO REGION. "Restoration of Existing Buildings - Arena Structures", Proceedings, Regional Seminar, CSCE Ontario Region, held in London, Ontario, Canada, 1977.
5. CANADIAN STANDARDS ASSOCIATION (CSA). "Code for Engineering in Wood, National Standard of Canada CAN3-086-M80", CSA, Rexdale, Ontario, Canada, 1980.
6. FOREST PRODUCTS LABORATORY (FPL). "Wood Handbook: Wood as an Engineering Material", Agriculture Handbook No. 72, FPL, U.S. Department of Agriculture, Madison, Wisconsin, U.S.A., 1974.
7. FREAS, A. D., and TUOMI, R. "Manual on Evaluation, Maintenance and Upgrading of Wood Structures", Annual Convention, ASCE, held in Hollywood-by-the-Sea, Florida, U.S.A., 1980.



8. HORNE, F. "Hi-Rise in Wood", Annual Convention, ASCE, held in Philadelphia, Pennsylvania, U.S.A., 1976.
9. KNUDSEN, R. M., and SCHNIEWOOD, A. P. "Performance of Structural Wood Members Exposed to Fire", Forest Products Journal, Vol. 25, No. 2, 1975.
10. LANIUS, R. M., TICHY, R., and BULLEIT, W. M. "Strength of Old Wood Joists", Journal of the Structural Division, ASCE, Vol. 107, No. ST12, 1981.
11. MALHOTRA, S. K., and VAN DYER, D. B. "Rational Approach to the Design of Built-Up Timber Columns", Wood Science, Vol. 9, No. 4, 1977.
12. MALHOTRA, S. K. and RITCHIE, R.A.G. "Some Research and Development Studies in Nailed Laminated Timber Construction", International Convention, ASCE, New York, N.Y., U.S.A., 1981.
13. MALHOTRA, S. K. "Probability-Based Design Methods and Their Application to Timber Buildings", 9th CIB Congress, Stockholm, Sweden, 1983.
14. NATIONAL FOREST PRODUCTS ASSOCIATION (NFPA). "National Design Specification for Wood Construction", NFPA, Washington, D.C., U.S.A., 1982.
15. POWELL, R. M. "Reinforcing Structural Wood Members", Fall Convention, ASCE, held in Chicago, Illinois, U.S.A., 1978.
16. QUAILE, A. T., and KEENAN, F. J., "Repair and Reinforcement of Timber Structures", Annual Meeting, Forest Products Research Society, held in San Francisco, California, U.S.A., 1979.
17. SANDERS, P. H., EMKIN, L. Z., and AVENT, R. P., "Epoxy Repair of Timber Roof Trusses", Journal of the Construction Division, Vol. 104, No. C03, 1978.
18. SHAFFER, E. L. "Effect of Pyrolytic Temperatures on Longitudinal Strength of Dry Douglas-Fir", Journal of Testing and Evaluation, Vol. 1, No. 4, 1973.
19. SHAFFER, E. L. "State of Structural Timber Fire Endurance", Wood and Fiber, Vol. 9, No. 2, 1977.
20. SHEFER, T. C., and VERRALL, A. F. "Principles of Protecting Wood Buildings from Decay", Forest Products Laboratory, U.S. Department of Agriculture, Research Paper FPL 170, Madison, Wisconsin, U.S.A., 1973.
21. SILVA, R. F. "Wood Arch Relamination By Epoxy Grouting", Annual Convention, ASCE, held in Hollywood-by-the-Sea, Florida, U.S.A., 1980.

Leere Seite  
Blank page  
Page vide



## A Method to Assess the Reliability of Actual Buildings

Méthode d'évaluation de la sécurité des bâtiments

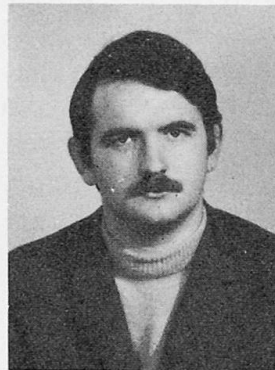
Methode zur Abschätzung der Gebäudesicherheit

**Francesco ZAUPA**  
Civil Engineer  
Università di Padova  
Padova, Italy



Born 1944, received his civil engineering degree at the University of Padova where he has been assistant professor at the department of civil engineering since 1970.

**Claudio MODENA**  
Civil Engineer  
Università di Padova  
Padova, Italy



Born 1946, received his civil engineering degree at the University of Padova, where he has been assistant professor at the department of civil engineering since 1972.

**Stefano ODORIZZI**  
Civil Engineer  
Università di Padova  
Padova, Italy



Born 1949, received his civil engineering degree at the University of Padova, where he has been research worker at the department of civil engineering since 1980.

### SUMMARY

A reliable and easy to use procedure is proposed, for the quantitative evaluation of the safety level of a building. The information coming from large scale and primary exterior inspections on a suitable sample of buildings is described in terms of symbolic entities, which are automatically processed. On this basis, once an appropriate safety criterion is fixed, a numerical determination of a statistically significant safety level can be obtained for a large urban settlement.

### RESUME

Une procédure sûre et d'application aisée est proposée pour évaluer quantitativement le niveau de sûreté d'un bâtiment. Les informations provenant de travaux d'inspection extérieure effectués à grande échelle sur un échantillon représentatif de bâtiments, sont traduites en termes symboliques, traités automatiquement par l'ordinateur. Sur cette base, et après avoir fixé un critère de sûreté approprié, on peut obtenir une détermination numérique d'un niveau de sûreté statistiquement représentatif pour un grand ensemble urbain.

### ZUSAMMENFASSUNG

Es wird ein zuverlässiges und leicht anwendbares Verfahren vorgeschlagen um den Sicherheitsgrad des Gebäudebestandes einer Region quantitativ zu erfassen. Die Informationen, die von einer Bestandaufnahme einer grossen Anzahl bestehender Gebäude stammen, werden auf symbolische Zeichen übertragen, die dann automatisch verarbeitet werden. Mit diesem Mittel kann ein statistisch signifikanter Sicherheitsgrad von grossen Siedlungen bestimmt werden, sobald ein geeignetes Sicherheitskriterium angenommen worden ist.



## 1. INTRODUCTION

A general approach to the problem of giving practically a quantitative evaluation, in the statistical sense, to the safety level of a regional building consistence was presented in a previous paper [1], where reference was made to the old, most frequent, masonry works and to their vulnerability to the seismic actions.

The matter of discussion was concerned with the establishment of those criteria which could lead to the formulation on a function of safety of a building, on the base of relevant parameters giving a measure of resistance and stability.

A procedure was also described in some details to process the informations which could be obtained only from exterior, widespread and quick inspections, to develop automatically the structural parameters.

Here some new parameters are introduced, and a multiple regression analysis is carried out within the whole series to find out the most representative ones.

A quite homogeneous sample of 41 buildings of the provincia of Trento is employed as a test case. The sample shows multiple correlation coefficients which are approximately 0.8 in the case of the structural indexes of geometric kind, when related to the VK ratios of the well-known POR and VET methods.

This application has been worked out also to control the reliability of the procedure and the arrangement of function of the global safety level.

## 2. RELIABILITY OF A SAFETY CRITERION WITH REFERENCE TO A SAMPLE OF MASONRY BUILDINGS.

The structural consistence of a building was drawn in [1] from the values of some dimensionless parameters, which were called structural status indexes.

In another paper [2] a method of survey was described which could produce the quantities to form such status indexes. For the sake of completeness a standard survey schedule is shown in figure 1 and the status indexes employed are listed in the table presented in the following, together with their classification. The geometrical ones are explicated in figure 2.

In this study all the mentioned indexes are preliminarily taken into account. Restricting practically the sample to a set of buildings which could be sufficiently homogeneous as age, architecture, technology and utilization, the number of indexes seems but to be reducible to few significant ones, whose choice can be pointed out through statistical dependencies like linear correlations.

As to the evaluation of the global safety level, the authors proposed in [1,2] to use a convenient combination of the status indexes. In fact a linear combination was employed, whose weighting coefficient were said to be significant of the risk of being the corresponding parameters close to certain limit values, and, by comparison, a linear multiplication of some normalized parameters was worked out. Introducing the problem of the definition of the weighting coefficients, and hence of the reliability of the safety function, a useful starting information seems to be the degree of correlation of the structural parameters with those coming from the methods which are most commonly adopted while drawing or verifying a structure. In the present work reference was made to the italian code for the restoration of masonry buildings damaged dur-

## STRUCTURAL STATUS INDEXES

SOIL AND FOUNDATION PARAMETERS	SUPERSTRUCTURES PARAMETERS																																																				
<p>a) Foundation soil.</p> <table border="1"> <thead> <tr> <th>Identifier</th> <th>Attribution</th> </tr> </thead> <tbody> <tr> <td>1</td> <td>Lack of information.</td> </tr> <tr> <td>2</td> <td>Loose soil with sloping surface.</td> </tr> <tr> <td>3</td> <td>Clayey soil with sloping surface.</td> </tr> <tr> <td>4</td> <td>Loose soil with horizontal surface.</td> </tr> <tr> <td>5</td> <td>Clayey soil with horizontal surface.</td> </tr> <tr> <td>6</td> <td>Sloping hard rock.</td> </tr> <tr> <td>7</td> <td>Horizontal hard rock.</td> </tr> </tbody> </table> <p>b) Groundwater level.</p> <table border="1"> <thead> <tr> <th>Identifier</th> <th>Attribution</th> </tr> </thead> <tbody> <tr> <td>1</td> <td>Lack of information.</td> </tr> <tr> <td>2</td> <td>Water table at ground level.</td> </tr> <tr> <td>3</td> <td>Medium deep level (<math>1 &lt; d &lt; 3m</math>).</td> </tr> <tr> <td>4</td> <td>Deeper level (<math>d &gt; 3m</math>).</td> </tr> </tbody> </table> <p>c) Structural typology.</p> <table border="1"> <thead> <tr> <th>Identifier</th> <th>Attribution</th> </tr> </thead> <tbody> <tr> <td>1</td> <td>Lack of information.</td> </tr> <tr> <td>2</td> <td>Non-existent foundation. Ground floor walls unbound and built directly on the ground.</td> </tr> <tr> <td>3</td> <td>Non-existent foundation. Well connected ground floor walls.</td> </tr> <tr> <td>4</td> <td>Individual footings.</td> </tr> <tr> <td>5</td> <td>Unbound continuous beams and individual footings.</td> </tr> <tr> <td>6</td> <td>Continuous beams or combined foundations with regular connections.</td> </tr> <tr> <td>7</td> <td>Mat foundations.</td> </tr> </tbody> </table> <p>d) Constitutive material of the foundations.</p> <table border="1"> <thead> <tr> <th>Identifier</th> <th>Attribution</th> </tr> </thead> <tbody> <tr> <td>1</td> <td>Lack of information.</td> </tr> <tr> <td>2</td> <td>Natural stone walls.</td> </tr> <tr> <td>3</td> <td>Chain bond or brickwork.</td> </tr> <tr> <td>4</td> <td>Reinforced or unreinforced masonry.</td> </tr> </tbody> </table>	Identifier	Attribution	1	Lack of information.	2	Loose soil with sloping surface.	3	Clayey soil with sloping surface.	4	Loose soil with horizontal surface.	5	Clayey soil with horizontal surface.	6	Sloping hard rock.	7	Horizontal hard rock.	Identifier	Attribution	1	Lack of information.	2	Water table at ground level.	3	Medium deep level ( $1 < d < 3m$ ).	4	Deeper level ( $d > 3m$ ).	Identifier	Attribution	1	Lack of information.	2	Non-existent foundation. Ground floor walls unbound and built directly on the ground.	3	Non-existent foundation. Well connected ground floor walls.	4	Individual footings.	5	Unbound continuous beams and individual footings.	6	Continuous beams or combined foundations with regular connections.	7	Mat foundations.	Identifier	Attribution	1	Lack of information.	2	Natural stone walls.	3	Chain bond or brickwork.	4	Reinforced or unreinforced masonry.	<p>a) Global indexes.</p> <p>aa) Ground floor.</p> <p>I 1 : Geometrical regularity index. I 2 : Compactness index. I 3 : Concentration index.</p> <p>ab) Vertical section.</p> <p>I 4 : Index of outer walls slenderness. I 5 : Index of main walls slenderness. I 6 : Index of standard story height.</p> <p>b) Local indexes.</p> <p>ba) Plant characteristics.</p> <p>I 7 : Index of eccentricity of the center of twist (in two orthogonal directions x, y); I 9 : Index of masonry percentage on the gross total area of walls. I 10 : Index of masonry percentage on the covered area. I 11 : Ratio between external pier and adjacent opening widths. I 12 : Ratio between internal pier and adjacent opening widths. I 13 : Index of linear density of stiffening walls. I 14 : Index of linear density of stiffening walls per unit length. I 15 : Index of normalized free length of a wall. I 16 : Index of openings percentage of a wall. I 17 : Ratio between external pier length and adjacent opening height.</p> <p>bb) Vertical section characteristics.</p> <p>I 18 : Index of slenderness of a wall between two rigid floors. I 19 : Index of normalized height of a story.</p>
Identifier	Attribution																																																				
1	Lack of information.																																																				
2	Loose soil with sloping surface.																																																				
3	Clayey soil with sloping surface.																																																				
4	Loose soil with horizontal surface.																																																				
5	Clayey soil with horizontal surface.																																																				
6	Sloping hard rock.																																																				
7	Horizontal hard rock.																																																				
Identifier	Attribution																																																				
1	Lack of information.																																																				
2	Water table at ground level.																																																				
3	Medium deep level ( $1 < d < 3m$ ).																																																				
4	Deeper level ( $d > 3m$ ).																																																				
Identifier	Attribution																																																				
1	Lack of information.																																																				
2	Non-existent foundation. Ground floor walls unbound and built directly on the ground.																																																				
3	Non-existent foundation. Well connected ground floor walls.																																																				
4	Individual footings.																																																				
5	Unbound continuous beams and individual footings.																																																				
6	Continuous beams or combined foundations with regular connections.																																																				
7	Mat foundations.																																																				
Identifier	Attribution																																																				
1	Lack of information.																																																				
2	Natural stone walls.																																																				
3	Chain bond or brickwork.																																																				
4	Reinforced or unreinforced masonry.																																																				

Table 1 Structural status indexes.



ing the last Irpinia earthquake [ 3 ] .

The sample to which the analysis is applied is an extension of the one illustrated in [ 1 ], excluding the coded buildings whose data were not complete.

As an example the statistical distribution of indexes I 3 and I 4 are shown in figure 3.

The high degree of correlation exhibited by some couples of structural indexes, e.g. I 4 and I 6, I 13 and I 14, whose linear correlation coefficients are about 0.8, clearly indicates the possibility to reduce their number.

On the same sample the VK values (i.e. the ratio V between the ultimate shear force at a floor level to the total weight, multiplied by a safety coefficient K) have been computed, according to the POR and VET methods, taking in case as reference values those given by the italian standards [ 3 ] .

The statistical distributions of VK are shown in figure 5a(POR method) and 5b(VET method), for seismic forces acting in one of the principal directions of the buildings.

The reliability of the obtained results can be firstly judged by comparison of figures 5a,b, and figures 4a,b, where the statistical distribution of the global safety indexes obtained from the two formulations of the safety function proposed in [ 1 ] are plotted, for a slightly reduced sample.

Obviously the VK values define only the safety against horizontal actions.

Hence a total safety function should be more reliable if expressed by means of more comprehensive parameters, like those proposed above.

### 3. CONCLUSIONS

The aim of this study has been to assess the reliability of a general procedure which should lead to evaluate the structural state of existing buildings.

The procedure was proposed by the authors in [ 1 ] and [ 2 ] . Quite a significant agreement has been found with the outcome of some standard methods to calculate the horizontal resistance of a building.

To the authors opinion the procedure is still to be improved as regards the choice of the representative parameters and their relative calibration, even with respect to the different characteristics of the sample examined and to the different limit states which can be considered. In this light a sample of buildings of Castelgrande (Potenza), which suffered various damages during the last Irpinia earthquake (table 2), is actually under investigation.

### REFERENCES

1. ZAUPA F., MODENA C., ODORIZZI S., Evaluation of the safety level of existing buildings with particular reference to seismic actions. 7th ECEE, September 1982, Athens.
2. ZAUPA F., MODENA C., ODORIZZI S., Sul problema della valutazione del livello di sicurezza degli edifici esistenti con particolare riferimento alle azioni sismiche. L'Industria delle Costruzioni, Gennaio 1982.
3. Circolare LL.PP. 30 Luglio 1982, n. 21745. Istruzioni relative alla normativa tecnica per le riparazioni ed il rafforzamento degli edifici in muratura danneggiati dal sisma.

BUILDINGS PROPERTIES						DAMAGES DISTRIBUTION									
Building Identifier	Number of stories	Vertical structures	Horizontal structures	Roof structure	Roof covering	Damage investigation made at story	Splitting of orthogonal not connected walls	Slipping of floor joists/roof struc. from bearing walls	Cracks at the headers over opening	Vertical/horizontal cracks in the walls	Diagonal cracks in the walls	Cracks nearby flues or niches	Distributed cracks on the walls	Damages at the roof covering	Other failures
1	(*) U.G.+2	Stonework	Timber	Timber	Brick	R.S.	*						****	*	
4	U.G.+2	Mixed stonework	Steel joists and brick	Timber		U.G.	*								
			Timber			1 <sup>o</sup>	*		**		*	**			
			Timber			2 <sup>o</sup>	****		**			**			
5	3+R.S.					R.S.	*	*				*			
6	2	Mixed stonework	Steel joists and brick	Timber		1			**				****		
						2			*		**				
7	2+R.S.	Stonework	Steel joists and brick	Timber	Brick	2 <sup>o</sup>				*			***	*	
10	U.G.+1 +R.S.	Mixed stonework	Steel/timber joists and brick	Timber		1 <sup>o</sup>	****		*	*****			**		
12	U.G.+2	Mixed stonework	Timber	Timber		1 <sup>o</sup>	**	**	***	*		****	*		
						2 <sup>o</sup>	*	*	***	*		**			
13	1+R.S.	Stonework	Steel joists and brick			1			*						*
15	U.G.+3	Mixed stonework	Steel joists and brick	Timber		2 <sup>o</sup>			****	**	***	*			*
			Timber joists			3 <sup>o</sup>	*	*		*		**			
16	2	Steel				6.	**			**					
						1 <sup>o</sup>	***					*			
17	1+R.S.	Stonework	Timber	Timber	Brick	R.S.	*			*			*		

Table 2 Damages distribution on a building sample after Campania-Lucania earthquake of 23-11-1980.

(\*) Note: U.G.: underground story; G.: ground story; R.S.: roof story.



COMUNE DI ROVERETO, Via M. Flamin, 20  
C. C. Rovereto: F.M. 18, p. ed. 1033. Proprietà comunale



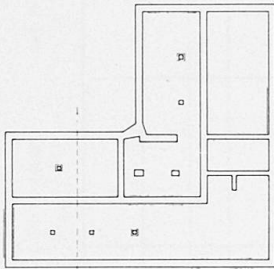
**A. UBICAZIONE**  
COMUNE DI  
Fraz. o località  
Via  
C.C.  
PROPRIETÀ

Civ. n°  
p.ed.  
F. Mapa n°

Schema N° 1  
FONDAZIONI

Data  
Il Tecnico rilevatore

B. RILIEVO - 1 : 200



Natura del terreno di fondazione  
 materiale sciolto  
 roccia compatta

Livello falda:  
 allorante  
 compreso fra 1 e 3 ml. sotto p.c.  
 oltre i 3 ml. sotto p.c.

**C. LEGENDA**

C.1. TIPOLOGIA STRUTTURE	C.2. TIPOLOGIA LESIONI
<ul style="list-style-type: none"> <li>C.1.1. FONDAMENTI SUPERFICIALI</li> <li>C.1.2. FONDAMENTI PROFONDI</li> <li>C.1.3. MURAGLIE</li> <li>C.1.4. TRAVI</li> <li>C.1.5. COLONNINE</li> <li>C.1.6. SOLAI</li> <li>C.1.7. COPERTURE</li> </ul>	<ul style="list-style-type: none"> <li>C.2.1. CRACKING</li> <li>C.2.2. DEFORMAZIONI</li> <li>C.2.3. CORROSIONI</li> <li>C.2.4. ROTTURE</li> <li>C.2.5. ALI</li> <li>C.2.6. ROTTURE</li> <li>C.2.7. ROTTURE</li> <li>C.2.8. ROTTURE</li> <li>C.2.9. ROTTURE</li> <li>C.2.10. ROTTURE</li> <li>C.2.11. ROTTURE</li> <li>C.2.12. ROTTURE</li> <li>C.2.13. ROTTURE</li> <li>C.2.14. ROTTURE</li> <li>C.2.15. ROTTURE</li> <li>C.2.16. ROTTURE</li> <li>C.2.17. ROTTURE</li> <li>C.2.18. ROTTURE</li> <li>C.2.19. ROTTURE</li> <li>C.2.20. ROTTURE</li> </ul>

ANNOTAZIONI:

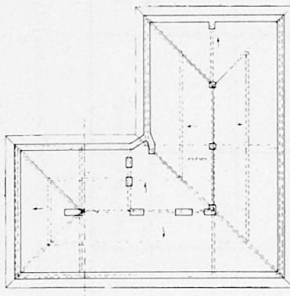
**A. UBICAZIONE**  
COMUNE DI  
Fraz. o località  
Via  
C.C.  
PROPRIETÀ

Civ. n°  
p.ed.  
F. Mapa n°

Schema N° 7  
COPERTURA

Data  
Il Tecnico rilevatore

B. RILIEVO - 1 : 200



Quota del colmo del coperto: 15,00 ml.  
 Quota d'imposta del coperto sui muri d'angolo: 12,40 ml.  
 Quota di calpestio dell'ultimo solaio: 12,00 ml.

**C. LEGENDA**

C.1. TIPOLOGIA STRUTTURE	C.2. TIPOLOGIA LESIONI
<ul style="list-style-type: none"> <li>C.1.1. FONDAMENTI SUPERFICIALI</li> <li>C.1.2. FONDAMENTI PROFONDI</li> <li>C.1.3. MURAGLIE</li> <li>C.1.4. TRAVI</li> <li>C.1.5. COLONNINE</li> <li>C.1.6. SOLAI</li> <li>C.1.7. COPERTURE</li> </ul>	<ul style="list-style-type: none"> <li>C.2.1. CRACKING</li> <li>C.2.2. DEFORMAZIONI</li> <li>C.2.3. CORROSIONI</li> <li>C.2.4. ROTTURE</li> <li>C.2.5. ALI</li> <li>C.2.6. ROTTURE</li> <li>C.2.7. ROTTURE</li> <li>C.2.8. ROTTURE</li> <li>C.2.9. ROTTURE</li> <li>C.2.10. ROTTURE</li> <li>C.2.11. ROTTURE</li> <li>C.2.12. ROTTURE</li> <li>C.2.13. ROTTURE</li> <li>C.2.14. ROTTURE</li> <li>C.2.15. ROTTURE</li> <li>C.2.16. ROTTURE</li> <li>C.2.17. ROTTURE</li> <li>C.2.18. ROTTURE</li> <li>C.2.19. ROTTURE</li> <li>C.2.20. ROTTURE</li> </ul>

ANNOTAZIONI:

N.B. Quotare i colmi e le imposte del piano di copertura



**A. UBICAZIONE**  
COMUNE DI  
Fraz. o località  
Via  
C.C.  
PROPRIETÀ

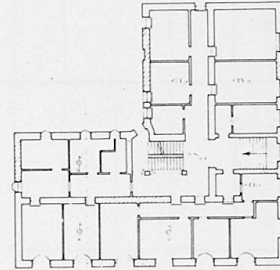
Civ. n°  
p.ed.  
F. Mapa n°

Schema N° 3  
PIANO RIALZATO

Data  
Il Tecnico rilevatore

B. RILIEVO - 1 : 200

Quota riferita al piano strada 1,40 ml.

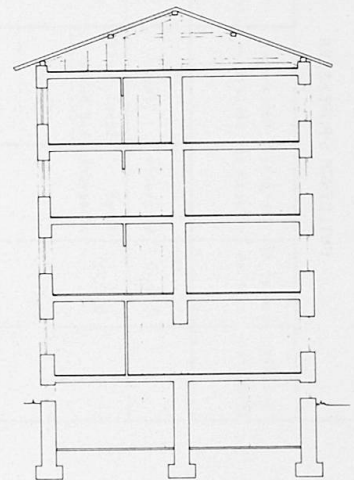


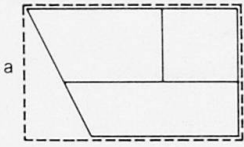
N.B. Quotare il piano campagna presente rilevante, pendente riportare sezione verticale indicata

**C. LEGENDA**

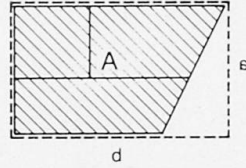
C.1. TIPOLOGIA STRUTTURE	C.2. TIPOLOGIA LESIONI
<ul style="list-style-type: none"> <li>C.1.1. FONDAMENTI SUPERFICIALI</li> <li>C.1.2. FONDAMENTI PROFONDI</li> <li>C.1.3. MURAGLIE</li> <li>C.1.4. TRAVI</li> <li>C.1.5. COLONNINE</li> <li>C.1.6. SOLAI</li> <li>C.1.7. COPERTURE</li> </ul>	<ul style="list-style-type: none"> <li>C.2.1. CRACKING</li> <li>C.2.2. DEFORMAZIONI</li> <li>C.2.3. CORROSIONI</li> <li>C.2.4. ROTTURE</li> <li>C.2.5. ALI</li> <li>C.2.6. ROTTURE</li> <li>C.2.7. ROTTURE</li> <li>C.2.8. ROTTURE</li> <li>C.2.9. ROTTURE</li> <li>C.2.10. ROTTURE</li> <li>C.2.11. ROTTURE</li> <li>C.2.12. ROTTURE</li> <li>C.2.13. ROTTURE</li> <li>C.2.14. ROTTURE</li> <li>C.2.15. ROTTURE</li> <li>C.2.16. ROTTURE</li> <li>C.2.17. ROTTURE</li> <li>C.2.18. ROTTURE</li> <li>C.2.19. ROTTURE</li> <li>C.2.20. ROTTURE</li> </ul>

Schema N° 8  
SEZIONE VERTICALE

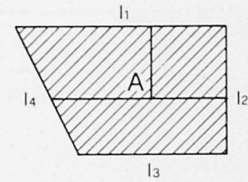




$$I_1 = a/b$$

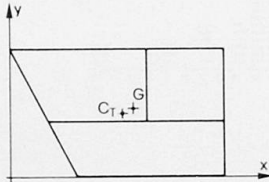


$$\frac{A}{b^2} = \zeta I$$



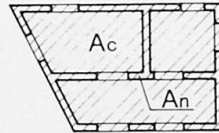
$$p = l_1 + l_2 + l_3 + \dots + l_n$$

$$I_3 = \frac{A}{p} / \frac{A}{4\sqrt{A}} = \frac{4\sqrt{A}}{p}$$

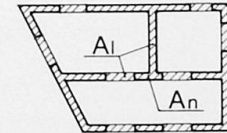


$$I_7 = \frac{x_{CT} - x_G}{x_{max} - x_{min}}$$

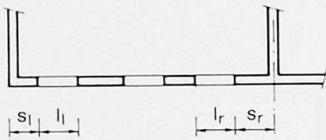
$$I_8 = \frac{y_{CT} - y_G}{y_{max} - y_{min}}$$



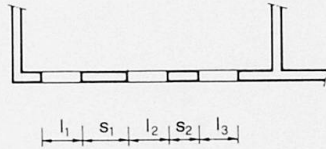
$$I_9 = \frac{A_n}{A_c}$$



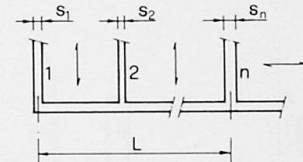
$$I_{10} = \frac{A_n}{A_l}$$



$$I_{11} = \left( \frac{s_e}{l_e} \right); [e = l, r]$$

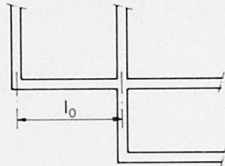


$$I_{12} = \left( \frac{s_i}{l_i + l_{i+1}} \right)_{min}$$

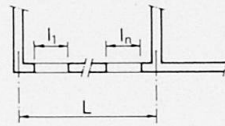


$$I_{13} = \frac{s_1 + s_2 + \dots + s_n}{L}$$

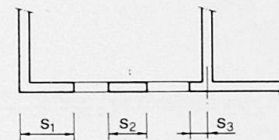
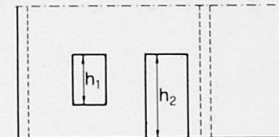
$$I_{14} = \frac{s_1 + s_2 + \dots + s_n}{n \cdot L}$$



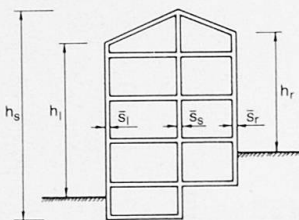
$$I_{15} = \frac{l_0}{l_{rif}}; [l_{rif} = 7.00 \text{ m}]$$



$$I_{16} = \frac{l_1 + l_2 + \dots + l_n}{L}$$

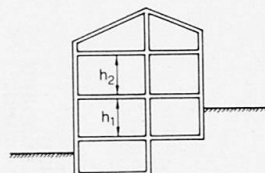


$$I_{17} = \left( \frac{s_i}{h_{i(i-1)}} \right)_{min}$$

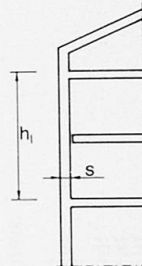


$$I_4 = \left( \frac{h_e}{s_e} \right)_{max}; [e = l, r]$$

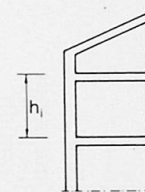
$$I_5 = \left( \frac{h_s}{s_s} \right)_{max}$$



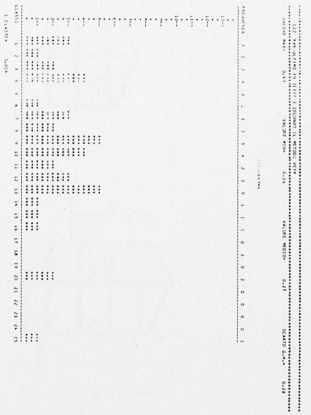
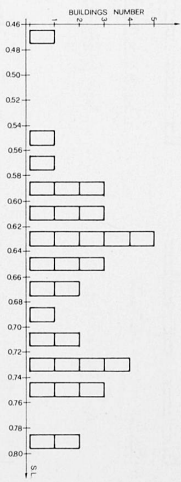
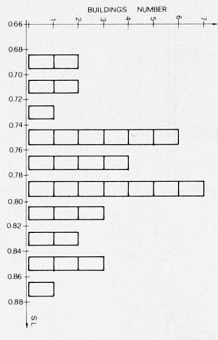
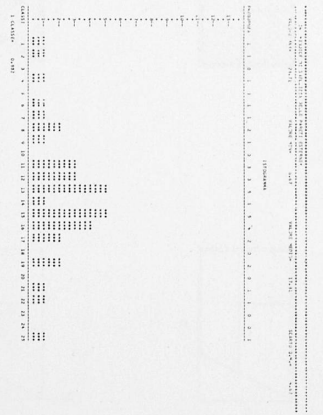
$$I_6 = \frac{1}{n} \frac{\sum h_i}{h_{rif}}; [h_{rif} = 3.00 \text{ m}]$$



$$I_{18} = \frac{h_e}{s}$$



$$I_{19} = \frac{h_i}{h_{rif}}; [h_{rif} = 3.00 \text{ m}]$$



## Decision Models for the Diagnosis and Treatment of Structural Defects

Modèles de décision pour le diagnostic et le traitement de dommages structuraux

Entscheidungsmodelle für die Diagnose und Behandlung von Bauschäden

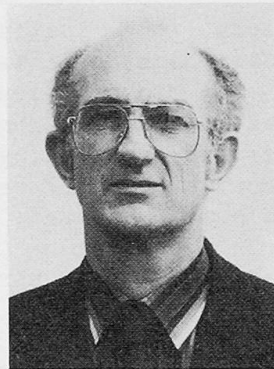
### R.F. WARNER

Prof. of Civil Eng.  
Univ. of Adelaide  
Adelaide, Australia



### J.N. KAY

Sen. Lecturer in Civil Eng.  
Univ. of Adelaide  
Adelaide, Australia



### SUMMARY

Statistical decision theory provides a useful basis for deciding whether or not to proceed with corrective work on a possibly defective structure, and for choosing from a range of options for carrying out such work. Minimum expected cost, adjusted to allow for risk aversion, is used as the decision criterion. The importance of additional data gathering is discussed.

### RESUME

Une théorie, basée sur des statistiques, permet de décider de la réparation ou du renforcement d'une structure défectueuse et de choisir la méthode à utiliser dans un cas particulier. Les critères de décision incluent le coût minimum prévisible pour un niveau de risque donné. La nécessité de récolter des informations complémentaires est discutée.

### ZUSAMMENFASSUNG

Die statistisch fundierte Entscheidungstheorie gibt eine nützliche Grundlage für den Entscheid, ob und wie eine Reparatur an einer schadhafte Konstruktion ausgeführt werden soll. Als Entscheidungskriterium dient das Verhältnis der zu erwartenden Minimalkosten zum erlaubten Risiko. Die Bedeutung zusätzlicher Dateninformationen wird diskutiert.



## 1. ASSESSMENT OF STRUCTURAL DEFECTS

Structural defects are defects which adversely affect the safety and serviceability of a structure. They have a wide variety of causes, including design error, construction error, material deterioration, steel corrosion, accidental damage, foundation movement, overload, and fire damage.

Before corrective work on a defective structure can be undertaken, some form of assessment is needed in order to identify the defects and diagnose their causes, and hence provide a prognosis of the future performance of the structure in both the defective and the repaired conditions. Unfortunately, systematic procedures for proper structural assessment are usually both costly and time-consuming [1]. For example, diagnostic charts prepared for concrete buildings [2] show that a small number of common symptoms are produced by a large range of different defects, so that careful, costly and time-consuming investigatory procedures are needed to diagnose and assess a structure accurately.

In practical situations, the initial decisions concerning the repair of a defective structure often have to be taken promptly on incomplete information without the benefit of a proper, accurate assessment. In these circumstances, difficult, risky and expensive decisions have to be taken, with the possibility of two types of assessment error being made. These may be referred to as Type I and Type II errors, because of their resemblance to the errors of statistical hypothesis testing and quality control [1].

A Type I error is made if the structure is assessed, incorrectly, as being defective.

A Type II error arises if the structure is assessed as being adequate when in fact it is defective.

Type II errors can endanger property and possibly life and are therefore potentially less acceptable than Type I errors, which may incur unnecessary, but possibly costly, repair work.

After an inspection and initial assessment has been made of a defective structure, it is necessary to identify the available courses of action and the range of possible consequences of each course of action, so that the most appropriate action can be chosen. While the nature and severity of the structural defect will greatly influence the choice of specific repair procedures, the following options will usually be included among the available courses of action:

- (a) do nothing, the structure being assessed as adequate to fulfil its intended function;
- (b) do not undertake corrective work, but monitor the structure for further signs of defect or deterioration;
- (c) carry out a thorough structural assessment, if necessary after taking it out of service for safety reasons;
- (d) undertake corrective work while maintaining the structure in-service;
- (e) take the structure out of service temporarily for safety reasons and carry out corrective work;
- (f) take the structure out of service indefinitely and investigate the alternatives of repair, reconstruction, demolition and replacement.



## 2. EXPECTED COST MODELS

A convenient framework for choosing the most appropriate of the available courses of action for a defective structure may be provided by statistical decision theory. One of the simplest decision criteria is based on expected values. It can be used to deal with defective structures, and can also be modified to allow for risk aversion, which is an important consideration in engineering decision making.

In a given situation, the courses of action to be considered will be referred to as  $A(1), A(2), \dots, A(i), \dots$ . For practical purposes it is convenient and usually adequate to lump the possible outcomes of any action  $A(i)$  into a finite number of distinct possibilities. For example, if action  $A(1)$  is do nothing (option (a) above), then possible outcomes would range from satisfactory structural behaviour over the entire design life of the structure to sudden, catastrophic collapse while in-service. The latter outcome would be an example of a Type II error of assessment. The finite set of outcomes of action  $A(i)$  will be expressed as  $S(i,1), S(i,2), \dots, S(i,j), \dots, S(i,N_i)$ . The total cost of outcome  $S(i,j)$ , including the cost of the original action  $A(i)$ , will be expressed as  $C(i,j)$ .

It is not possible to predict accurately which of the possible outcomes will in fact follow a particular action. Imperfect knowledge of the structural system, the approximate nature of structural theories, random variations in system parameters and uncertainty with regard to real world demands on the structure (loads, temperature gradients, etc) all prevent precise predictions from being made. On the other hand, the structural engineer can usually estimate the relative likelihood of each outcome, which can be expressed in the form of a probability. The probability, as perceived by the engineer, that outcome  $S(i,j)$  will follow from action  $A(i)$  can be expressed as  $P[S(i,j)|A(i)]$  or simply as  $P[S(i,j)]$  where

$$\sum_{j=1}^{N_i} P[S(i,j)] = 1.0 \quad (1)$$

The expected cost of any course of action  $A(i)$  is defined as follows:

$$EC[A(i)] = \sum_{j=1}^{N_i} P[S(i,j)] \cdot C(i,j) \quad (2)$$

According to the expected value criterion, the preferred course of action is the one which has the minimum expected cost.

It will be recognised that the probabilities  $P[S(i,j)]$  are likely to be educated guesses in many cases. However, the use of these numbers in a formal calculation process is more rational and more reliable than the conventional approach of intuitive selection.

## 3. EXAMPLE OF EXPECTED COST CRITERION

Extensive inclined torsion-type cracks developed in a prestressed concrete building during construction and were diagnosed as being caused by temperature warping of the floor slabs. Warping of the slabs had imposed torsional deformations in the supporting beams. Concern was felt for the safety of the building, because the cracked beams, being fully prestressed, contained no transverse reinforcement. Unusual loads (blast, earth tremor, etc) which might well occur at some future time, could result in partial collapse. Four courses



Table 1 : Calculation of Minimum Expected Cost and Utility  
(Cost shown in millions of dollars)

		Expected Cost calculation			Expected Utility calculation	
		(1)	(2)	(3)	(4)	(5)
A(1)	S(1,1)	0.50	0.00	0.00	0.0	0.00
	S(1,2)	0.30	0.70	0.21	-2.4	-0.72
	S(1,3)	0.10	1.00	0.10	-3.6	-0.36
	S(1,4)	0.10	10.00	1.00	-100	-10.00
Cost = 0		$\Sigma = 1.31$			$\Sigma = -11.08$	
A(2)	S(2,1)	0.50	0.01	0.05	0.0	-0.00
	S(2,2)	0.42	0.71	0.30	-2.5	-1.05
	S(2,3)	0.04	1.01	0.04	-3.6	-0.14
	S(2,4)	0.04	10.01	0.40	-100	-4.00
Cost = 0.01		$\Sigma = 0.79$			$\Sigma = -5.19$	
A(3)	S(3,1)	0.90	1.10	0.99	-4.0	-3.60
	S(3,2)	0.10	1.80	0.17	-7.0	-0.70
	S(3,3)	0.00	-	0.00	-	0.00
	S(3,4)	0.00	-	0.00	-	0.00
Cost = 1.10		$\Sigma = 1.16$			$\Sigma = -4.30$	
A(4)	S(4,1)	0.95	0.80	0.76	-2.8	-2.70
	S(4,2)	0.05	1.50	0.08	-5.8	-0.29
	S(4,3)	0.00	-	0.00	-	0.00
	S(4,4)	0.00	-	0.00	-	0.00
Cost = 0.80		$\Sigma = 0.84$			$\Sigma = -2.99$	

Notes :

(1) =  $P[S(i,j)]$  ; (2) =  $C(i,j)$  ; (3) =  $P[S(i,j)].C(i,j)$

(4) =  $U(i,j)$  ; (5) =  $P[S(i,j)].U(i,j)$



of action were identified:

- A(1) : do nothing;
- A(2) : take no immediate action but monitor the building;
- A(3) : provide permanent protective propping around the columns,  
thereby causing partial impairment of the building;
- A(4) : introduce additional external prestress to correct the defect.

As a result of action (A1), the possible outcomes were considered to be as follows:

- (a) S(1,1) : the structure survives satisfactorily;
- (b) S(1,2) : further cracking occurs, especially in the roof system,  
and the client is forced to undertake repair work;
- (c) S(1,3) : non-catastrophic local failure occurs as a result  
of an adverse combination of external forces;
- (d) S(1,4) : sudden collapse occurs due to a rare combination of external loads.

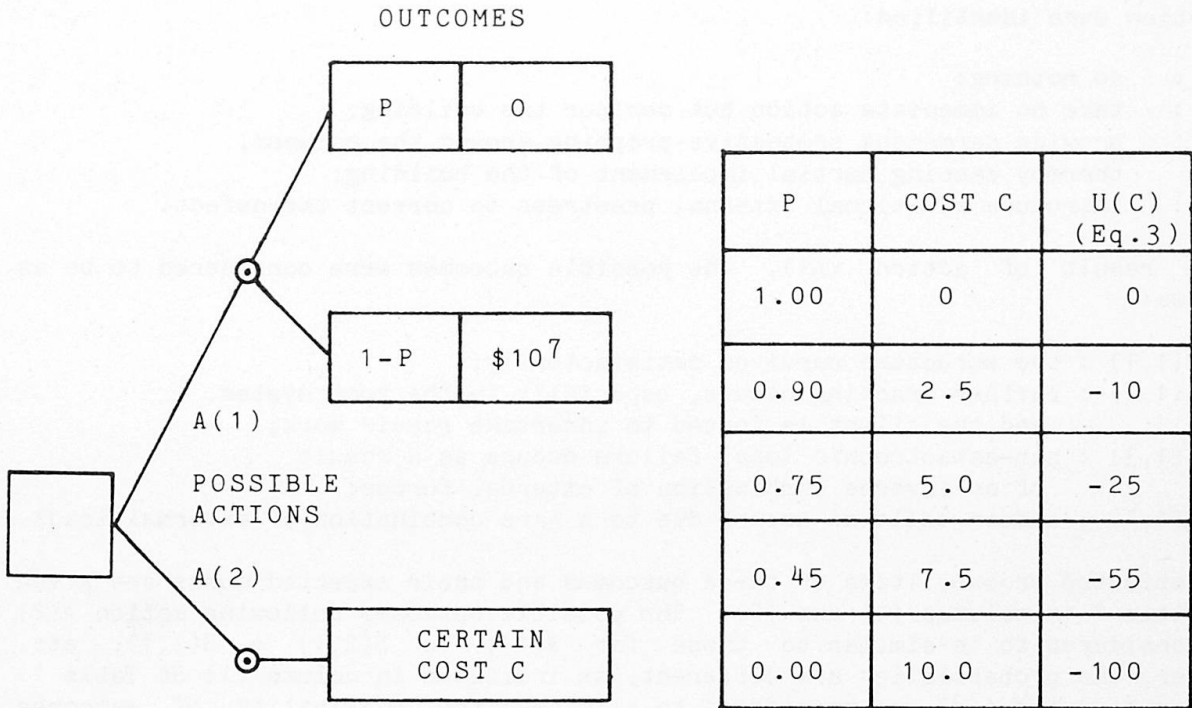
The estimated probabilities of these outcomes and their expected costs are given in Table 1 in columns (1) and (2). The possible outcomes following action A(2) are considered to be similar to those for A(1); ie  $S(2,1) = S(1,1)$ , etc. However, the probabilities are different, as indicated in column (1) of Table 1. Actions A(3) and A(4) are considered to eliminate the possibility of outcomes (c) and (d). This is taken into account in Table 1 with zero probabilities as appropriate. In column (2) of Table 1 the costs C(3,1) and C(3,2) include an estimate of the reduced value of the building due to partial impairment. According to the expected costs calculated in column (3) by means of Eq 2, the preferred course of action is A(2).

In this simplified example, the range of possible outcomes listed above as items (a) to (d) happen to be the same for each of the courses of action considered, and a simplified notation S(1), S(2), etc could obviously have been used. In many situations, the range of outcomes will depend on the course of action and the notation adopted here reflects this more general situation.

Two aspects of the expected cost approach as used in this example require further consideration and comment. The first concerns the aptness, or otherwise, of the expected monetary value criterion; the second arises from difficulties experienced by many engineers in choosing appropriate probabilities for use in the calculations. Each aspect will be considered in turn in the following sections of this paper.

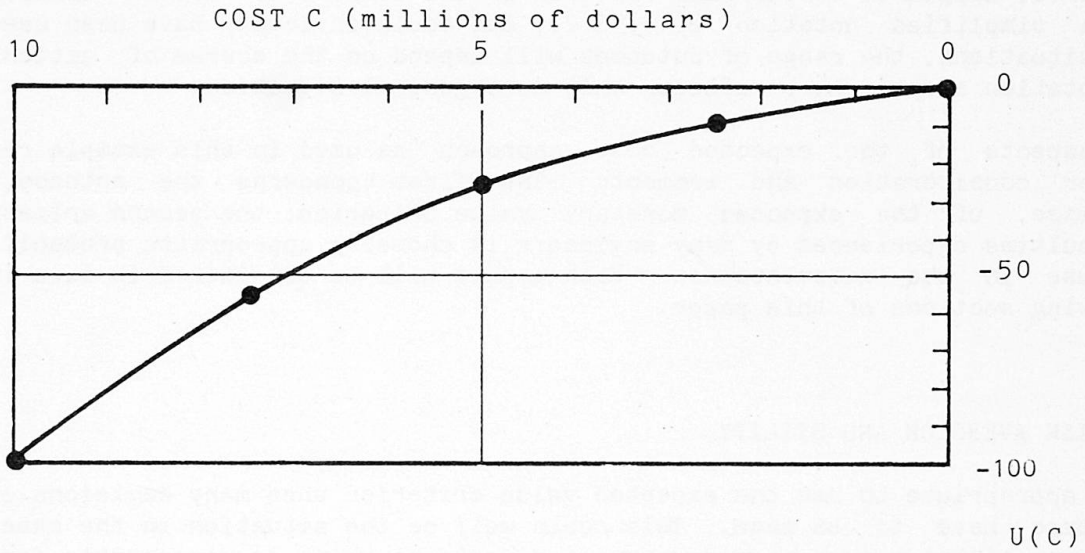
#### 4. RISK AVERSION AND UTILITY

It is appropriate to use the expected value criterion when many decisions of the one type have to be made. This could well be the situation in the case of a large organisation such as a government department which is responsible for the operation and maintenance of a large number of buildings or structures. The situation is rather different when the risk taker is a small organisation or an individual, facing an important one-off decision. Problems such as cash flow and possible loss of income create a high aversion to courses of action which might entail large costs, even when the associated probabilities are very slight. Strong aversion to risk is also likely to exist when low-probability outcomes entail loss of reputation or injury or loss of life. Professional reputation is an important consideration to the engineer, whether or not he is involved personally with the financial aspects of the problem.



COST C is in millions of dollars  
 $U(C)$  = Utility of Cost C (see Eq.3)

(a) Utility Function Decision Tree



(b) Utility Function

Fig. 1 : Construction of Utility Function



Allowance can be made for any desired degree of risk aversion by making a non-linear transformation of monetary values into utility values [4,5]. An arbitrary range of utility values is chosen to correspond to the range of monetary values. In Fig 1b, utilities of zero and minus one hundred units are equivalent to zero dollars and ten million dollars, respectively. A simple hypothetical decision situation such as the one indicated in Fig 1a is then used to obtain other intermediate utility values which allow a smooth transformation curve to be plotted as in Fig 1b. In Fig 1a two possible courses of action are considered. If action A(1) is chosen, there is a probability P that a loss of zero dollars will occur, but a probability of (1 - P) of a loss of ten million dollars. For various specific values of P, the decision maker chooses the maximum certain cost C which he is prepared to pay for action A(2) in order to avoid A(1). As (1) and A(2) are of equal value the utility of C dollars is equal to the expected utility of A(1), ie

$$U(C) = (0.0).P + (-100).(1 - P) = 100(P - 1) \quad (3)$$

It is convenient to use readily visualised values of P. In the present example, P values of 0.45, 0.75 and 0.90 produced C values of 7.5, 5.0 and 2.5 million dollars, respectively, and these were used to plot the points and hence the curve in Fig 1b.

When the expected values are calculated in terms of utilities instead of dollars in columns (4) and (5) in Table 1, it is found that A(4) is the preferred course of action. This result is consistent with a strong aversion to risk.

In the construction of the utility function, it is important that the risk aversion characteristics of the risk taker be properly represented, as these may not coincide with those of the engineer or professional decision maker. A further advantage of introducing utilities is that non-monetary aspects of the possible outcomes can often also be allowed for.

## 5. SUBJECTIVE PROBABILITIES AND THE PURCHASE OF NEW INFORMATION

As already pointed out, many engineers would have difficulty in giving values to the probabilities  $P[S(i,j)|A(i)]$ . Indeed it could be argued that such values are in most cases subjective, since there is insufficient information available to produce such values, except by educated guessing.

In many situations an attractive course of action open to the decision maker is to make the structure safe temporarily and then acquire additional information by any of the means used in structural assessment [2] such as:

- (a) study of available documentation concerning the design and construction of the structure;
- (b) quantitative measurement and analysis of environmental conditions;
- (c) non-destructive testing and inspection of structural components;
- (d) sampling and laboratory testing of materials;
- (e) retrospective analysis of structural behaviour to confirm an original diagnosis;
- (f) load testing of the in-situ structure (proof testing).

It will be noted that of the six common courses of action recommended in Section 1 of this paper which might be taken in the case of a defective structure, two involve gathering further information about the state of the structure. However, a difficulty arises when the expected value approach is used to consider information gathering as a possible course of action: before the



expected value of this course of action can be calculated, the range of possible outcomes of the information gathering exercise must be identified and their probabilities also estimated.

In Table 1, actions A(1) and A(2) are unattractive because of the very high cost associated with the relatively unlikely outcomes S(i,3) and S(i,4). If a relatively inexpensive in-situ load test could be devised to check the possibility of local or general collapse, it would be very cost-effective. For example, if the cost of such a test is \$100,000 then A(1) clearly becomes the best course of action if the test is likely to show that the structure can resist the unusual load combinations. Otherwise A(4) remains the best course of action.

A formal procedure for incorporating test results into the decision analysis is available through Bayes Theorem [4,5,6]. Suppose a test is conducted with potential results T(1), T(2),...T(r)...T(Nj). Each outcome S(i,j) of the decision process can be considered in turn and an estimate made of the probability that, given outcome S(i,j), test result T(r) would occur. This information, together with the original probabilities associated with the S(i,j), can be used with Bayes Theorem to determine an improved set of probabilities for the outcomes S(i,j), given a specific test result. The relation is:

$$P [S(i,j)|T(r)] = \frac{P [S(i,j)] \cdot P [T(r)|S(i,j)]}{\sum_{j=1}^{Nj} P [S(i,j)] \cdot P [T(r)|S(i,j)]} \quad (4)$$

The denominator of the right hand side is simply a normalising term which ensures that

$$\sum_{j=1}^{Nj} P [S(i,j)|T(r)] = 1.0 \quad (5)$$

This provides a means for deciding whether to test or not to test in situations where testing is one of the courses of action to be considered [6]. The probabilities and utilities may be manipulated to provide the expected cost of each of the testing alternatives and from these, together with the expected costs of the non-testing alternatives, the best course of action can be chosen.

## 6. REFERENCES

1. WARNER R.F., Strengthening, Stiffening and Repair of Concrete Structures, IABSE Periodica, 2-1981, Zuerich, 1981.
2. WARNER R.F., Structural Assessment of Existing Concrete Buildings, Concrete Symposium 1981, Institution of Engineers Australia, Adelaide, 1981.
3. RAIFFA H. and SCHLAIFER R., Applied Statistical Decision Theory, MIT Press Paperback, 1961.
4. RAIFFA H. and SCHLAIFER R., Decision Analysis: Introductory lectures on choices under uncertainty, Addison-Wesley, Reading Mass., 1970.
5. de NEUFVILLE R. and STAFFORD J.H., Systems Analysis for Engineers and Managers, McGraw-Hill Book Co, New York., 1971.
6. BENJAMIN J.R. and CORNELL C.A., Probability, Statistics and Decision for Civil Engineers, McGraw-Hill Book Co, New York, 1970.